The AAA-ATPase p97 in mitosis and fertilization

Dissertation der
Fakultät für Biologie der
Ludwig-Maximilians-Universität
München

vorgelegt von
Diplom-Biochemikerin
Simone Heubes

Juli 2007

Hiermit erkläre ich, dass ich die vorliegende Dissertation selbstständig und ohne unerlaubte Hilfe angefertigt habe. Ich habe weder anderweitig versucht, eine Dissertation einzureichen oder eine Doktorprüfung durchzuführen, noch habe ich diese Dissertation oder Teile derselben einer anderen Prüfungskommission vorgelegt.

München, den 17. Juli 2007

Promotionsgesuch eingereicht am: 19. Juli 2007

Tag der mündlichen Prüfung: 29. Oktober 2007

Erster Gutachter: Prof. Dr. Stefan Jentsch

Zweite Gutachterin: PD Dr. Angelika Böttger

Die vorliegende Arbeit wurde zwischen November 2003 und Juli 2007 unter Anleitung von Dr. Olaf Stemmann in der Abteilung von Prof. Dr. Stefan Jentsch am Max-Planck-Institut für Biochemie in Martinsried durchgeführt.

Wesentliche Teile dieser Arbeit sind in folgenden Publikationen veröffentlicht:

Heubes, S. and Stemmann, O. (2007). The AAA-ATPase p97-Ufd1-Npl4 is required for ERAD but not for spindle disassembly in Xenopus egg extracts. *J Cell Sci* 120, 1325-9.

Pfleghaar, K., **Heubes, S.**, Cox, J., Stemmann, O. and Speicher, M. R. (2005). Securin is not required for chromosomal stability in human cells. *PLoS Biol* 3, e416.

CONTENTS

1 SUMMARY

Late mitotic events are chiefly controlled by proteolysis of key regulatory proteins via the ubiquitin-proteasome pathway. In this pathway ubiquitin ligases modify substrates by attachment of ubiquitin ("ubiquitylation"), which usually results in their subsequent degradation by the 26S proteasome. The crucial ubiquitin ligase involved in late mitosis is the anaphase-promoting complex or cyclosome (APC/C). Among the many substrates of the APC/C is the anaphase inhibitor securin, whose destruction leads to activation of separase, which in turn triggers sister chromatid separation by proteolytic cleavage of cohesin. The APC/C also targets cyclin B1, an activating subunit of Cdk1 kinase, whose inactivation is a prerequisite for mitotic exit. The unstable APC/C substrates are often found in association with stable partner proteins. How single subunits of multi-protein complexes are selectively extracted and eventually degraded is largely unknown, but there is increasing evidence that additional factors assist to extract ubiquitin-carrying subunits from stable binding partners. One such factor is vertebrate p97 (Cdc48 in yeast), an abundant and highly conserved member of the AAA-ATPase family. It is involved in such diverse processes as transcriptional regulation, membrane fusion, and ER-associated protein degradation (ERAD). The unifying scheme in these seemingly unrelated functions is that p97 is able to "extract" preferentially ubiquitylated proteins from their environment. Roles of p97 in mitosis have recently emerged: p97 was reported to be required for spindle disassembly and for nuclear envelope reformation during mitotic exit in *Xenopus*. Furthermore, a genetic interaction between p97, separase and securin, as well as a requirement of p97 for separase stability, were discovered in fission yeast.

Given these hints and the importance of ubiquitylation in both mitosis and p97 pathways, this study intended to elucidate additional mitotic roles of p97 in vertebrates. Towards this end, tools to interfere with p97 function in *Xenopus* egg extracts were developed. These included immunodepletion of the p97 adaptors Npl4, Ufd1 and p47 and addition of recombinant dominant-negative p97-mutants. ERAD, which could be established here for the first time in *Xenopus* egg extracts, was greatly impaired in the absence of p97 function. However, many aspects of mitosis were found to be unaffected. Importantly, p97's proposed role in spindle disassembly was clearly falsified within this thesis. Furthermore, p97 was shown

to be dispensable for activity and stability of vertebrate separase. Disassembly of the mitotic checkpoint complex, which prevents premature APC/C activation by sequestering its activator Cdc20, did also not require functional p97 despite its dependence on ubiquitylation of Cdc20. However, a novel function of p97 at fertilization was discovered. p97 was found to interact with nucleoplasmin, a histone-binding chaperone that catalyzes the exchange of sperm-specific basic proteins (SBPs) to histones. Indeed, interference with p97 function delayed sperm decondensation in *Xenopus* egg extracts, thereby confirming a novel role of this AAA-ATPase in sperm chromatin remodelling.

In another project the role of securin in human cells was investigated. Human cells lacking securin had been reported to suffer from massive chromosome missegregation, which was in sharp contrast to the mild phenotype of securin knockout mice. In collaboration with the group of M. Speicher it could be demonstrated that chromosome losses in *securin*^{-/-} cells are transient and give way to a stable segregation pattern after just a few passages. This was despite persisting biochemical defects such as reduced level and activity of separase. These data demonstrate that securin is dispensable for chromosomal stability in human cells.

2 INTRODUCTION

This work mainly constitutes a study of p97, a AAA-ATPase with the ability to segregrate protein complexes. It focuses on p97's involvement in diverse processes during mitosis and fertilization. Therefore, these processes, as well as p97 itself, are introduced in the following chapters.

2.1 The eukaryotic cell cycle – An overview

During the eukaryotic cell cycle the genetic material of a cell is duplicated and subsequently partitioned into two newly forming daughter cells. Precise regulation of the chromosome cycle is critical since mistakes may lead to aneuploidy which is associated with cancer in multicellular organisms.

The cell cycle can be divided into four phases: In S phase (for DNA <u>s</u>ynthesis) chromosomes are replicated while their subsequent separation as well as cell division take place in M phase (for <u>m</u>itosis). Both phases are separated by so called <u>g</u>ap phases, G1 before and G2 after S phase. The G1, S and G2 phases together are referred to as interphase. Sister chromatids are paired concomitantly with their generation by replication in S-phase. They are mainly held together by a multi-subunit protein complex called cohesin (see below) and are disjoined only in M phase. M phase consists of mitosis - subdivided into prophase, prometaphase, metaphase, anaphase and telophase - and cytokinesis. In prophase chromosomes condense and become visible in the light microscope as well-defined structures (Fig. 1). At the same time assembly of the mitotic spindle is initiated by formation of asters of microtubules (MTs) around centrosomes, specialized organelles that constitute the microtubules organizing centers (MTOCs) in animal cells. Nuclear envelope breakdown marks the end of prophase and entry into prometaphase. The mitotic spindle fully assembles and chromosomes get attached to MTs of the spindle via specialized protein complexes called kinetochores that assemble on top of distinct chromosomal regions, the centromeres. Chromosomes start to migrate until metaphase, when they become aligned in a plane between the spindle poles, the metaphase plate. Every chromosome is now attached to opposite poles of the spindle via its two sister kinetochores and held under tension. Separation of sister chromatids occurs in anaphase when every chromatid is pulled towards the spindle pole that

it faces. Movement is achieved by shortening of kinetochore MTs (anaphase A) and increase of the interpolar distance (anaphase B). In telophase, chromosomes have arrived at the poles and start to decondense. The mitotic spindle disassembles and the nuclear envelope starts to reform around the chromosomes. Cell division is completed in cytokinesis by cleavage of the cytoplasm, leading to two separate daughter cells with identical sets of chromosomes (Fig. 1).
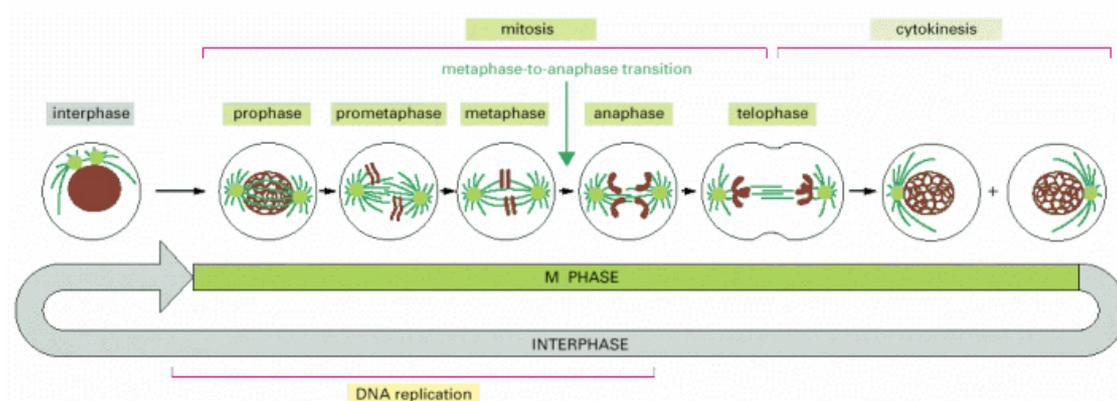
Fig.1: The eukaryotic cell cycle. Sister chromatids are generated by replication in S-phase and remain paired until their separation in mitosis. Mitosis and cytokinesis are referred to as M-phase. G1, S and G2 phase are referred to as interphase. See text for details. Chromatin is shown in brown, microtubules in dark green and centrosomes in light green (Alberts et al., 2002).

2.1.1 Establishment and resolution of cohesion between sister chromatids

In contrast to bacteria, chromosome replication and segregation are timely separated processes in eukaryotes, taking place in S and M phase, respectively. Separation of both events was possible only upon the evolution of chromatid cohesion in eukaryotes allowing assignment of corresponding sister chromatids to each other long after their replication. Cohesion between sister chromatids is established concomitantly with their generation by replication in S-phase by a ring-shaped protein complex called cohesin. The cohesin ring, which is assumed to embrace both DNA strands in its middle (Ivanov and Nasmyth, 2005), is mainly built out of the two Smc (<u>s</u>tructual <u>m</u>aintainance of <u>c</u>hromosomes) proteins Smc1 and Smc3 as well as the kleisin subunit Scc1/Rad21. Scc3, occuring in two isoforms SA1 and SA2 in higher eukaryotes, constitutes the fourth subunit of the complex and binds to Scc1 (Nasmyth and Haering, 2005). Cohesin is loaded onto DNA already in G1 phase with the help of the Scc2/Scc4 complex (Ciosk et al., 2000) and co-replicative establishment of sister chromatid cohesion in S phase

4

requires the acetyltransferase Eco1/Ctf7 (Skibbens et al., 1999). Sister chromatids are held together until M phase when cohesion is resolved to allow sister chromatid separation. In higher eukaryotes removal of cohesin occurs in two waves: The majority of cohesin along chromosome arms dissociates in prophase. This early dissociation requires phosphorylation of the cohesin SA2 subunit and the mitotic kinases Polo and Aurora B (Waizenegger et al., 2000; Hauf et al., 2005). Only a small fraction of cohesin around centromeres persists and preserves cohesion of sister chromatids until metaphase. Protection of centromeric cohesin in prophase is mediated by a protein called shugoshin ("guardian spirit" in Japanese). Shugoshin likely protects cohesin by recruiting the protein phosphatase 2A (PP2A), which antagonizes phosphorylation-dependent opening of the cohesin ring (Kitajima et al., 2004, Riedel et al., 2006). Additionally, shugoshin might physicially shield cohesin (Kitajima et al., 2004). Centromeric cohesin is finally removed when a large protease, called separase (see below), is activated in anaphase. Separase cleaves the Scc1 cohesin subunit, leading to opening of the cohesin ring and thus separation of sister chromatids (Uhlmann et al., 2000).

2.1.2 Regulation of separase

Separase exists in all eukaryotes and belongs to the family of cysteine-endopeptidases. Despite low conservation of their primary structures, separases from different species seem to have highly conserved tertiary structures (Jager et al., 2004). The active site of the 180 - 250 kDa protein is located near the C-terminus and contains a conserved histidine and cysteine residue forming the catalytic dyad (Uhlmann et al., 2000). Before anaphase, separase is kept inactive by two different inhibitory mechanisms. The first is represented by the stoichiometric separase inhibitor securin, which is conserved in function but not in sequence among different eukaryotic species (Funabiki et al., 1996; Yamamoto et al., 1996; Zou et al., 1999). In human cells it accumulates in G1 phase and blocks separase until the metaphase-to-anaphase transition when it gets degraded via the ubiquitin/proteasome pathway (see below). Surprisingly, securin not only functions as an inhibitor but also as an activator of separase since knockout of securin in vertebrates leads to a reduced level and activity of separase (Jallepalli et al., 2001). How securin exerts its positive effect on

separase is not yet elucidated. It might be involved in proper localization of separase (Jensen et al., 2001) or act as a chaperone assisting in correct folding (Nagao et al., 2004). Neither the inhibitory nor the activating function of securin seem to be essential in vertebrates since *securin*^{-/-} mice are viable and show only a mild phenotype (Mei et al., 2001). However, Jallepalli et al. (2001) reported that securin is required for chromosomal stability in the human cell line HCT116, pointing to a much more important role of securin and contradicting these results. A second mechanism that leads to inhibition of separase is phosphorylation-dependent binding of Cdk1/cyclinB1. Cdk1 can be considered the master regulator of mitosis and consists of the catalytic subunit Cdk1 and the regulatory subunit cyclin B1. Cdk1 is only active when associated with B-type cyclins and mediates phosphorylation of key proteins in mitosis. The cell cycle state directly correlates with Cdk1/cyclin B1 activity being high in mitosis and low in interphase. Accumulation of cyclin B1 is necessary and sufficient to trigger entry into mitosis whereas degradation of cyclin B1 and thus Cdk1 inactivation is essential for mitotic exit (Murray and Kirschner, 1989; Murray et al., 1989). Accordingly, a non-degradable mutant of cyclin B1 arrests cells in mitosis (Holloway et al., 1993; Wheatley et al., 1997). Using *Xenopus* anaphase egg extracts (see below) arrested in late mitosis by addition of non-degradable cyclin B1Δ90 (cyclin B1 with an N-terminal deletion of 90 aa), Stemmann et al. (2001) discovered that separase can be inhibited in the absence of securin when Cdk1 activity is kept high. Subsequent studies showed that under these conditions separase is phosphorylated by Cdk1 at Ser1126 and within a domain referred to as CLD. These phosphorylations create a binding site for the kinase, which then stably associates with separase in a second step, thereby inhibiting its proteolytic activity (Stemmann et al., 2001; Gorr et al., 2005). Binding of Cdk1/cyclin B1 and securin to separase is mutually exclusive (Gorr et al., 2005). Separase is thus tightly controlled by two independent mechanisms, which comes as no surprise given its great importance as ultimate trigger of anaphase. Indeed, abrogating both inhibitory mechanisms leads to premature activation of separase, cleavage of cohesin and, consequently, results in chromosome missegregation (Holland and Taylor, 2006; Huang et al., 2005).

Once activated in anaphase by degradation of both securin and cyclin B1, vertebrate separase not only cleaves Scc1 but also itself. The function of

separase self-cleavage is not yet understood but it might be important for G2-M transition and early mitosis (Papi et al., 2005).

2.1.3 Anaphase and the spindle assembly checkpoint

Progression through mitosis is controlled by proteolysis of key proteins via the ubiquitin-proteasome pathway. In this pathway target proteins are "marked" by ubiquitylation leading to recognition and degradation by the 26S proteasome, a large protease complex in eukaryotes. Ubiquitylation is achieved with a specific set of enzymes including a ubiquitin-activating enzyme E1, a ubiquitin-conjugating enzyme E2 and a ubiquitin-ligase E3. In the process the small (79 aa) protein ubiquitin is covalently bound to a lysine side chain of the substrate protein. Attached ubiquitin can itself be coupled to a further ubiquitin allowing formation of polyubiquitin chains on the target protein. Ubiquitin is first activated by ATP-dependent formation of a high-energy thioester bond of its C-terminal glycine residue with a cysteine side chain of the E1. The E1 transfers this activated form of ubiquitin to the E2 which in turn uses the high energy from the thioester bond to generate an isopeptide bond between the ubiquitin glycine residue and a lysine residue on the substrate protein (or on the ubiquitin that is already attached to the substrate protein) (Pickart and Eddins, 2004). The E3 confers substrate specificity by serving as a platform that brings E2 and substrate protein together (Fig. 2).
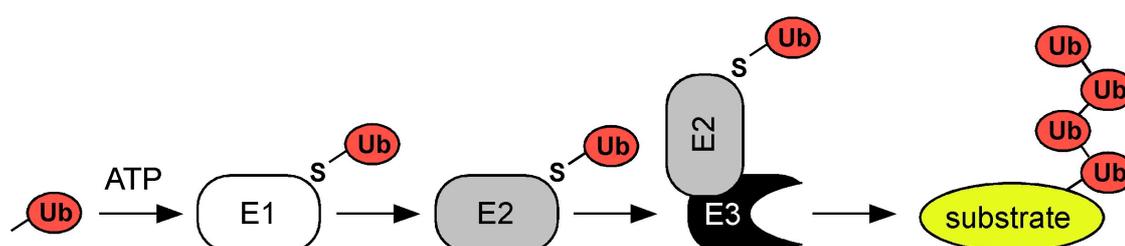
Fig. 2: Enzymatic thioester casacade of the ubiquitin conjugation system (simplified portrayal, applying to RING finger E3 ligases). Ubiquitin (Ub) is activated by E1 and subsequently passed to an E2. Ubiquitylation of substrates occurs in conjunction with an E3 which is responsible for substrate specificity. See text for details.

The E3 involved in late mitosis is the anaphase-promoting complex or cyclosome (APC/C). Prominent examples for the many substrates of the APC/C are securin, A- and B-type cyclins, Aurora B or Polo-like kinase 1 (Plk1) (Glotzer et al., 1991;

Peters, 2002; Zur and Brandeis, 2001). APC/C collaborates with either UbcH5 or UbcH10 as E2 enzyme (Aristarkhov et al., 1996; Yu et al., 1996). UbcH5 can also interact with other E3 enzymes, while UbcH10 seems to support APC/C exclusively. Although both E2 enzymes can support APC/C activity *in vitro*, UbcH10 is essential for the initiation of anaphase in human cells, *Drosophila* and *S. pombe,* indicating that UbcH5 cannot replace UbcH10 *in vivo* (Townsley et al., 1997; Seino et al., 2003; Mathe et al., 2004). Mitotic APC/C activity is dependent on the presence of one out of the two co-activator proteins Cdc20 or Cdh1 that associate with APC/C. APC/C^{Cdc20} mediates the degradation of cyclin B1 and securin at the metaphase-to-anaphase transition until it is inactivated in anaphase/telophase by APC/C^{Cdh1}-dependent removal of Cdc20. APC/C^{Cdh1} stays active throughout G1, thereby preventing premature reaccumulation of cyclins and ensuring a proper length of G1 phase. Once all G1 substrates are degraded, APC/C^{Cdh1} mediates degradation of UbcH10, thus inactivating itself and promoting S-phase entry (Rape and Kirschner, 2004).

It is evident that APC/C activation must be tightly controlled considering the fatal consequences of premature degradation of key regulators such as securin or cyclin B1. Accordingly, eukaryotic cells possess a special surveillance mechanism, the spindle assembly checkpoint (SAC) that keeps APC/C^{Cdc20} in check until all chromosomes have become bi-oriented on the metaphase plate of the mitotic spindle. Remarkably, the presence of a single kinetochore that has not properly attached to MTs is sufficient to prevent activation of APC/C^{Cdc20} and thus progression into anaphase. Although the mechanism of SAC signalling is not fully elucidated, structural and biochemical analyses point towards the so called "template model" (De Antoni et al., 2005; Nasymth, 2005). Major player in this model is the SAC protein Mad2 (mitotic arrest deficient), which can either interact with Mad1 or with Cdc20. Mad1 stably associates with unattached kinetochores and thereby recruits Mad2. Mad1-Mad2 complexes at kinetochores are thought to function as templates that catalyze assembly of Cdc20-Mad2 complexes and thus initiate formation of the MCC (mitotic checkpoint complex). The MCC, consisting of Cdc20, Mad2 and two other SAC proteins BubR1 (budding uninhibited by benzimidazole) and Bub3, tightly associates with APC/C leading to its inactivation. Once all kinetochores are properly attached, SAC signaling is silenced resulting in disassembly of the MCC and consequently in activation of

APC/C^{Cdc20}. The transition from strong APC/C^{Cdc20} inhibition to APC/C^{Cdc20} activation occurs very rapidly and in a switch-like manner. Recent results from the Kirschner and Elledge groups provide a possible explanation of how this switch-like transition is achieved (Reddy et al., 2007; Stegmeier et al., 2007). They demonstrated that disassembly of the MCC is not a passive process, as long been assumed, but that disassembly is actively promoted by, surprisingly, APC/C itself. APC/C in collaboration with UbcH10 mediates polyubiquitylation of Cdc20 resulting in destabilization and dissociation of the MCC. During this process polyubiquitylation of Cdc20 does not lead to its degradation by the 26S proteasome but only to disassembly of the complex (Reddy et al., 2007). APC/C therefore permanently antagonizes its own inhibition raising the question of how it is ever inhibited. The newly identified SAC protein USP44 discovered in a parallel approach by Stegmeier and co-workers (2007) provides an answer to this question. USP44 belongs to the family of de-ubiquitylating enzymes that hydrolyze ubiquitin chains previously attached by E2 enzymes on target proteins. As long as SAC signaling is active, USP44 de-ubiquitylates Cdc20, thereby antagonizing ubiquitylation mediated by UbcH10. Consequently, USP44 promotes MCC stabiliziation and APC/C inactivation. Despite these new discoveries and other previously elucidated inactivation mechanisms (Xia et al., 2004; Zhang et al., 2007; Wassmann et al., 2003) many aspects of SAC remain a mystery. It is unclear how ubiquitylation drives dissociation of Cdc20 from Mad2, BubR1 and Bub3 and whether this process requires additional proteins. Moreover it remains to be elucidated whether degradation of USP44 that occurs in late mitosis constitutes the primary switch for checkpoint inactivation or rather is a consequence of APC/C activation.

2.1.4 Assembly and disassembly of the mitotic spindle

In interphase cells, MTs extend through the cytoplasm as long polymers constituting a part of the cytoskeletal system. These interphase MT arrays govern the localisation of cell organelles and contribute to both cell motility and polarity. The building block of MTs are heterodimers of $\alpha-$ and $\beta-$tubulin that polymerize to form protofilaments which assemble into cylindrical tubes with 25 nm in diameter. Purified MTs are dynamic structures that switch between periods of polymerization and depolymerization, a behavior called "dynamic instability"

(Desai and Mitchison, 1997). While interphase MT arrays are relatively stable, mitotic MTs switch very frequently between growth and shrinkage. Upon entry into mitosis, MTs emanating from centrosomes are thus enabled to "search-and-capture" chromosomal kinetochores and to build up the spindle (Kirschner and Mitchison, 1986). Consequently, the transformation of an interphase MT array into a mitotic spindle involves dramatic changes in dynamics and movements of MTs. Dynamic instability not only lies within the nature of MTs themselves but are also strongly influenced by MT-stabilizing and -destabilizing factors. Additionally, motor proteins contribute to self-organization of the mitotic spindle through directional movement and cross-linking of MTs (Heald et al., 1996). These regulators of MT-behaviour are themselves primarily regulated by phosphorylation as exemplified by the control of MT-dynamics and steady-state length by cdk1 in *Xenopus* (Verde et al., 1990; Verde et al., 1992). Apart from mitotic kinases, the small GTPase Ran also contributes to spindle formation by releasing spindle assembly factors from inactive complexes with nuclear import receptors (Hetzer et al., 2002). This occurs in the vicinity of chromosomes where Ran is converted into its GTP-bound, active form by its chromatin-associated guanine exchange factor RCC1. It is conceivable that the regulatory mechanisms triggering spindle formation early in mitosis must be reversed to bring about spindle disassembly upon exit from mitosis. However, the transition of mitotic spindles into interphase MT arrays has hardly been studied so far. Although Cdk1 inactivation is clearly essential for spindle disassembly (Murray, 1989), Zheng and co-workers recently reported that, surprisingly, it was not sufficient (Cao et al., 2003). Spindle disassembly additionally required the activity of the AAA-ATPase p97 (see below), as reported by these researchers.

2.2 The AAA-ATPase p97

p97 (Cdc48 in yeast; valosin-containing protein (VCP) in humans - an unfavorable name given after an artefact) is an abundant and highly conserved member of the AAA-ATPase (ATPases associated with various cellular activities) family. It is involved in such diverse processes as transcriptional regulation, membrane fusion and ubiquitin-dependent protein degradation. The unifying scheme in these seemingly unrelated functions is that p97 uses the chemical energy from ATP hydrolysis to "extract" target proteins from their environment, an

activity that earned p97 the epithet "segregase". p97 seems to have a strong preference for ubiquitylated substrates although there is some debate whether ubiquitylation is an absolute requirement (Ye et al., 2003). p97 either only dissociates its target proteins from their environment or subsequently transfers them to the 26S proteasome resulting in their degradation. The former activity is exemplified by the activation of the membrane-bound transcription factor SPT23. In this process p97 dissociates ubiquitylated truncated SPT23 from membrane-bound full-length SPT23 allowing its transport into the nucleus (Rape et al., 2001). The dissocation of SNARE complexes in homotypic fusion events of endoplasmatic reticulum (ER) and Golgi membranes is another example of p97-catalyzed disassembly without subsequent degradation (Uchiyama et al., 2005; Ye, 2006). In contrast, p97 also has a well characterized role in ER-associated protein degradation (ERAD). This pathway, mainly investigated in *S. cerevisiae*, mediates the export of e.g. incorrectly folded proteins from the ER into the cytosol where they get degraded by the 26S proteasome (Rabinovich et al., 2002, Meusser et al., 2005). During this process p97 extracts substrates from the ER membrane and releases them for cytosolic degradation. In vertebrate cells involvement of p97 in ERAD has been shown for several substrates including major histocompatibility complex (MHC) class I heavy chains and cystic fibrosis transmembrane conductance regulator (CFTR) (Ye et al., 2001; Weihl et al., 2006).

In its native state p97 exists as a homohexamer with its subunits arranged in a ring-like manner leaving a pore in the centre (Pye et al., 2006; DeLaBarre and Brunger, 2003). Each monomer with 97 kDa in size is composed out of an N-domain responsible for substrate binding and two AAA-domains called D1 and D2 (Fig. 3A). The characteristic AAA-cassettes comprise approximately 250 aa each and are responsible for nucleotide binding. Since both the N- together with the D1-domains and the D2-domains oligomerize, a p97 hexamer appears like two rings on top of each other (Fig. 3B and C). The D2-ring is responsible for the catalytic activity of p97 by binding and hydrolyzing ATP. In contrast, the D1-domains do not seem to hydrolyze ATP but rather be important for hexamer stabilization (DeLaBarre and Brunger, 2003).
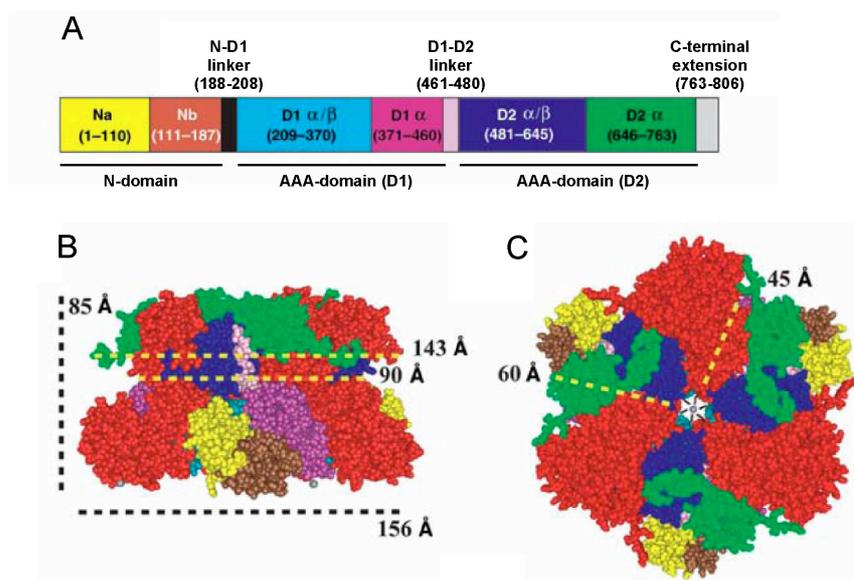
Fig. 3: Structure of p97. (A) Primary structure of a p97 monomer consisting out of a N-domain and two AAA-domains called D1 and D2. **(B)** Quarternary structure of a p97 hexamer (side view). p97 monomers are arranged in a ring-like manner forming a pore in the middle. See text for details. **(C)** Quarternary structure of a p97 hexamer (top view).

Adaptor proteins, which bind to the N-domain of p97 (Bruderer et al., 2004), play crucial roles in p97 substrate specificity and recruitment. Of these, the heterodimer Ufd1-Npl4 (Ufd1 for ubiquitin fusion degradation 1 and Npl4 for nuclear protein localization 4) and p47 are the best characterized ones. While p47 is essential in p97-catalyzed membrane fusion events, the Ufd1-Npl4 complex is involved in ERAD. Both adaptors bind p97 in a mutually exclusive manner (Meyer et al., 2000; Meyer et al., 2002).

As discussed, the majority of p97's well-established and characterized roles lie outside mitosis. However, p97/Cdc48 was first discovered in budding yeast by a cell division cycle mutant, *cdc48-1*, which causes arrest in mitosis with undivided nuclei and medium-sized spindles (Moir et al., 1982; Frohlich et al., 1991). Likewise, knockdown of p97 in HeLa cells leads to transient accumulation in a prometaphase-like state (Wojcik et al., 2004). The molecular details that form the basis of these phenotypes are not yet elucidated. Additional hints on important roles for p97 in mitosis come from from Yanagida and co-workers who demonstrated a strong genetic interaction of fission yeast Cdc48 with Cut1 (separase) (Yuasa et al., 2004). Using a newly isolated *cdc48* mutant strain they also demonstrated that Cdc48 is necessary to prevent degradation of Cut1 in

anaphase when its inhibitor Cut2 (securin in fission yeast) is proteolyzed (Ikai and Yanagida, 2006). In *Xenopus* and budding yeast, specific roles of p97 at mitotic exit have recently been proposed: p97 with its ability to mediate membrane fusion seems to be important for reformation of the nuclear envelope, which becomes fragmented in mitosis (Hetzer et al., 2001). Moreover, Cao et al. (2003) reported a requirement for p97 in spindle disassembly at the end of mitosis and suggested a mechanism by which spindle stabilizing factors are displaced from microtubules through p97 action. All these results underline the significance of p97 also for mitosis and indicate that additional important roles of p97 are very likely to exist.

2.3 Fertilization

Fertilization marks the beginning of one of the most remarkable phenomena in nature – the development of a new individual. It requires the preceding formation of specialized haploid cells, egg and sperm, that fuse to build a diploid zygote, which then undergoes embryogenesis. The formation of both egg and sperm begins in a similar way, with meiosis. Starting with a diploid germ stem cell, homologous chromosomes, which have been paired to from so-called tetrades, are separated in meiosis I. Importantly, sister chromatids remain paired during this first nuclear division and are segregated from each other only during meiosis II, which follows meiosis I and closely resembles a normal mitotic division.

Despite many similarities between egg and sperm formation (oogenesis and spermatogenesis, respectively) there are important differences. In contrast to sperm, mature eggs from many vertebrates including humans arrest in metaphase of meiosis II until fertilization. This metaphase II arrest is achieved by the presences of a cytostatic factor (CSF) which was recently identified as XErp1 (*Xenopus* Erp1) in *Xenopus*. XErp1 represents an inhibitor of APC/C^{Cdc20}, which is degraded via the ubiquitin/proteasome system in response to a rise in intracellular Ca^{2+} (Rauh et al., 2005; Schmidt et al., 2005; Schmidt et al., 2006). While eggs are usually large and immotile cells bearing all material needed for early embronic development, sperm are small cells optimized for motility and speed. Sperm DNA is extremely tightly packed resulting in condensation of the nucleus to 10% of its original volume (Bergmann, 2005). During spermatogenesis this is achieved by replacement of somatic histones with sperm-specific basic

proteins (SBPs), which include both arginine-rich protamines and sperm-specific histone variants (Ausió, 1999).

Mammalian fertilization begins when the head of the sperm bind to the zona pellucida, a glycoprotein-rich coat surrounding the egg. After traversing the zona pellucida the sperm binds to and fuses with the plasma membrane thereby triggering a sudden increase of cytosolic Ca^{2+} that releases the egg from CSF-arrest. While the egg completes meiosis II forming the so-called female pronucleus, the sperm nucleus is released into the egg cytoplasm. Transformation of the injected sperm nucleus into the male pronucleus is a prerequisite for successful fertilization and includes two steps called sperm decondensation stage I and II (Alberts et al, 2002; Long and Kunkle, 1978). During stage I decondensation the sperm nucleus undergoes membrane breakdown followed by rapid decondensation of its chromatin. SBPs are replaced back by somatic histones, a process which is mediated by a protein called nucleoplasmin. Nucleoplasmin is an acidic histone-binding protein (Laskey et al., 1978) and constitutes the most abundant protein in egg cytoplasm. It has been reported to be both necessary and sufficient for sperm chromatin decondensation (Philpott et al., 1991; Philpott and Leno, 1992) in *Xenopus*. Formation of the male pronucleus is completed with stage II decondensation, which culminates in formation of a new nuclear envelope (Kunkle and Longo, 1975). Male and female pronuclei finally migrate towards each other and combine their chromosomes. Formation of a single diploid nucleus completes fertilization thereby starting embryonal development.

2.4 The African clawed frog as model organism

A powerful and common system to study mitosis and meiosis are egg extracts of the African clawed frog (*Xenopus laevis*). These frogs are easy to breed and have been kept as laboratory animals since the 1940's, originally for pregnancy diagnosis. After injecting female frogs with the hormone chorionic gonadotropin (which is also present in pregnant womens' urine) they react by laying eggs. Freshly layed eggs are arrested in metaphase II (CSF-arrest) and are used for the preparation of cytosolic extracts by low-speed (13 000 g) centrifugation (Fig. 4).
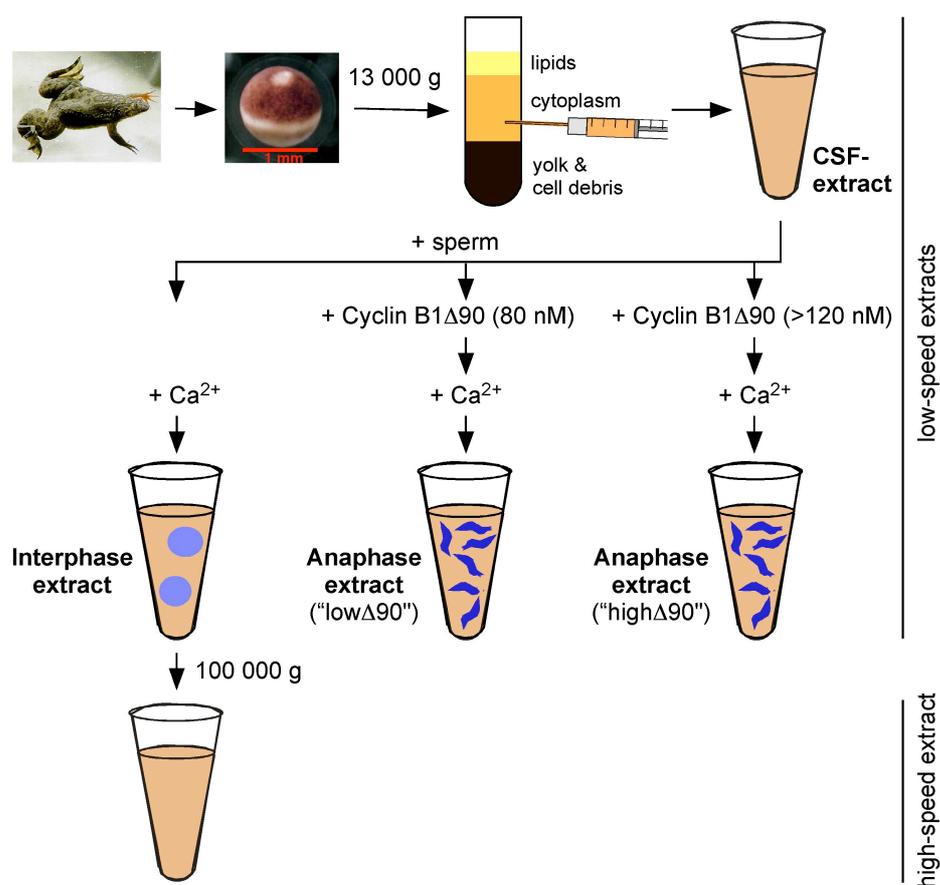
Fig. 4: Preparation of *Xenopus* egg extracts mimicking various cell cycle stages. Metaphase II arrested eggs obtained from female frogs after hormone injection are crushed by low-speed centrifugation (13 000 g). The cytosolic fraction is recovered (CSF-extract) and can be released by addition of Ca^{2+} in the presence or absence of cyclin B1Δ90 resulting in interphase, "lowΔ90" or "highΔ90" anaphase extracts. Sperm chromatin (blue) is usually added to extracts to visualize cell cycle stages by microscopy after DAPI staining. Low-speed extracts can be centrifuged by a second, high-speed (100 000g) centrifugation resulting in high-speed extracts that are devoid of all membranes.

These extracts are still arrested in metaphase II and are thus referred to as CSF-extracts. Importantly, they can be released by the addition of Ca^{2+} which mimics sperm entry and triggers exit from meiosis. Major advantages of the extracts are their synchrony regarding the cell cycle state and their amenablity to biochemical manipulations such as protein additions or depletions. This provides the great opportunity to investigate the involvement of specific proteins in mitotic/meiotic processes. A multitude of different extracts can be prepared starting from a CSF-extract. Addition of Ca^{2+} alone triggers progression into interphase. If CSF-extracts are released by Ca^{2+} in the presence of non-degradable cyclin B1Δ90, they progess into anaphase but no further since Cdk1/cyclinB1 activity is

maintained and blocks meiotic exit. Depending on the concentration of cyclin B1Δ90, "lowΔ90"- or "highΔ90"- extracts with active APC/C^{Cdc20} but either active or inhibited separase can be prepared. By a second high-speed (100 000 g) centrifugation, usually starting with interphase extracts, so called "high-speed extracts" are obtained. In contrast to low-speed extracts they do not contain any membranes and support only few cell biological processes including stage I (but not stage II) sperm decondensation. Unless stated otherwise, "extract" is used to describe low-speed extract in this thesis.

2.5 Aim of this work

Although it is long known that the APC/C controls late mitotic transitions many questions remain to be answered. Most of the APC/C substrates are engaged in complexes with stable partner proteins and it is largely unknown how selective extraction and/or degradation of single subunits out of protein complexes is achieved. The AAA-ATPase p97 is an attractive candidate to assist in extracting ubiquitin-carrying APC/C substrates from their binding partners since it has been demonstrated to act as a ubiquitin-selective "segregase" in other processes. Roles of p97 in mitosis recently emerged. Importantly, p97 was reported to be required for spindle disassembly and nuclear envelope reformation in late mitosis. p97 was additionally found to be necessary for separase stability after securin degradation in fission yeast. Therefore, this thesis aimed to elucidate novel roles of p97 in vertebrate mitosis. In particular, the requirement of p97 for separase activation and stability, as well as for liberation of Cdc20 from the mitotic checkpoint complex, should be addressed. To this end, tools to interfere with p97 function in *Xenopus* egg extracts had to be established and should be first used in spindle disassembly experiments as an activity assay for p97. Since, unexpectedly, these experiments revealed that the proposed role of p97 in spindle disassembly is wrong, further controls had to be established to validate these results. During the establishment of depleting p97 and its adaptors, nucleoplasmin, a histone-binding chaperone was identified as a novel interactor of p97. Since nucleoplasmin plays a major role in sperm chromatin remodelling at fertilization, the physiological relevance of this interaction should be further characterized and a putative involvement of p97 in this reaction be investigated (Fig. 5).
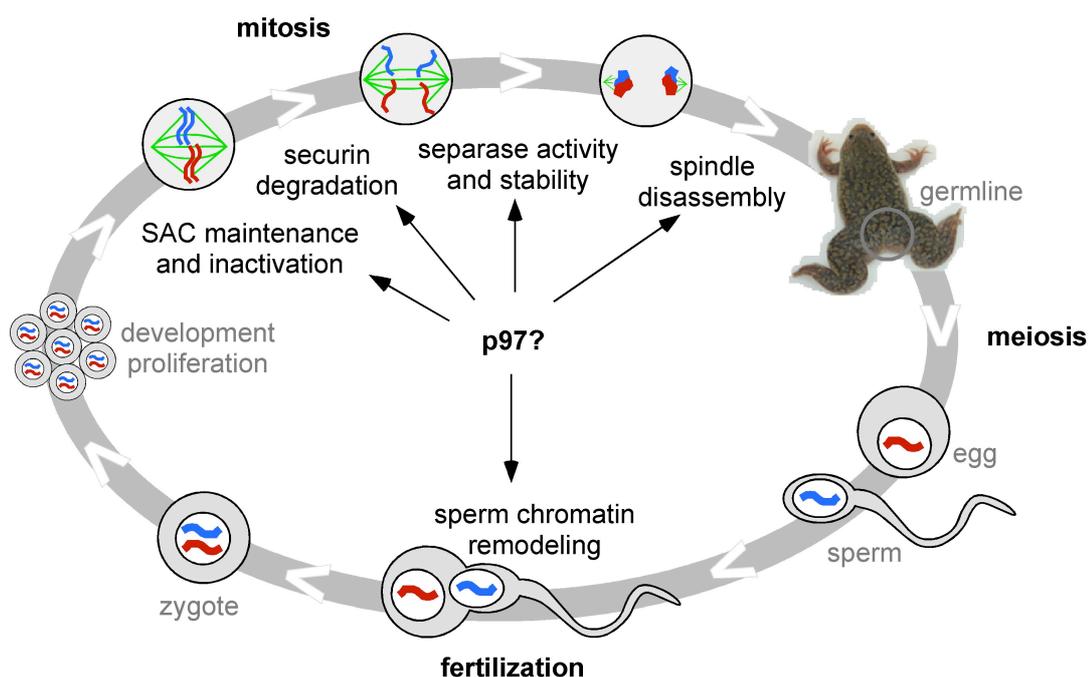
Fig. 5: Overview of molecular mechanisms investigated within this study for a potential involvement of p97. See text for details.

An additional project in collaboration with the group of M. Speicher addressed the relevance of securin for chromosomal stability in human cells. Previously, human cells lacking securin had been reported to display frequent losses and gains of chromosomes which contrasted with results from mouse cells. To solve this discrepancy, human *securin*^{-/-} cells had to be investigated in more detail.

3 RESULTS

3.1 The AAA-ATPase p97 in mitosis and fertilization

3.1.1 Interference with p97 function in *Xenopus* egg extracts

3.1.1.1 Depletion of p97 using the UT6-domain of Ufd1

At the beginning of this work tools to interfere with p97 function in *Xenopus* egg extracts had to be established. Hetzer et al. (2001) had described a method where p97 was successfully removed from *Xenopus* high-speed extract using the N-terminal UT6-domain of Ufd1 immobilized on beads. Due to the strong interaction of the UT6-domain with p97, these beads depleted p97 from high-speed extract. Adopting the approach of Hetzer et al. (2001), the UT6-fragment was PCR-amplified and cloned from *Xenopus* egg mRNA, expressed as GST fusion protein in bacteria and affinity-purified over glutathione sepharose. Indeed, these beads proved to reduce the amount of p97 in high-speed extract to more than 95% within two rounds of depletion (Fig. 6).
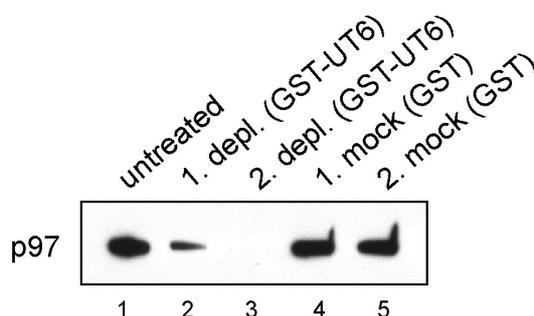
Fig. 6: Depletion of p97 from *Xenopus* high-speed extract. High-speed extract was depleted in two rounds using immobilized, GST-tagged UT6. Mock-depletion was performed with immobilized GST alone. Equivalent amounts before (lane 1) and after the 1st (lanes 2 and 4) and 2nd depletion (lanes 3 and 5) were immunoblotted against p97. Equal loading was confirmed by Ponceau staining (data not shown).

In contrast to high-speed extract, only low-speed extract fully supports translation, protein degradation and replication and can thus be cycled through mitosis and interphase. Since the aim of this PhD thesis was to investigate roles of p97 at mitotic exit, there was a need to successfully interfere with p97 in low-speed extract while maintaining its ability to cycle. However, depletion of p97 by the UT6-approach turned out to be unsuitable for low-speed extract. Likely due to the presence of membranes and membrane-bound p97, quantitative removal of

p97 from low-speed extract involved several, lengthy depletions resulting in dilution and long incubation times which were incompatible with the maintenance of the mitotic state. Therefore, additional ways to interfere with p97 function had to be searched that also worked in low-speed extract.

3.1.1.2 Immunodepletion of p97

An alternative approach aimed to immunodeplete p97 from extract using newly raised polyclonal antibodies against *Xenopus* p97. To this end, the open reading frame of *Xenopus* p97 was PCR-amplified and cloned into a modified pQE80 for His-tagging and into a modified pGEX for GST-tagging. His- and GST-tagged proteins were expressed in *E. coli* and purified over Ni^{2+}-NTA-agarose and glutathione sepharose, respectively. His_6-p97 was used to immunize a rabbit, while GST-p97 was used to prepare the affinity column for antibody purification. While immunoblotting with pre-immune serum did not result in any signal (Fig. 7, left panel), as little as 5 ng of recombinant His_6-p97 were easily detected by anti-serum (Fig. 7, middle panel). Moreover, the specificity was high as only a single band was detected in *Xenopus* egg extract. Given the high sequence conservation of p97 from different phlya, it comes as no surprise that the newly raised antibody recognized even *S. cerevisiae* Cdc48 with high specificity (data not shown). To remove unspecific IgG the antibody was affinity-purified over immobilized GST-p97. The amount of antibody present in the rabbit anti-serum was quite low resulting in approximately 600 μg of purified antibody from 10 ml. Since the concentration of p97 in low-speed extract is very high (0.25 mg/ml), immunodepleting p97 using the novel antibody failed again because of limiting amounts of antibody and the requirement of multiple rounds of depletion that were incompatible with cycling of the extract, similar to the UT6-approach.
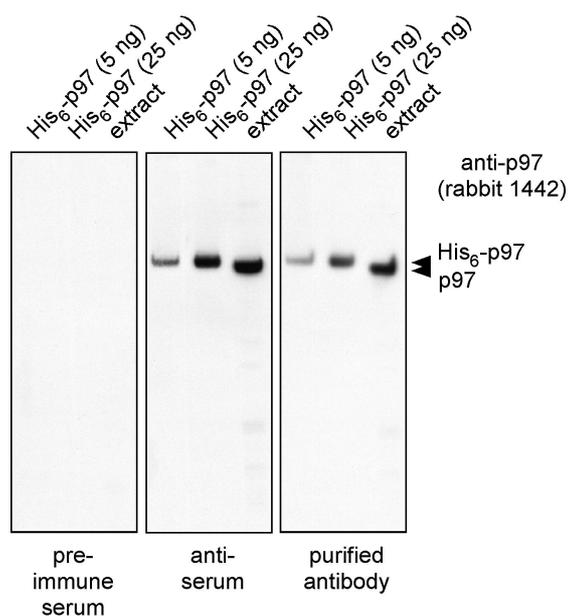
Fig. 7: Characterization of a novel antibody against *Xenopus* p97. Five and 25 ng of recombinant His_6-Xep97 or 0.25 µl of extract were loaded and immunoblotted with pre-immune serum (left), anti-serum (middle) or anti-p97-antibody (0.05 ng/µl final) affinity-purified from anti-serum (right).

3.1.1.3 Immunodepletion of p97 adaptors

While p97 itself is present in high concentrations in extract, its adaptor proteins are less abundant. Therefore, antibodies against the most common and best characterized adaptors of p97, p47 and the heterodimeric Ufd1-Npl4, were raised with the aim to establish their immunodepletions from extract. Towards this end, the open reading frames of *Xenopus* Ufd1, Npl4, and p47 were amplified by RT-PCR from *Xenopus* egg mRNA. Each PCR-product was then cloned into a modified pQE80 vector for His-tagging and into a modified pGEX vector for GST-tagging. Following expression in *E. coli*, His- and GST-tagged proteins were purified over Ni^{2+}-NTA-agarose and glutathione sepharose, respectively. While His-tagged proteins were used to immunize rabbits (2 in case of Ufd1 and Npl4, 1 in case of p47), immobilized GST-tagged proteins were used for affinity purification of antibodies. Since His- and GST-tagged Ufd1 alone turned out to be largely insoluble but preparation of the affinity column for antibody purification required soluble Ufd1, His_6-Ufd1 was co-expressed with GST-Npl4 and the soluble His_6-Ufd1/GST-Npl4 complex purified via Ni^{2+}-NTA-agarose. A mixture of this His_6-Ufd1/GST-Npl4 and GST-UT6 was covalently coupled to N-hydroxysuccinimid (NHS)-activated beads to prepare the affinity column. After

purification from rabbit anti-serum with the respective immunoaffinity column, antibodies anti-Ufd1-1, anti-Ufd1-2, anti-Npl4-1 and anti-p47 were characterized by immunoblotting of recombinant proteins and extract (Fig. 8). In case of all four antibodies immunoblotting with corresponding pre-immune serum did not result in any signal at the expected size of Ufd1, Npl4 or p47 (Fig. 8, left panels of A-D), confirming specificity of signals obtained with anti-sera (Fig. 8, middle panels of A-D). Affinity purification of antibodies from anti-serum did not improve their specificity as immunoblotting with purified antibodies gave rise to the same background bands as immunoblotting with anti-serum (compare right and middle panel of Fig. 8A-D). However, the specific and absolute concentration of the antibodies was highly increased during purification, facilitating subsequent immunodepletions and allowing antibody addition experiments (see below). Both anti-Ufd1-1 and anti-Ufd1-2 recognized recombinant His_6-Ufd1 and endogenous Ufd1 in extract. Anti-Ufd1-1 gave a stronger signal with endogenous Ufd1 (Fig. 8A and B) but at the same time was less specific than anti-Ufd1-2 as it also detected recombinant GST-Npl4 (Fig. 8A and B). Anti-Npl4-1 detected recombinant GST-Npl4 and endogenous Npl4 in extract with high specificity, producing only few and weak unspecific bands (Fig. 8C). The same was true for anti-p47 which was highly specific for recombinant His_6-p47 and endogenous p47 (Fig. 8D). The second rabbit immunized with His_6-Npl4 died before final bleeding and anti-Npl4-2 could thus be purified only in very limited amounts from the first testblood of this rabbit. Since anti-Npl4-2 was used in some few experiments of this study, its characterization is also shown (Fig. 9). Immunoblotting with pre-immune serum did not give a signal at the size of Npl4 in contrast to anti-serum obtained from the first testblood oft this rabbit (Fig. 9, left and middle panels). Both recombinant His_6-Npl4 and endogenous Npl4 in extract were specifically recognized (Fig. 9, middle panel). The specificity could be further enhanced by affinity purification of anti-Npl4-2 as judged by reduced background bands in the immunoblot performed with purified anti-Npl4-2 (Fig. 9, right panel).
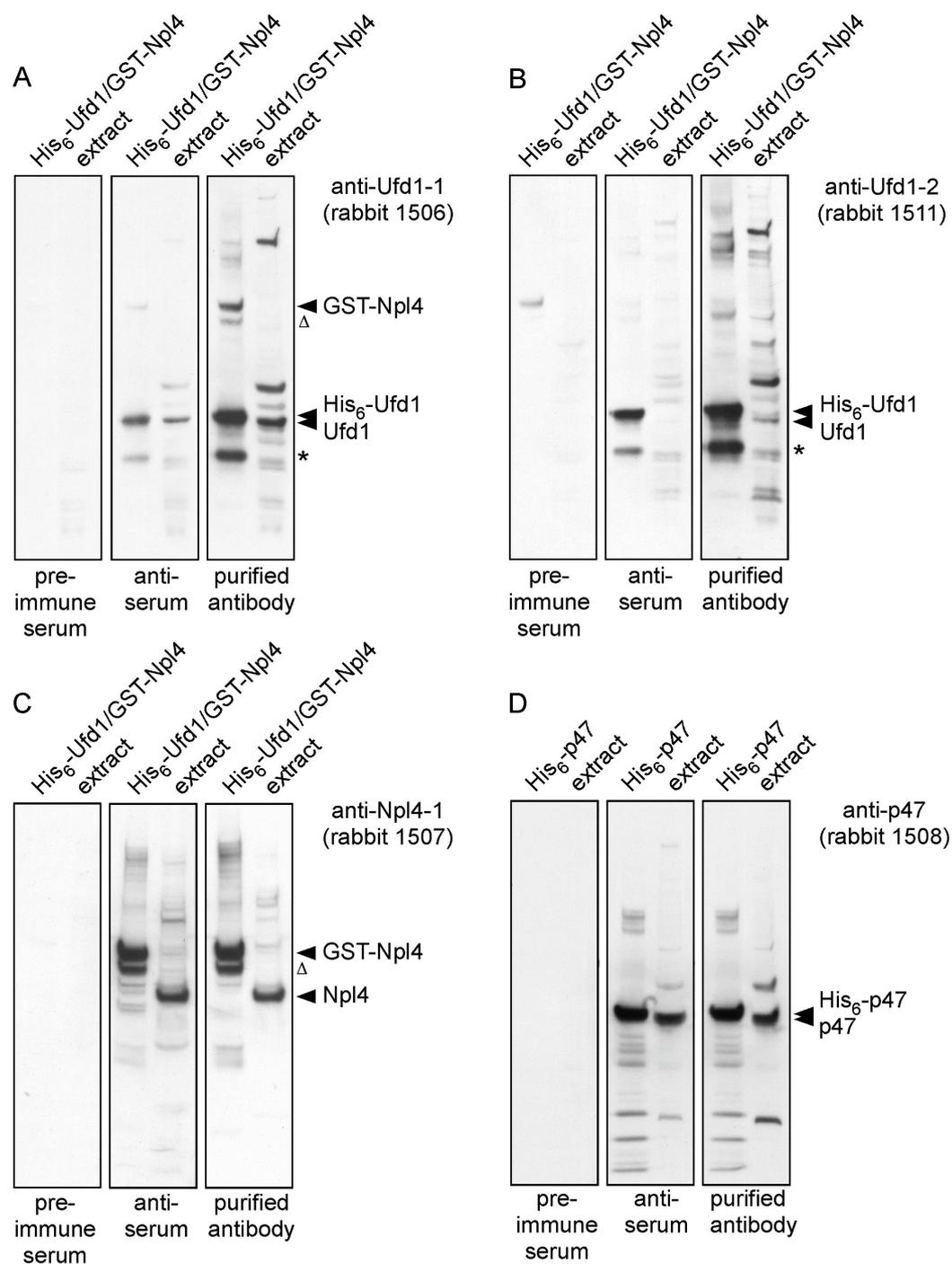
Fig. 8: Characterization of novel antibodies against *Xenopus* Ufd1, Npl4 and p47 by immunoblotting. 50 ng of His₆-Ufd1/GST-Npl4 (left lane in each panel of A, B, C), 50 ng of His₆-p47 (left lane in each panel of D) and 0.5 µl of extract (right lane in each panel of A-D) were loaded and immunoblotted with respective pre-immune serum (left panel), anti-serum (middle panel) and affinity-purified antibody in a final concentration of 0.3 ng/µl (anti-Ufd1-1), 0.2 ng/µl (anti-Ufd1-2), 0.4 ng/µl (anti-Npl4-1) and 0.3 ng/µl (anti-p47) (right panel). Triangle and star denote degradation products of recominant GST-Npl4 and His₆-Ufd1, respectively.
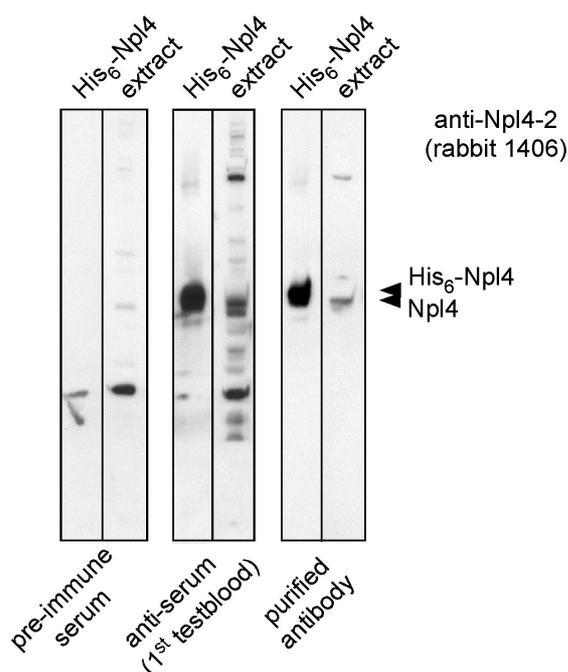
Fig. 9: Characterization of novel antibody anti-Npl4-2 by immunoblotting. 50 ng of His$_6$-Npl4 (left lane in each panel) and 0.5 µl of extract (right lane in each panel) were loaded and immunoblotted with respective pre-immune serum (left panel), anti-serum (middle panel) and affinity-purified antibody in a final concentration of 0.05 ng/µl (right panel).

After characterization of the antibodies in immunoblotting experiments, their ability to immunoprecipitate corresponding endogenous proteins from extract was tested. Towards this end, antibodies were coupled to magnetic protein A beads and incubated in highΔ90-extract for 30 min. Beads were re-isolated afterwards and analyzed by immunoblotting (Fig. 10).
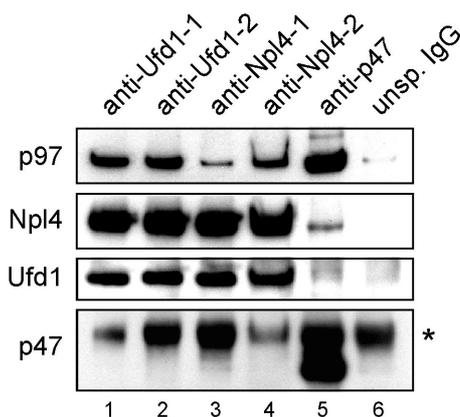
Fig. 10: Immunoprecipitation from *Xenopus* egg extract with novel anti-Ufd1-1, anti-Ufd1-2, anti-Npl4-1, anti-Npl4-2 and anti-p47 antibodies. 10 µg of anti-Ufd1-1 (lane 1), anti-Ufd1-2 (lane 2), anti-Npl4-1 (lane 3), anti-Npl4-2 (lane 4), anti-p47 (lane 5) or unspecific rabbit IgG (lane 6) were bound to magnetic protein A beads and incubated in highΔ90-extract. After re-isolation, beads were analyzed by immunoblotting. Star denotes IgG heavy chain.

Anti-Ufd1-1 and anti-Ufd1-2 immunoprecipitated endogenous Ufd1 with similar efficiencies and led to co-immunoprecipitation of Npl4 and p97, due to the strong interaction of these proteins with each other (Fig. 10, lanes 1 and 2). Anti-Npl4-1 and anti-Npl4-2 efficiently immunoprecipiated endogenous Npl4, at the same time co-immunoprecipitating Ufd1 (Fig. 10, lane 3 and 4). However, only anti-Npl4-2 but not anti-Npl4-1 efficiently co-immunoprecipitated p97 indicating that anti-Npl4-1 covers the p97 binding site on Npl4 and is able to dissociate Ufd1-Npl4 from p97 (Fig. 10, lane 3 and 4). Neither anti-Ufd1-1, anti-Ufd1-2 nor anti-Npl4-1 or anti-Npl4-2 co-immunoprecipitated p47, consistent with the mutual exclusive binding of p47 and Ufd1-Npl4 to p97 (Meyer et al., 2000). As expected, anti-p47 efficiently immunoprecipitated p47 and co-immunoprecipitated p97 but did not co-immunoprecipitate Ufd1 or Npl4 (Fig. 10, lane 5). Unspecific rabbit IgG served as negative control for all immunoprecipitations (Fig. 10, lane 6). In summary, specific antibodies against *Xenopus* Ufd1, Npl4 and p47 have been generated and carefully characterized by immunoblotting and –precipitation.

Next, immunodepletions of Ufd1, Npl4 and p47 were established from extract. For this purpose, antibodies were coupled to magnetic protein A beads as before and incubated in CSF-arrested extracts. After removal of the beads, extracts were analyzed by immunoblotting for remaining amounts of endogenous Npl4, Ufd1 and p47. Varying incubation time, temperature, amounts of beads, and amounts of antibodies, optimal conditions for depletions were identified under which the CSF-arrest of the extracts was maintained. Two rounds of 30-min depletion at 12°C with 15 μg anti-Ufd1-1, 20 μg anti-Npl4-1, or 10 μg anti-p47 turned out to be best to deplete 50 μl of CSF-extract. As controls, egg extracts were mock-depleted using corresponding amounts of unspecific rabbit IgG (Fig. 11). Using anti-Ufd1-1 for two rounds of depletion, the amount of Ufd1 could be reduced by roughly 90% (Fig. 11A). At the same time at least 95% of the Ufd1-binding Npl4 were co-depleted indicating that Ufd1 is present in slight excess over Npl4 in LSX. With anti-Npl4-1 antibodies, estimated 99% of Npl4 and 90% of Ufd1 were removed from the extract (Fig. 11B). However, the most complete depletion of >95% and >99% for Ufd1 and Npl4, respectively, was achieved by a combination of both antibodies (Fig. 11C), performed with 15 μg anti-Ufd1-1 in the first and 20 μg anti-Npl4-1 in the second round. Similarly, reduction of p47 was estimated to be 99% complete (Fig. 11D). Although p97 co-

immunoprecipitated with Ufd1 and p47, the overall p97 levels remained unchanged in all depletions due to the vast excess of p97 over its adaptors. Anti-p97 immunoblots therefore served as loading controls for the documentation of immunodepletion experiments. Importantly, all depletions were compatible with the CSF-arrest of the extract as revealed by the fact that added sperm chromatin stayed condensed (data not shown). Thus, removal of p97's essential adaptors constitutes an efficient tool to interfere with its function in mitotic extract.
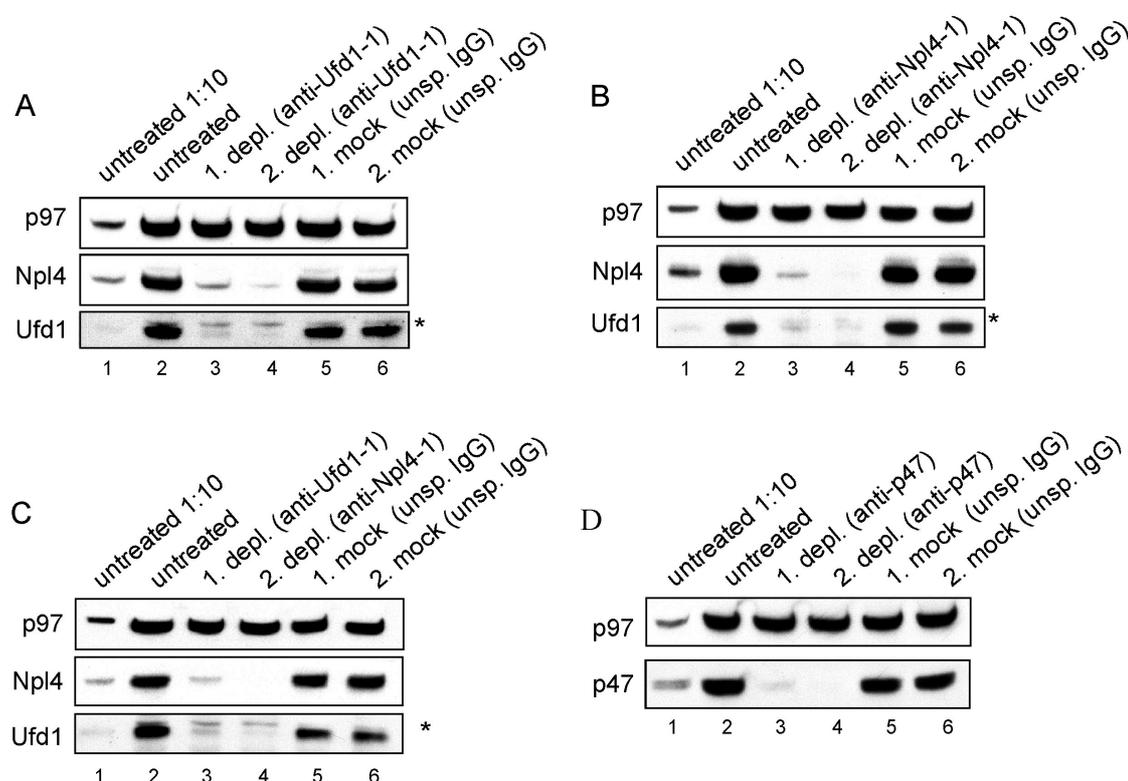
Fig. 11: Immunodepletion efficiently removes p97 adaptors from mitotic *Xenopus* egg extracts. CSF-extracts were immunodepleted in two rounds with anti-Ufd1-1 (**A**, lanes 3 and 4), anti-Npl4-1 (**B**, lanes 3 and 4), anti-Ufd1-1 plus anti-Npl4-1 (**C**, lanes 3 and 4), anti-p47 (**D**, lanes 3 and 4), or unspecific IgG (lanes 5 and 6 in all panels). Aliquots were taken after the 1st and after the final depletion and immunoblotted for p97, Ufd1, Npl4 and/or p47 as indicated. Equivalent amounts of untreated extract (lane 2 in all panels) and 1/10th thereof (lane 1 in all panels) served as controls. Star denotes unspecific band.

3.1.1.4 Generation of dominant-negative p97 mutants

Apart from depletion of p97 or adaptors, a dominant-negative mutant of murine p97 has been described to successfully interfere with its function in astrocytoma cell lysates (Ye et al., 2001). This dominant-negative mutant is able to bind substrates but – due to its ATPase-deficiency – is unable to release them. Suppression of p97 function was therefore achieved by simply adding the p97 mutant to lysates, leading to sequestration of substrates.

To obtain a second, independent tool for interference with p97 function in *Xenopus* extract, the analogous dominant-negative version of *Xenopus* p97 was generated by changing the conserved glutamates residues 305 in D1 and 578 in D2 to glutamines. Inactivation of the AAA-domains was confirmed by comparing the ATPase activities of the resulting QQ-mutant with wild type (wt) p97 in a malachite green assay which measures the enzymatic release of free phosphate from added ATP (Fig. 12). Although p97 contains two AAA domains, D1 and D2, several studies indicate that in the p97 hexamer, the D2 ring is responsible for catalytic activity and that the D1 ring rather functions to stabilize the quarternary structure (DeLaBarrre and Brunger, 2003; Wang et al., 2003; Song et al., 2003). Conceivably, the E305Q mutation in the D1 domain might disfavour association of p97 subunits thereby weakening the dominant-negative effect *in vivo*. Although Wang et al. (2003) have shown that the E305Q mutation does not affect hexamer formation in dissociation-reassembly assays, versions of *Xenopus* p97 with an intact D1 but inactivated D2 domain were also generated by replacing only lysine 524 with alanine (Kitami et al., 2006) and/or glutamate 578 with glutamine. Again, ATPase activities were tested and proven to be greatly diminished or eliminated (Fig. 12). Finally, p97 mutants from other species were also produced to exclude that deviations from the sequence of *Xenopus* p97 might enhance their dominant-negative character in extract. Towards this end, human p97-QQ was generated and the original clones of murine p97-wt and QQ were requested, which had been also used by Cao and colleagues. Again, all these dominant-negative mutants were not only sequenced but also confirmed by measuring their ATPase activity in a malachite green assay (Fig. 12).
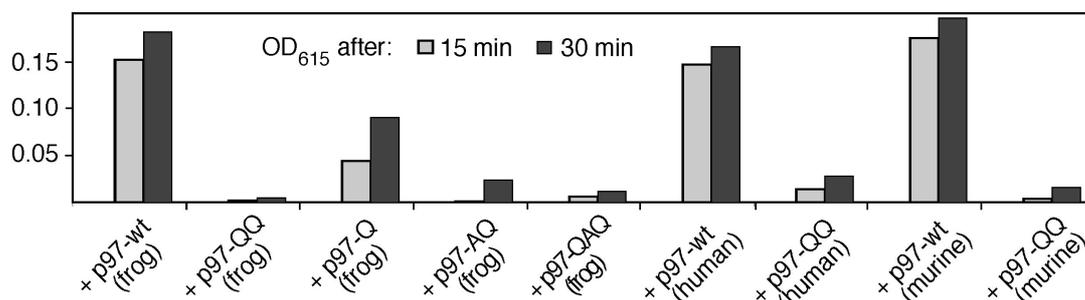
Fig. 12: Malachite green ATPase assay of wt p97 and dominant-negative p97 mutants. Malachite green assays were performed as described in Materials and Methods. Extinction of aliquots taken after 0, 15 and 30 min were measured and the 0 min-values substracted from corresponding 15 and 30 min- values.

In summary, various dominant-negative p97 mutants were generated and confirmed as being ATPase defective. In contrast to adaptor depletion, which specifically inactivates either p97-Ufd1-Npl4 or p97-p47, this approach allows a general inactivation of p97 in extract independent of a distinct adaptor.

3.1.2 p97 is not required for spindle disassembly at the end of mitosis

As discussed in the introduction, the function of p97 has been mainly investigated outside mitosis. In all its diverse functions, p97 seems to act as a "segregase" that selectively extracts ubiquitylated subunits out of their environment, i.e. membranes, or protein complexes. Several mitotic regulators are bound to stable partner proteins and dissociated/degraded in a ubiquitin-dependent manner. Additonal hints on mitotic functions of p97 had emerged with reports of a genetic interaction of separase and securin with this AAA-ATPase in fission yeast (Yuasa et al., 2004; Ikai and Yanagida, 2006) and a proposed role for p97 in spindle disassembly in budding yeast and *Xenopus* (Cao et al., 2003).

3.1.2.1 p97-Ufd1-Npl4 interacts with tubulin

Fitting to a role of p97 in spindle disassembly, an interesting discovery was made during establishment of p97 depletion from extract. Tubulin co-precipitated with UT6 (Fig. 13). To confirm the interaction of tubulin with p97-Ufd1-Npl4, an immunoprecipitation using anti-Npl4-2 was performed. Indeed, tubulin was found to co-precipiate with Npl4 and p97.
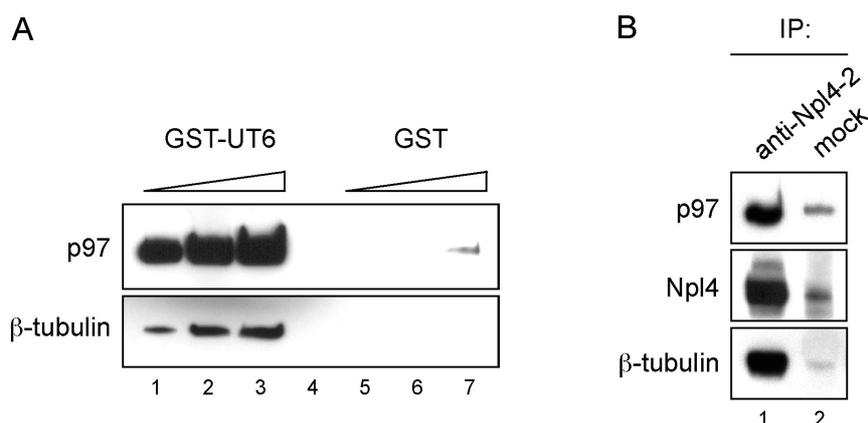
Fig. 13: Tubulin interacts with p97-Ufd1-Npl4. (A) GST-UT6 or GST coupled to glutathione sepharose was incubated in high-speed extract, re-isolated and analyzed by immunoblotting. 2.5, 5 and 7.5 μl of GST-UT6 (lanes 1-3) or GST (lanes 5-7) beads were examined. Equal loading of beads with GST-UT6 or GST was confirmed by coomassie staining (data not shown). Lane 4 is empty. **(B)** Anti-Npl4-2 or unspecific rabbit IgG were bound to protein G sepharose, incubated in high-speed extract and beads were analyzed by immunoblotting after re-isolation. Equal loading was confirmed by Ponceau staining (data not shown).

Being encouraged by the discovery of tubulin interacting with p97-Ufd1-Npl4, the experiments of Cao et al. (2003) were first revisited with the aim to use spindle disassembly as an activity assay for p97. These researchers had reported that immunodepletion of p97 or addition of dominant-negative murine p97-QQ completely blocked spindle disassembly but not inactivation of Cdk1 in *Xenopus* extracts.

3.1.2.2 Depletion of p97 adaptors has no effect on spindle disassembly

Ufd1 was depleted from CSF-extract that was then supplemented with sperm nuclei and rhodamine-labeled tubulin and incubated for 30 min at 20°C to allow for assembly of MT-asters (which occasionally fused into bipolar spindle-like structures). Mitotic exit was then triggered by addition of Ca^{2+} and the state of the MT-cytoskeleton was monitored by fluorescence microscopy over a period of 60 min. Using the same assay, Cao et al. had reported that spindle disassembly was completely blocked in Ufd1-depleted extract for up to 80 min despite normal inactivation of Cdk1 (Cao et al., 2003). But when this experiment was repeated, spindle disassembly occurred normally within 40 min after Ca^{2+} addition (Tab. 1) despite the fact that Ufd1-Npl4 had been efficiently removed (Fig. 11).

CSF extract	tested concentrations (final; mg/ml)	- Ca^{2+}	+ Ca^{2+}
ΔNpl4	---	+	+
ΔUfd1	---	+	+
ΔNpl4/ΔUfd1	---	+	+
ΔNpl4/ΔUfd1 + anti-Ufd1	0.25	+	+
ΔNpl4/ΔUfd1 + anti-Npl4	0.25	+	+
Δp47	---	+	+
+ CyclinB1Δ90	0.03	+	-

Tab. 1: Neither p97-Ufd1-Npl4 nor p97-p47 is required for spindle disassembly at the end of mitosis. CSF-extracts were depleted (Δ) with either anti-Ufd1-1 or anti-Npl4-1 alone, with a combination of anti-Ufd1-1 and anti-Npl4-1, or anti-p47 alone and, where indicated, additionally supplemented with antibodies against Ufd1 or Npl4 to final concentrations of 0.25 μg/μl (+ anti-Ufd1/+ anti-Npl4). CSF-extract supplemented with stable human cyclinB1 served as control. Sperm-induced spindles were allowed to form for 30 min at 20°C. Then, rhodamine-labelled MTs and DAPI-stained sperm chromatin were examined right before and 60 min after triggering release into interphase by Ca^{2+}. Scale bars correspond to 10 μm.

To clarify this issue, spindle disassembly was additionally assayed in CSF-extracts depleted by use of anti-Npl4-1 or a combination of anti-Ufd1-1 and anti-Npl4-1. Furthermore, extracts which had been depleted of >95% and >99% of Ufd1 and Npl4, were supplemented with soluble anti-Ufd1-1 or anti-Npl4-1 to 0.25 μg/μl, respectively, before triggering mitotic exit. As these antibodies were generated against full-length proteins, their presence likely interferes with function of residual trace amounts of Ufd1-Npl4. However, in no case any impairment of spindle disassembly was observed (Tab. 1). Finally, the effect of depleting p47, the adaptor known to be involved in p97-mediated membrane fusions, was checked. Again, about 40 min after Ca^{2+} addition all spindles had disappeared irrespective of the presence or absence of p47 (Tab. 1). As a positive control for block of spindle disassembly, a non-degradable version of cyclin B1 (cyclin B1Δ90) was added to CSF-extract prior to Ca^{2+} addition. This regulatory subunit of Cdk1 blocks exit from mitosis by maintaining a constitutively high activity of this crucial mitotic kinase. Consistently, MT-asters persisted

despite successful inactivation of CSF as judged by APC/C-dependent degradation of securin (Tab. 1 and data not shown). This experiment shows that MT-asters do not depolymerize independent of mitotic exit and simply due to prolonged incubation. Thus, neither p97-Ufd1-Npl4 nor p97-p47 are necessary to bring about the transition from mitotic spindles into interphase MT-arrays in *Xenopus* egg extracts.

3.1.2.3 Dominant-negative p97 mutants do not interfere with spindle disassembly

Apart from Ufd1-depleted extracts, Cao et al. also reported block of spindle disassembly in extracts supplemented with dominant-negative p97-QQ at final concentrations of 0.5 to 0.6 mg/ml. To check whether this part of their observations was reproducible, CSF-extract was pre-incubated for 30 min at 4°C with reference buffer, wild type or dominant-negative version of recombinant *Xenopus* p97 at 0.5 mg/ml. Spindle disassembly was assayed as before and, remarkably, was again normal in all samples, i.e. all astral structures disappeared within 40 min (Tab. 2). Spindles disassembled on schedule even when the final concentration of p97-QQ was raised up to 2 mg/ml or when pre-incubation of the extract with the dominant-negative mutant was extended to 60 min (Tab. 2 and data not shown). Furthermore, the effect of additional dominant-negative p97 variants on spindle disassembly was tested. *Xenopus* mutants with intact D1 domain and/or additional mutation in D2, namely p97-Q, p97-AQ and p97-QAQ, were checked in various final concentrations, but none had any effect on spindle disassembly (Tab. 2). Similarly, even at final concentrations of up to 5 mg/ml, there was no effect on spindle disassembly upon addition of the same murine p97-QQ used by Zheng and co-workers, or human p97-QQ (Tab. 2).
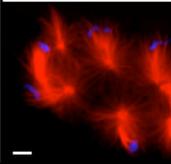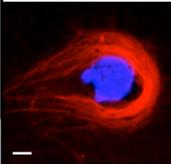
CSF extract	tested concentrations (final; mg/ml)	- Ca^{2+}	+ Ca^{2+}
---	---	+	+
+ p97-wt (frog)	0.5, 2, 4	+	+
+ p97-E305,578Q (frog)	0.5, 1, 2	+	+
+ p97-E578Q (frog)	0.5, 1	+	+
+ p97-E578Q,K524A (frog)	0.5, 1, 2	+	+
+ p97-E305,578Q, K524A (frog)	0.5, 1, 2	+	+
+ p97-E305,578Q (human)	0.5, 5	+	+
+ p97-wt (murine)	0.25, 0.5, 1, 5	+	+
+ p97-E305,578Q (murine)	0.25, 0.5, 1, 5	+	+

Tab. 2: Dominant-negative versions of p97 do not interfere with spindle disassembly at the end of mitosis.
CSF-extracts were supplemented with wild type or dominant-negative mutants of *Xenopus*, murine, or human p97 to various final concentrations as indicated. Sperm-induced spindles were allowed to form for 30 min at 20°C. Rhodamine-labelled MTs and DAPI-stained sperm chromatin were examined right before and 60 min after triggering release into interphase by Ca^{2+}. Scale bars correspond to 10 μm.

In summary, experiments using a multitude of dominant-negative mutants at up to 10-fold higher concentrations than used by Cao and co-workers indicated that p97 might be dispensable for spindle disassembly in *Xenopus* egg extracts.

3.1.2.4 Establishment of ERAD in *Xenopus* egg extract

The absence of any phenotype upon addition of dominant-negative p97 mutants could either mean that p97 plays indeed no role in spindle disassembly or that the dominant-negative approach is not suitable to interfere with p97 function in the *Xenopus* system. To exclude the latter possibility, there was a need for a positive control. Towards this end, ERAD was established in extract, since p97 has a well characterized role in this process. As substrate, an unstable mutant (ΔF508) of the human c̲ystic f̲ibrosis t̲ransmembrane conductance r̲egulator (CFTR) was chosen since it is degraded via ERAD in yeast and mammalian cell culture (Zhang et al., 2001; Varga et al., 2004; Okiyoneda et al., 2004; Weihl et al., 2006). As egg extracts do not exhibt transcription but actively support translation, CFTRΔF508-encoding mRNA was added to extracts. This gave rise to anti-CFTR-reactive proteins with apparent molecular weights of 140 and 160 kDa. As these bands represent fully and partially glycosylated CFTRΔF508 they were likely inserted properly into ER membranes which are abundant in low-speed extract (Fig. 14A). In contrast, standard rabbit reticulocyte lysates did not give corresponding signals, since they are lacking ER membranes (Fig. 14A). Next, steady-state levels of CFTRΔF508 were monitored in extract in the presence or absence of p97-QQ. Even at 0.25 mg/ml, which corresponds to the level of endogenous p97, the QQ-mutant greatly impaired ERAD, as judged by a 2.7-fold elevated level of CFTRΔF508 after 3 hours (Fig. 14B). The disappearance of CFTRΔF508 was also followed in a cycloheximide shut-off experiment. In control extract, roughly 90% of the ERAD substrate were degraded with a half-life of approximately 45 min (Fig. 14C). Degradation was, however, heavily impaired in the presence of p97-QQ. The inhibition of ERAD shows that the dominant-negative mutant efficiently interferes with p97 activity in *Xenopus* egg extracts, validating the earlier observation of its lacking effect on spindle disassembly.
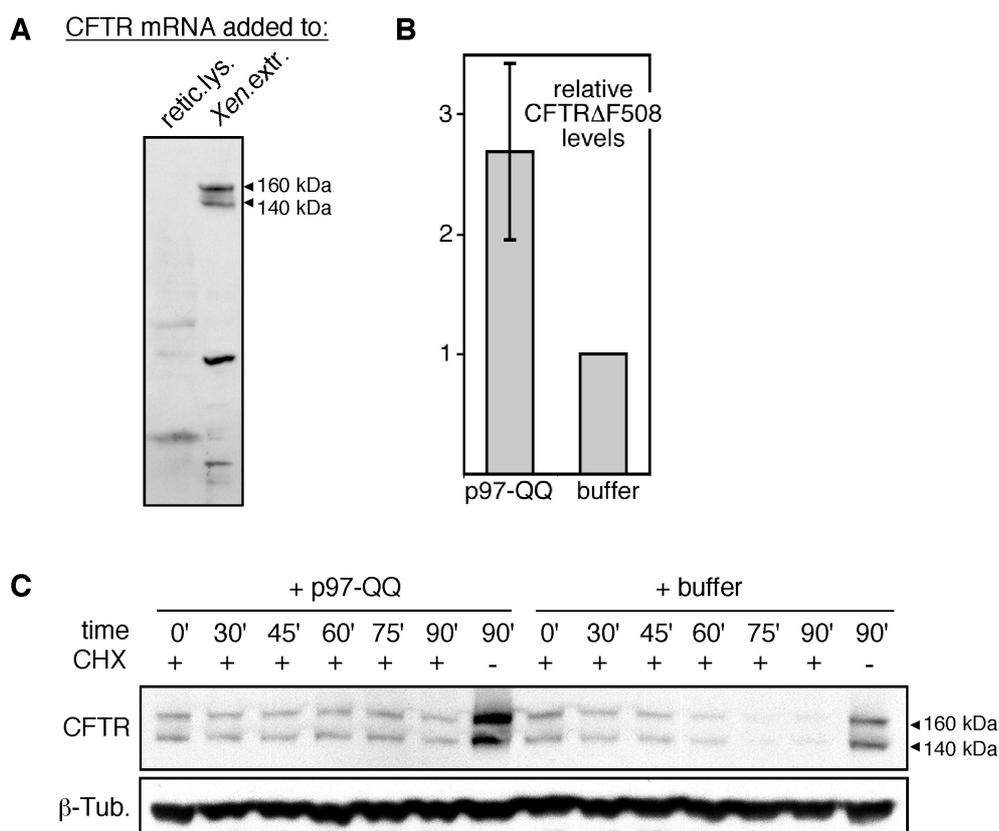
Fig. 14: Block of ERAD by ATPase-deficient mutant verifies dominant-negative effect on p97 function. (A) Translation of CFTRΔF508-mRNA in standard rabbit reticulocyte lysate (90 min at 30°C) or in *Xenopus* low-speed extracts (3h at 20°C) and examination of reaction products by anti-CFTR Western. Arrowheads indicate CFTR-specific bands. All unlabeled bands are unspecific (data not shown). **(B)** Quantification of steady-state levels of CFTRΔF508 in p97-QQ-supplemented extracts relative to buffer-supplemented controls. Egg extracts were incubated with CFTRΔF508-mRNA for 3 hours before determining protein levels by anti-CFTR-Western relative to corresponding ß-tubulin signals. Shown is the mean (+/- SD) of three independent experiments, each with values for the buffer-treated samples set to 1. **(C)** Egg extract was incubated with human CFTRΔF508-mRNA for 90 min at 20°C prior to addition of *Xenopus* p97-QQ (final 1 mg/ml) or reference buffer. Fifteen min later, translation was stopped with cycloheximide. Degradation of CFTRΔF508 was analyzed by anti-CFTR Western 0, 30, 45, 60, 75, 90 min thereafter. Anti-ß-tubulin Western served as loading control.

3.1.2.5 Spindle disassembly is not delayed in the absence of p97 function

Since block of spindle disassembly was never observed in the above experiments, it was checked whether there was at least a detectable delay in the absence of functional p97. For this purpose, kinetics of spindle disassembly were carefully monitored by taking aliquots of the egg extract every 5 min after Ca^{2+} addition and counting chromatin-associated MT-asters after fixation. First, spindle disassembly was compared in extracts supplemented with murine p97-QQ (1 mg/ml), murine p97-wt (1 mg/ml), or buffer. In all extracts, spindles disassembled with virtually identical kinetics (Fig. 15A). Second, extracts first co-depleted of Npl4 and Ufd1 and then supplemented with additional, soluble anti-Npl4-1 (0.25 μg/μl) were analyzed. Comparison with mock-depleted extract supplemented with unspecific IgG or non-depleted extract supplemented with buffer showed again that chromatin-associated, spindle-like structures disappeared with similar kinetics in all cases. In fact, Ufd1-Npl4-depleted extract even displayed a weak but reproducible acceleration of spindle disassembly (Fig. 15B and data not shown). In conclusion, the experiments of this work show unambiguously that interfering with p97 function neither blocks nor delays disassembly of sperm-induced spindles in *Xenopus* egg extracts exiting mitosis.

A

B
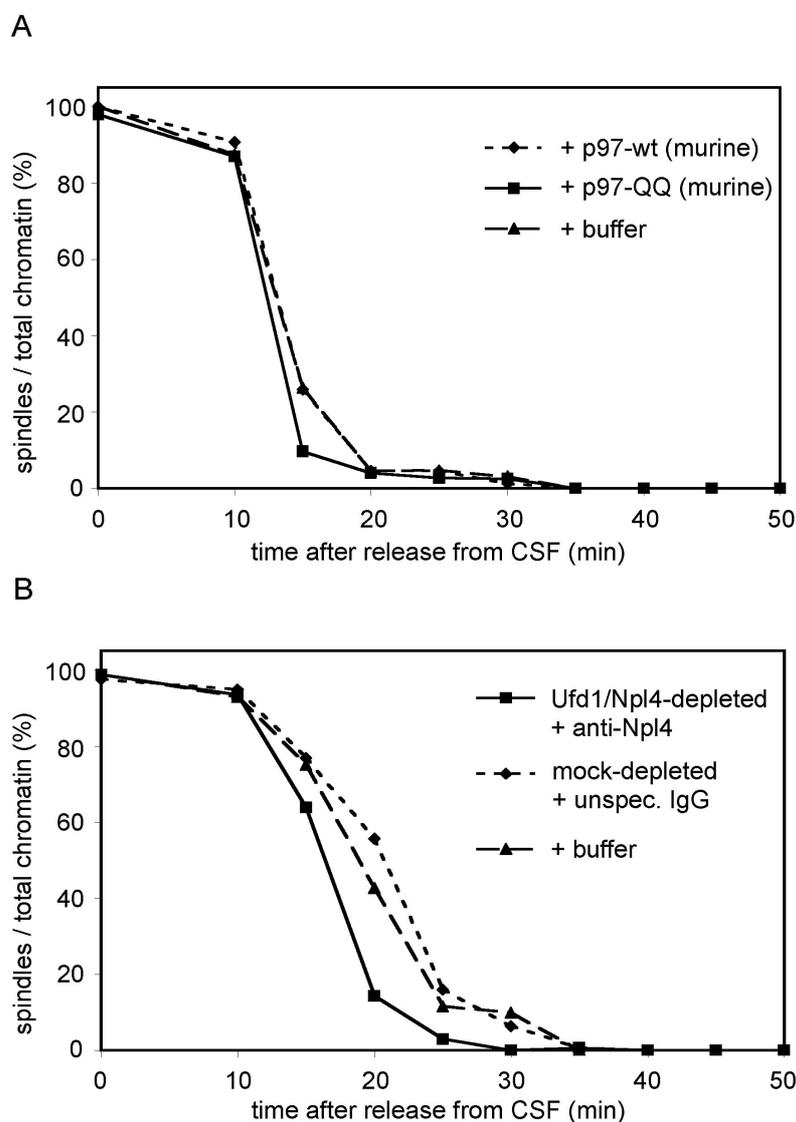
Fig. 15: Spindle disassembly is not delayed in the absence of p97 function. (A) CSF-extracts pre-incubated with murine p97 (wild type or E305,578Q) or buffer were supplemented with rhodamine-tubulin and 500 sperm nuclei per μl. Following Ca^{2+} addition (t = 0 min) kinetics of spindle disassembly were monitored by quantifying every 5 min the percentage of sperm nuclei associated with spindles. **(B)** CSF-extract was depleted of Ufd1-Npl4 and additionally supplemented with soluble anti-Npl4-1 antibody. Mock-depleted extract supplemented with unspecific rabbit IgG or untreated extract supplemented with reference buffer served as controls. Kinetics of spindle disassembly were monitored as in (A).

3.1.2.6 Dispensability of p97 is independent of sperm chromatin

Isolated sperm nuclei contain p97 and its adaptors in low concentrations (Fig. 16).
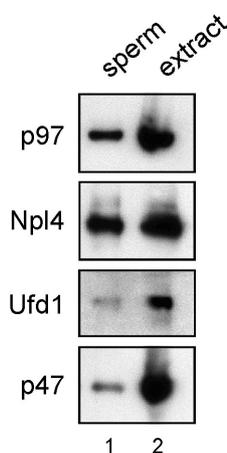
Fig. 16: Amount of p97 and adaptors in *Xenopus* sperm nuclei. 2.5 μl of isolated sperm nuclei (1.3×10^5/μl) were analyzed by immunoblotting with the indicated antibodies. 0.5 μl of extract were loaded as control.

The amounts added back with sperm nuclei to immunodepleted extracts are negligible, however. For Npl4, which - relative to extract - exhibits the highest concentration (Fig. 16), an estimated 0.036% is replenished by addition of 2000 sperm nuclei to 1 μl of depleted extract. Nevertheless, to fully exclude any influence of added chromatin on MT dynamics, formation of MT-asters was triggered by adding to mitotic extract purified centrosomes instead of sperm nuclei. Disappearance of these structures was then compared between extracts supplemented with *Xenopus* p97-QQ, p97-wt (both at 1 mg/ml), or reference buffer. As before, all samples were indistinguishable in the way spindle-like structures were replaced by interphase MT-arrays (Fig. 17A). Similarly, no difference in disassembly of centrosome-generated spindles was detected in Ufd1-Npl4-depleted versus mock-depleted extracts (Fig. 17B). Successful removal of Ufd1-Npl4 from the extract was confirmed by immunoblotting (Fig. 17C). Interestingly, a slightly accelerated disappearance of asters in Ufd1-Npl4- versus mock-depleted extract was again observed (data not shown).
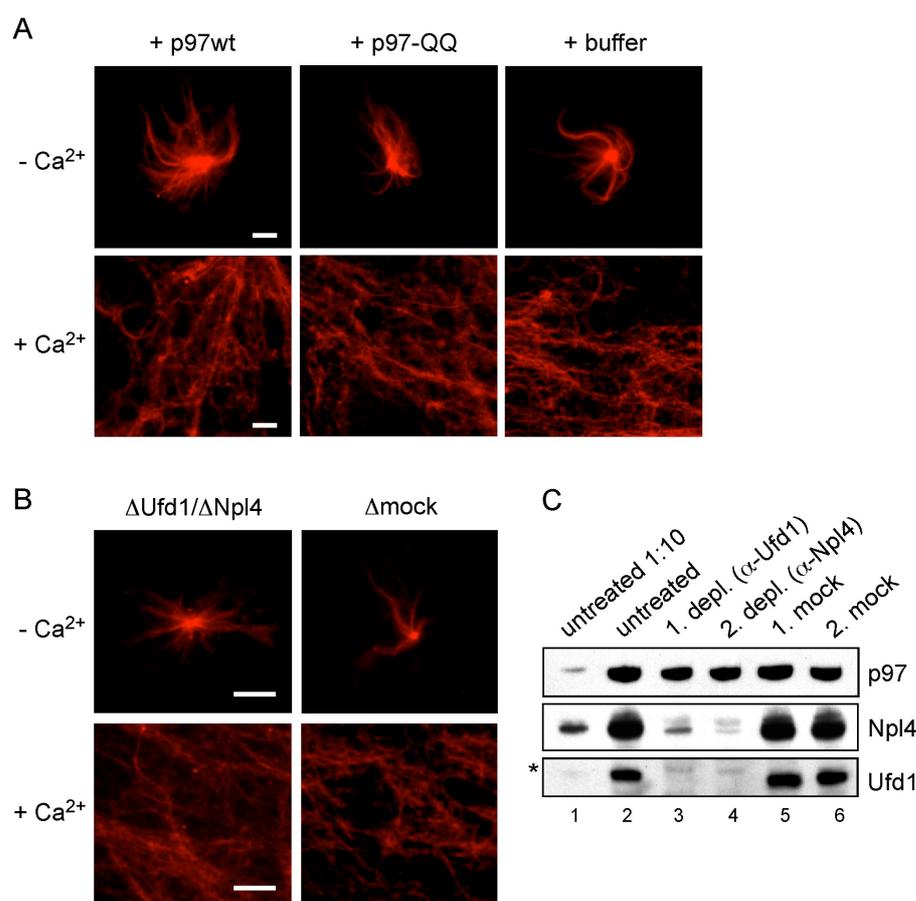
Fig. 17: Spindles induced by centrosomes instead of sperm nuclei disassemble normally in the absence of p97 function

(A) CSF-extract was pre-treated with murine p97-wt, murine p97-QQ, or reference buffer. 30 min after addition of purified human centrosomes, mitotic exit was triggered at 25°C by Ca^{2+}. Centrosome-induced, rhodamine-labelled asters were visualized right before and 60 min after release into interphase. Note that the pictures in the lower panel are overexposed relative to the upper images. Scale bars correspond to 10 μm. **(B)** CSF-extract was Ufd1-Npl4- or mock-depleted. Thereafter, extracts were combined with centrosomes to induce aster formation, released into interphase and analyzed as in (A). Scale bars correspond to 10 μm. **(C)** Verification of efficient removal of Ufd1-Npl4 in the experiment shown in (B). CSF-extracts were immunodepleted in two rounds with anti-Ufd1-1 and anti-Npl4-1 (lanes 3 and 4) or unspecific IgG (lanes 5 and 6). Equivalent amounts of untreated extract (lane 2) and 1/10th thereof (lane 1) served as controls. Star denotes unspecific band.

In conclusion, irrespective of whether their formation has been triggered by chromatin or centrosomes, MT-asters disassemble normally when *Xenopus* egg extracts leave mitosis in the absence of p97 function.

3.1.3 p97 and separase activation and stability

3.1.3.1 p97 is not required for securin degradation in *Xenopus*

Late mitotic transitions are chiefly controlled by the timely ubiquitylation of key proteins mediated by the E3 ligase APC/C. Ubiquitylated target proteins are dissociated from their stable binding partner(s) and subsequently degraded. It is still unclear whether additional factors assist the proteasome in "extracting" APC/C substrates from their environment. Among the many substrates of the APC/C is the anaphase inhibitor securin whose destruction leads to activation of separase (Uhlmann et al., 2000; Stemmann et al., 2001). Interestingly, Cut1/separase, Cut2/securin, and Cdc48/p97 show strong genetic interaction in *S. pombe* (Yuasa et al., 2004). Even more so, using a newly isolated *cdc48* mutant strain Yanagida and co-workers recently reported that Cut1/separase was degraded along with Cut2/securin in anaphase upon inactivation of Cdc48/p97 (Ikai and Yanagida, 2006). Therefore, an attractive hypothesis is that p97 assists in dissociating separase and securin in anaphase. To investigate whether such a connection exists in higher eukaryotes, the *Xenopus* system was used to examine if p97 was required for securin degradation, separase activation and/or separase stability in vertebrate anaphase.

Towards this end, the following experiments were performed: 293T cells were transiently transfected with expression constructs for human separase and securin. After nocodazole arrest, separase/securin complexes were isolated by chromatography on S-cation exchange columns and added to lowΔ90-extract. Active APC/C^{Cdc20} in this extract leads to securin degradation and activation of separase (Stemmann, 2001). Separase activity can be detected *in vitro* by cleavage of the cohesin subunit Scc1 which is added as ^{35}S-labelled IVT product. To check if p97 was involved in separase activation, human separase/securin complexes were incubated in lowΔ90-extracts that were either supplemented with p97-QQ or buffer and additionally with ^{35}S-Scc1. To monitor separase and securin levels, aliquots were taken every 10 to 30 min and subjected to immunoblotting (Fig. 18). The experiment showed that p97 was not required for securin degradation in *Xenopus* egg extract since securin was degraded equally well in the absence or presence of p97-QQ (Fig. 18A lower panel).
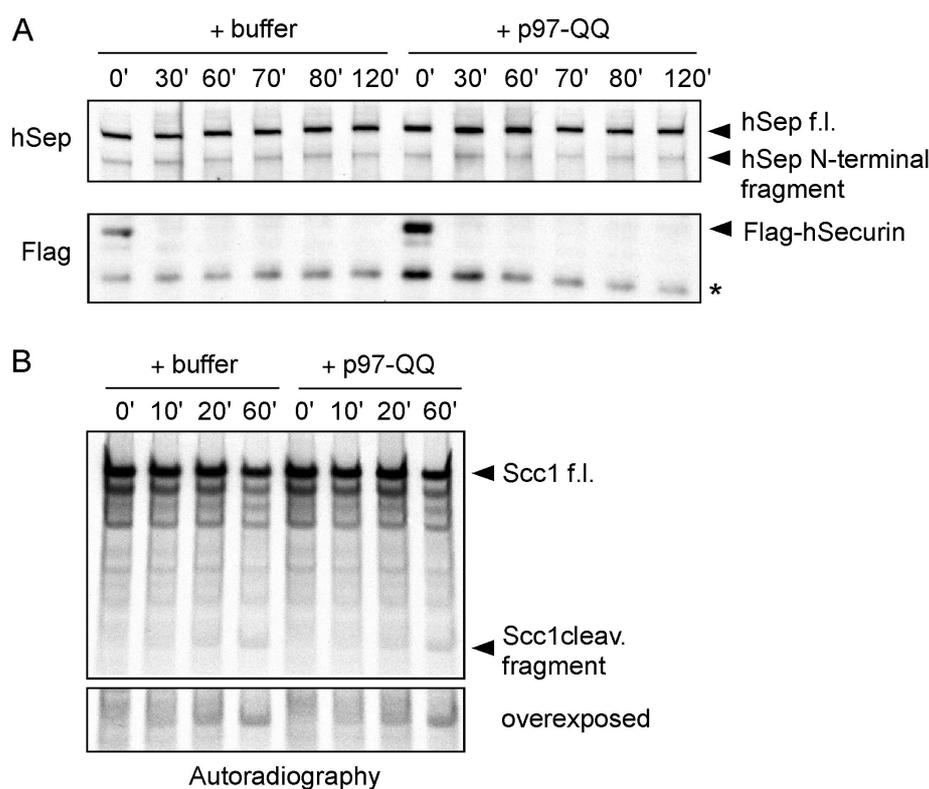
Fig. 18: Securin degradation, separase activation and separase stability in *Xenopus* egg extract is unaffected by addition of p97-QQ. **(A)** Human separase/securin complexes isolated from transfected 293T cells were added to lowΔ90-extract supplemented with buffer or p97-QQ at 2 mg/ml final. Separase and securin levels were monitored by immunoblotting of aliquots taken over time. **(B)** In-extract Scc1 cleavage assay. ^{35}S-Scc1 was added to extract at 0 min corresponding to time point 60 min in (A). Aliquots were taken 10, 20 and 60 min thereafter and analyzed by autoradiography.

This result was confirmed by additional experiments where closer time points were taken after Ca^{2+} release but nontheless no difference in securin degradation rates with or without p97 function was observed (data not shown). Separase levels remained constant in the presence of p97-QQ (Fig. 18A, upper panel) indicating that p97 function is not required for separase stability under these conditions. Furthermore, separase was activated normally in the presence of p97-QQ, i.e. Scc1 was cleaved with the same efficiency as in control extract (Fig. 18B). Thus, p97 function is dispensable for separase activation in *Xenopus* egg extracts. It should be stressed that cleavage of added human Scc1 by endogenous *Xenopus* separase has never been observed (data not shown; O. Stemmann, personal communication), which is why the observed Scc1 fragments have to be caused by the weak activity of the human separase added in trans. (The in-extract cleavage assay gives weak signals because of the 1:10 dilution of

the ^{35}S-Scc1 substrate into the extract and the limited amount of the highly concentrated egg extract that can be loaded onto SDS-PAGE gels.)

To confirm these results the requirement of p97 for separase activation was tested in a different experimental setup. To this end, human ZZ-Tev$_4$-separase/securin complexes were isolated from transfected 293T cells using IgG-beads that bind to the ZZ-tag (IgG binding domain of protein A) of separase. ZZ-separase/securin complexes bound to beads were then incubated in lowΔ90-extract to allow degradation of securin. Subsequently, beads were re-isolated from extracts and put into an Scc1 cleavage assay. To test the requirement of p97 for separase activation in this assay, mock-depleted extracts were compared with extracts from which Ufd1-Npl4 had been removed using anti-Npl4-1. Scc1 cleavage occured with similar efficiency irrespective of whether separase/securin-beads had been re-isolated from Ufd1-Npl4-less or mock-depleted extract (Fig. 19).
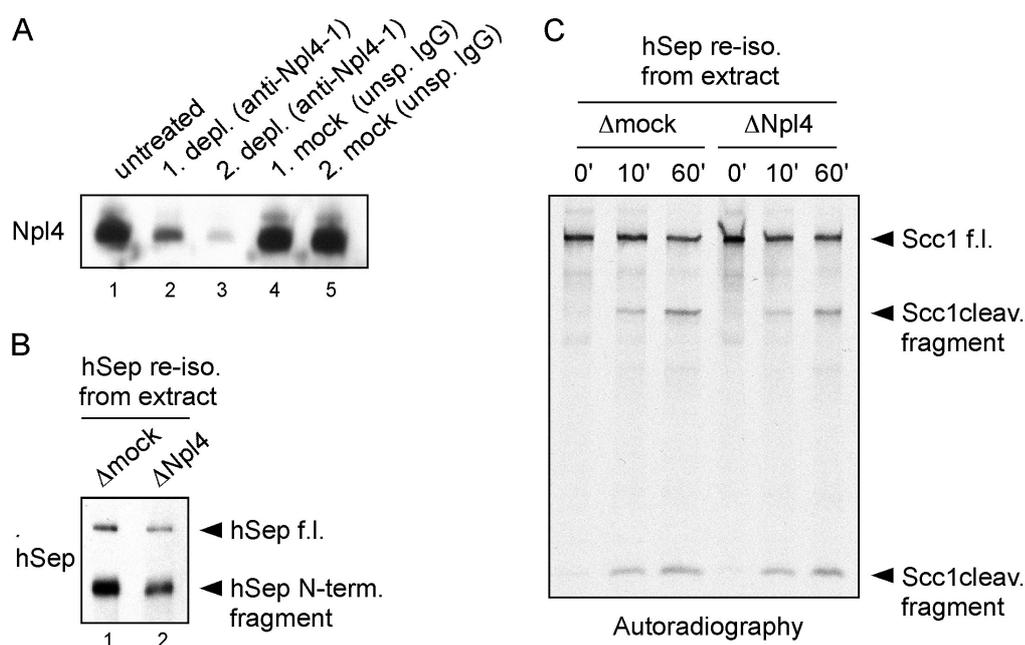
Fig. 19: p97-Ufd1-Npl4 is dispensable for separase activation in *Xenopus*. **(A)** Immunoblot confirming depletion of Npl4 from lowΔ90-extract. Aliquots were taken before (lane 1) and after the first and second depletion (lane 2 and 3) or mock-depletion (lane 4 and 5). Equal loading was checked by Ponceau staining (data not shown). **(B)** IgG-beads loaded with human ZZ-Tev$_4$-separase and re-isolated from extracts of (A) were analyzed by immunoblotting. **(C)** Separase eluted from beads after extract incubation was put into an Scc1 cleavage assay and Scc1-cleavage fragments were detected by autoradiography.

To further validate the dispensability of p97 for separase activation, the same experiment was repeated with the alteration that p47 instead of Ufd1-Npl4 was depleted (Fig. 20).
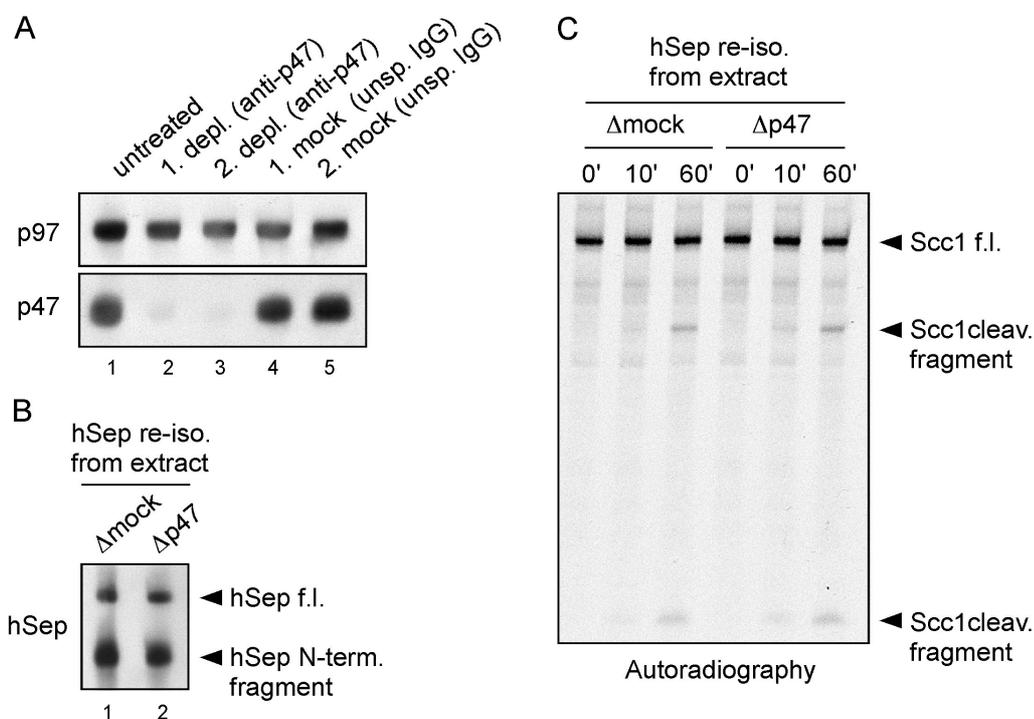
Fig. 20: p97-p47 is dispensable for separase activation in *Xenopus*. (A) Immunoblot confirming depletion of p47 from lowΔ90-extract. Aliquots were taken before (lane 1) and after the first and second depletion (lane 2 and 3) or mock-depletion (lane 4 and 5). p97 immunoblot served as loading control. (B) IgG-beads loaded with ZZ-Tev$_4$-separase and re-isolated from extracts of (A) were analyzed by immunoblotting. (C) Separase eluted from beads after extrac incubation was put into an Scc1 cleavage assay and Scc1-cleavage fragments were detected by autoradiography.

Again, Scc1 was cleaved by separase from both extracts with equal efficiency. Thus, using different approaches and experimental setups, it could be unambigiously demonstrated that p97-mediated dissociation of securin does either not occur at all or is at least dispensable for activation and stability of separase.

3.1.3.2 p97 does not act as a chaperone for vertebrate separase

Although these results argued against a connection between p97 and separase in vertebrates, an additional study was performed to ask whether p97 might be needed as a chaperone for proper folding of separase. Separase is a giant protease that might well need the assistance of chaperones during translation to

adopt its native state. Along this line, securin has been proposed to act as a chaperone since separase levels are reduced in its absence (Jallepalli et al, 2001; Pfleghaar et al., 2005). p97 might also function as such a chaperone although it has been attributed to unfolding rather than folding activity. This model would provide an explanation for the genetic link between p97 and separase in fission yeast. A function of p97 as a chaperone for separase might have been overlooked in the above experiments since p97 function was suppressed only after separase had been fully translated and thus folded. Therefore, the following experiment was conducted: A 7 kB mRNA of Myc_6-Tev_2-tagged human separase was generated *in vitro* and added to CSF-extract supplemented with p97-QQ. Translation of separase in the absence of functional p97 was allowed by incubation for 75 min. Subsequently, CSF-extracts were released into anaphase by addition of Ca^{2+} in the presence of cyclin B1Δ90 preventing mitotic exit. Immunoblotting showed that the overall separase levels were slightly reduced when p97-QQ was present during translation (Fig. 21A, compare lanes 3-6 with 9-12 in) However, impaired translation in the presence of p97-QQ was also observed for other mRNAs, e.g. CFTRΔF508 (data not shown), implying that this is a general effect of p97-QQ on translation. Consistent with the previous results (Fig. 18), there was again no sign of separase degradation upon release of the extract from CSF-arrest into anaphase. Due to the low amounts of separase obtained from translated mRNA, separase activity in the less sensitive Scc1 cleavage assay could not be detected in any of the samples even after affinity isolation of separase from the extracts (data not shown). However, as judged by the appearance of self-cleavage bands 90 min after release (Fig. 21A, lanes 4,6, 10 and 12), separase was partly activated in anaphase extracts and this activation was not affected by dominant-negative p97. The use of self-cleavage as a read-out for separase activity was possible because – as for Scc1 cleavage – endogenous *Xenopus* separase does not cleave added human separase in trans (data not shown; O. Stemmann, personal communication). Specificity of separase fragments was confirmed by immunoblotting with two different antibodies, anti-Myc and anti-Sep-N, both detecting full-length separase and the N-terminal separase cleavage fragment that appeared 90 min after release. Samples supplemented with buffer instead of mRNA served as negative controls (Fig. 21A, lanes 1, 2, 7 and 8).
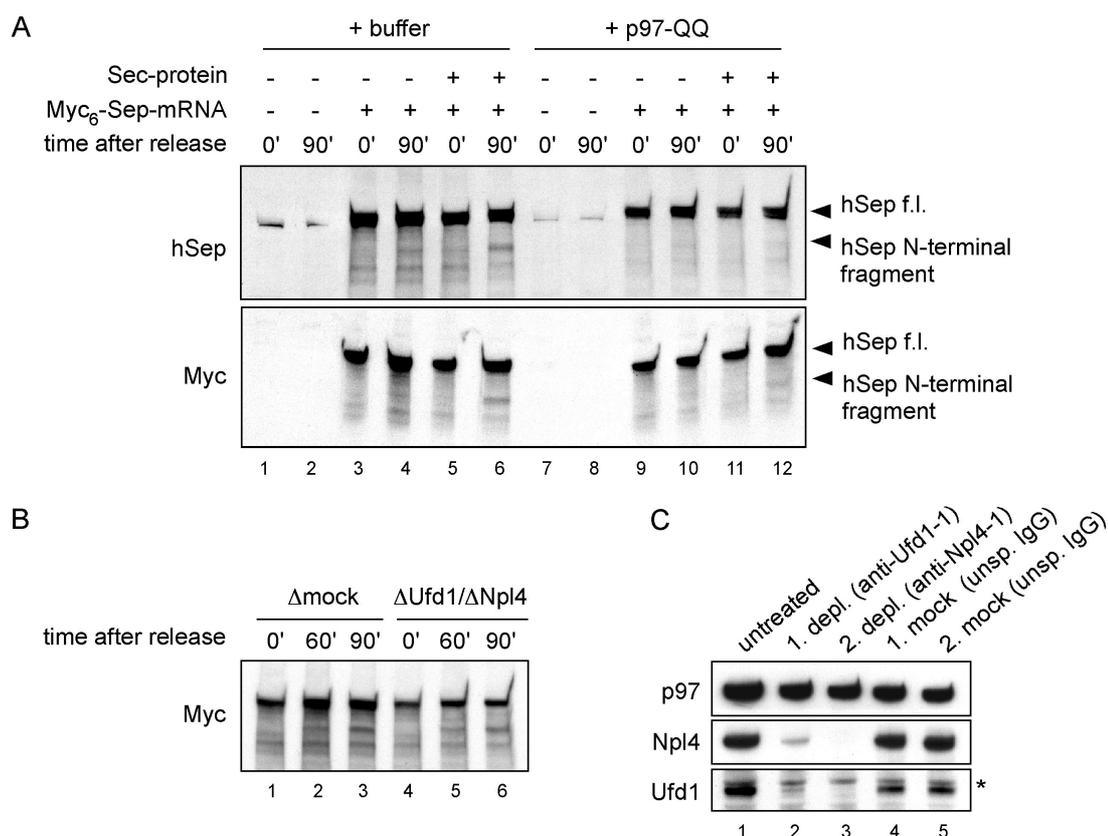
Fig. 21: p97 is not necessary for proper folding of separase. **(A)** CSF-extracts were supplemented with mRNA encoding human Myc$_6$-Tev$_2$-separase and with human securin, p97-QQ or buffer as indicated. After incubation for 75 min at RT, extracts were released by addition of Ca^{2+} (t = 0min) in the presence of cyclin B1Δ90 and incubated for another 90 min. Aliquots of 0 and 90 min time points were analyzed by immunoblotting with anti-SepN and anti-Myc antibodies. **(B)** CSF-extracts were depleted from Ufd1-Npl4 or mock-depleted, supplemented with mRNA encoding human Myc$_6$-Tev$_2$-separase, with human securin and buffer and processed as in (A). **(C)** Immunoblot confirming successful depletion of Ufd1-Npl4.

In a second experiment p97 function was blocked by depleting Ufd1-Npl4 instead of adding p97-QQ (Fig. 21B and C). Again, while overall separase levels were slightly reduced in samples with blocked p97 function, no specific decrease upon release from CSF could be detected. Furthermore, separase was activated equally well in depleted extracts as compared to control extracts despite efficient removal of Ufd1-Npl4 (Fig. 21C). Together, these experiments clearly demonstrated that p97 is not required as chaperone for separase. Thus, in contrast to the situation in *S. pombe*, no connection between separase and p97 in higher vertebrates could be detected. An explanation for this discrepancy might be that the effects in *S. pombe* are indirect, an idea supported by the fact that Ikai

and Yanagida (2006) were unable to show an interaction between Cut1/separase or Cut2/securin and Cdc48/p97 in *S. pombe.*

As endogenous *Xenopus* securin does not bind to added human separase, the effects of recombinant human securin could also be studied in this experimental setup. As expected, human separase translated in the presence of purified human securin is more active than in its absence as judged by the intensity of the N-terminal cleavage fragment (Fig. 21A, compare lanes 4 and 6, 10 and 12). However, total levels of human separase were almost unaffected by the presence or absence of human securin in extract (Fig. 21A, compare lanes 3, 4 with 5, 6 and lanes 9, 10 with 11, 12) – a result that contrasts with the situation *in vivo* (Fig.27).

3.1.4 p97 and UbcH10-dependent SAC override

3.1.4.1 p97 is dispensable for SAC inactivation

To prevent chromosome missegration, cells remain in metaphase until all chromosomes are aligned at the metaphase plate with proper bipolar attachment of their sister kinetochores to MTs originating from opposite spindle poles. As long as there are un- or misattached kinetochores, the mitotic checkpoint stays active and inhibits the APC/C by sequestering its activating subunit Cdc20 in a complex with the checkpoint proteins Mad2, BubR1 and Bub3 (Sudakin et al., 2001). Only when the checkpoint is silenced, Cdc20 is released and activates the APC/C, thereby leading to anaphase onset. The two ubiquitin-conjugating enzymes (E2s) that communicate with the APC/C are UbcH10 and, to a lesser extent, UbcH5. Addition of recombinant UbcH10 to mitotic extracts obtained from nocodazole-treated human cells leads to checkpoint-override and activation of APC^{Cdc20} (Reddy et al., 2007). This involves ubiquitylation of Cdc20 which triggers disassembly of the mitotic checkpoint complex (MCC) and liberation of Cdc20. As segregation of MCC-Cdc20 is reminiscent of p97-mediated disassembly reactions, it was asked whether p97 might be involved in UbcH10-dependent SAC override. The following questions were addressed: 1) Can surplus of UbcH10 override a mitotic checkpoint also in *Xenopus* egg extracts? 2) If yes, is p97 function required for this checkpoint override?

Early embryonic cell cycles (and hence egg extracts) usually lack SAC. Nevertheless, this surveillance mechanism can be established in egg extracts by

adding sperm nuclei to high density thereby mimicking a chromatin to cytosol ratio of late checkpoint-proficient embryogenesis (Minshull et al., 1994). To determine the required sperm density, nocodazole-containing CSF-extracts were first supplemented with sperm at different final concentrations. Extracts were then released from CSF-arrest by addition of Ca^{2+} and levels of added ^{35}S-securin were monitored over time. A concentration of 5000 sperm/µl was found to be sufficient to activate the checkpoint and keep APC/C inactive as judged by stablization of ^{35}S-securin (Fig. 22 and data not shown). Therefore, all following experiments were performed at this sperm concentration. Next, it was investigated whether checkpoint-override by UbcH10 is possible in the *Xenopus* system. To this end, CSF-extracts with activated checkpoint were additionally supplemented with recombinant human UbcH10 (kind gift from M. Rape) or reference buffer and then combined with Ca^{2+}. At a final concentration of ≥ 0.5 µg/µl, UbcH10 indeed forced *Xenopus* egg extracts into interphase despite the presence of unattached kinetochores at high concentrations (Fig 22). Having successfully established checkpoint activation and its override by UbcH10 in the *Xenopus* system, the requirement of p97 for UbcH10-dependent checkpoint override could finally be investigated. p97 function was disrupted by addition of p97-QQ to CSF-extracts supplemented with sperm, nocodazole and UbcH10 as described above. Supplementations with corresponding buffers served as controls. Upon release, ^{35}S-securin was degraded with identical kinetics in p97-QQ containing extract and respective controls (Fig. 22A, compare lanes 6-10 with lanes 1-5). Thus, p97 is not required for UbcH10-dependent checkpoint override. Furthermore, p97 function seems to be dispensable also for SAC maintaince since addition of p97-QQ alone did not cause a checkpoint override in the absence of UbcH10 (Fig. 22A, lanes 16-20). As an additional measure of checkpoint activity, sperm morphology was assessed 60 min after release. The persistance of condensed chromatin and ^{35}S-securin perfectly correlated, thereby confirming the SAC-mediated arrest of the corresponding extracts (data not shown).

A

B
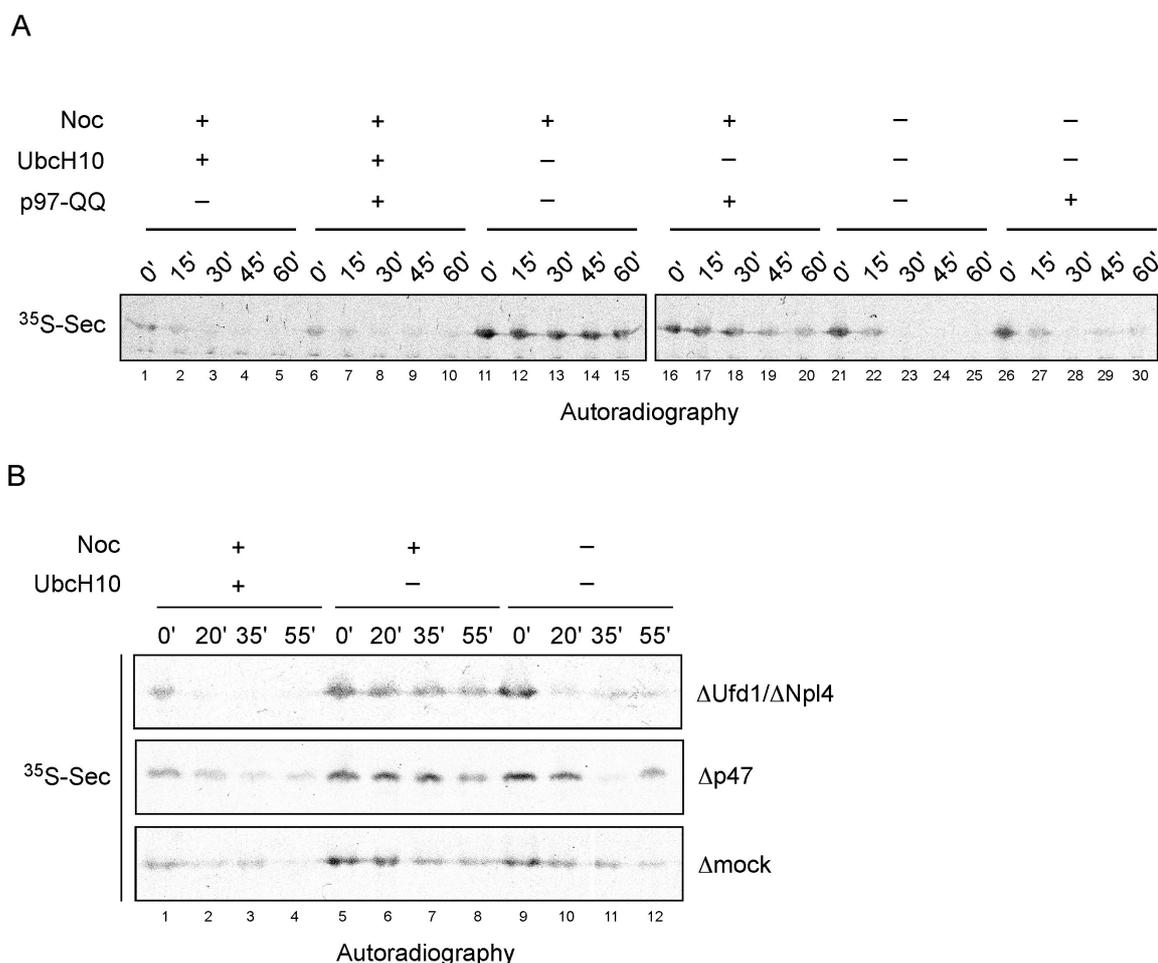
Fig. 22: p97 is dispensable for UbcH10-dependent checkpoint override. **(A)** CSF-extracts were supplemented with *in-vitro* translated ^{35}S-securin (1/20 volume), nocodazole (Noc, 0.01 µg/µl final), UbcH10 (0.5 µg/µl final) and p97-QQ (1 µg/µl final) as indicated, released from CSF by addition of Ca^{2+} (t=0 min) and aliquots taken after 0, 15, 30, 45 and 60 min were analyzed by autoradiography. **(B)** CSF-extracts were depleted with anti-Ufd1-1 and anti-Npl4-1, anti-p47 or unspecific IgG and subsequently supplemented with ^{35}S-securin, nocodazole and UbcH10 (0.5 µg/µl final) as indicated. Extracts were then released and analyzed as in (A). Successful immunodepletions were confirmed by immunoblotting (data not shown).

To validate these observations, p97 function was alternatively blocked by depleting its adaptors Ufd1-Npl4 or p47. Neither Ufd1-Npl4 (Fig. 22B, upper panel) nor p47 (Fig. 22B, middle panel) depletion had any effect on checkpoint override by UbcH10 as judged by degradation of ^{35}S-securin and sperm morphology (Fig. 22B and data not shown).

In conclusion, these experiments revealed that UbcH10-dependent checkpoint override in *Xenopus* occurs independent of p97 function, consistent with results recently obtained by Rape and co-workers in cultured human cells (M. Rape, personal communication).

3.1.4.2 Excess of UbcH10 triggers release from CSF-arrest

During the course of these experiments, an unexpected observation was made: In UbcH10-containing samples the majority of ^{35}S-securin had already been degraded at the time of Ca^{2+} addition (0 min). This was in contrast to controls in which ^{35}S-securin degradation was first detectable only 15 min after Ca^{2+} addition (Fig. 22A, compare lanes 1 and 6 with 11 and 16; Fig. 22B, compare lane 1 with 4 and 9). This raised the question whether UbcH10 not only leads to checkpoint override but also to release from CSF-mediated mitotic arrest. This hypothesis was examined in an additional experiment where ^{35}S-securin degradation was compared between extracts supplemented with either Ca^{2+} or UbcH10 (Fig. 23).
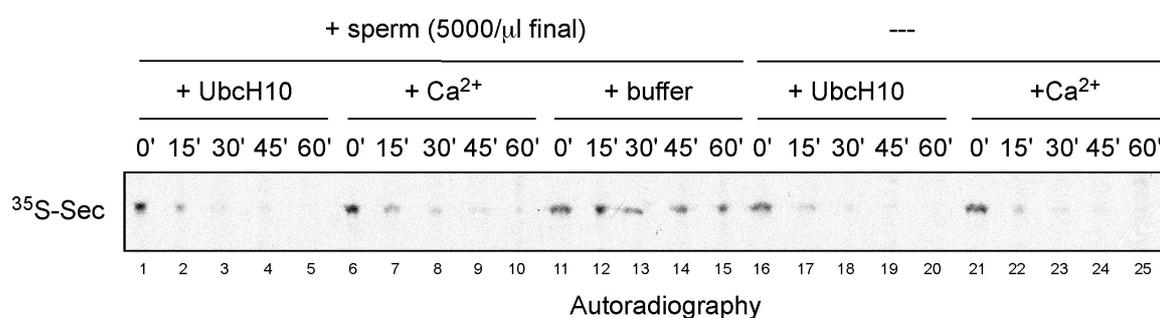
Fig. 23: UbcH10 addition leads to release from CSF arrest. ^{35}S-securin containing CSF-extracts were supplemented with UbcH10, Ca^{2+} or buffer in the presence or absence of sperm. Aliquots taken 0, 15, 30, 45 and 60 min thereafter were analyzed for ^{35}S-securin levels by autoradiography.

Indeed, in both extracts ^{35}S-securin was degraded with similar kinetics and sperm chromatin had formed nuclei after 60 min (Fig. 23 and data not shown). Thus, addition of UbcH10 alone leads to a release from CSF and circumvents any requirement of Ca^{2+} addition. This release was also observed in the absence of sperm (Fig. 23, lanes 16-20), i.e. under conditions when the mitotic checkpoint cannot be activated. UbcH10-mediated release from CSF therefore occurs via a a checkpoint-independent mechanism. Further studies will shed light on how UbcH10 mediates release from CSF and whether this is accompanied by degradation of Xerp1 as in Ca^{2+} triggered release.

3.1.5 p97 assists in sperm decondensation upon fertilization

While establishing depletions of p97 and its adaptors from *Xenopus* extract, not only tubulin (see 3.1.1), but yet another new interactor of p97 was discovered: Nucleoplasmin co-precipitated with the UT6-fragment of Ufd1 (Fig. 24A) and co-immunoprecipitated both with Npl4 (Fig. 24B) and p97 (Fig. 24C) from high-speed extract.
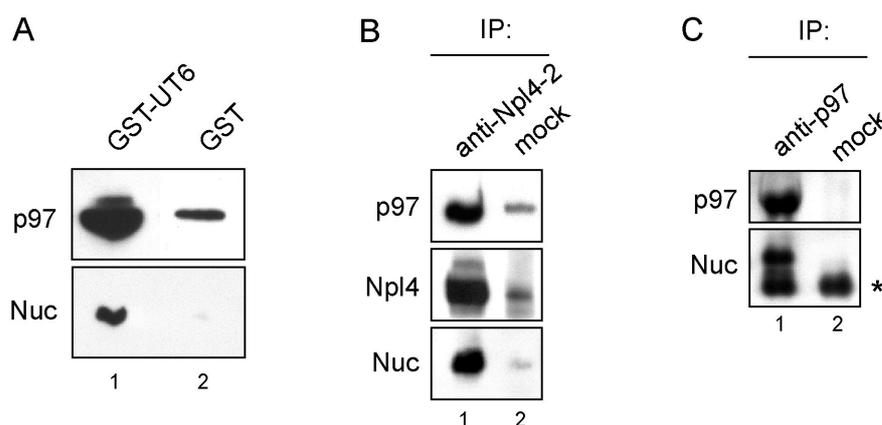
Fig. 24: Nucleoplasmin interacts with p97-Ufd1-Npl4. **(A)** Pulldown from high-speed extract using GST-UT6 or just GST coupled to glutathione sepharose beads. 5 µl of both GST-UT6 and GST beads were analyzed by immunoblotting using the indicated antibodies. Equal loading of beads with GST-UT6 or GST was confirmed by coomassie staining (data not shown). **(B)** IP from high-speed extract with anti-Npl4-2 or unspecific IgG coupled to protein G sepharose beads. Beads were analyzed as in (A). Equal loading was confirmed by Ponceau staining (data not shown). **(C)** IP from high-speed extract with selfmade anti-p97 antibody or mock IgG bound to protein G sepharose. Beads were analyzed as in (A). Star denotes IgG light chain serving as loading control.

Nucleoplasmin is an essential regulator of sperm chromatin decondensation at fertilization catalyzing the exchange of sperm specific basic proteins for histones (Philpott et al., 1991; Philpott et al., 1992). This "repacking" of sperm DNA is necessary for fusion of the male and female pronuclei in the zygote. While nucleoplasmin is highly abundant in egg cytoplasm, it is absent from sperm (Laskey et al., 1978; Mills et al., 1980).

Sperm decondensation can easily be monitored in the *Xenopus* system and manifests in enlargement of *Xenopus* sperm upon addition to egg extract. Sperm swelling starts immediately after addition of sperm to extract and is largely completed after 30 min. Examples of sperm at different stages of decondensation are shown in Fig. 25A. The newly discovered interaction of nucleoplasmin with

p97 suggested an involvement of p97 in sperm-specific chromatin remodelling. Philpott et al. (1991) had postulated that nucleoplasmin was sufficient for this process by demonstrating almost normal sperm decondensation with purified nucleoplasmin. However, these researchers did not take into consideration that sperm themselves might contain additional proteins assisting in sperm decondensation. Consistent with an involvement of p97, sperm contain significant amounts of p97 and adaptors as demonstrated before (Fig. 16). Furthermore, it could be shown by an ATP bioluminescense assay that sperm contain high concentrations of ATP (1.5-2 µM; sperm preparation with $1.3x10^5$ nuclei/µl) which could potentially be utilized by the AAA-ATPase. Therefore, the hypothesis of p97 assisting in sperm decondensation was investigated by interfering with its function both in high-speed extract and in sperm. High-speed extracts were depleted from Ufd1-Npl4 and permeablized sperm were pre-incubated with anti-Ufd1-1 antibody prior to their addition to the depleted extract. It is important to note that depletion of Ufd1-Npl4 did not lead to any detectable decrease of nucleoplasmin in the extracts (data not shown). As control, mock-depleted high-speed extract was supplemented with sperm pre-incubated with unspecific rabbit IgG (Fig. 25B). To exclude any influence of sperm pre-treatment on sperm length, aliquots of sperm were taken before addition to extract and analyzed for sperm length after DAPI-staining. Pre-incubation did not change sperm length as shown by identical sperm length distribution of 50 evaluated sperm for each sample (Fig. 25C, 0 min). Sperm decondensation was then started by addition of pre-treated sperm to correspondingly treated extracts. Aliquots were taken every 2 min over a total period of 30 min, DAPI-stained and analyzed for sperm length. Interestingly, interference with p97 function resulted in a weak but highly reproducible delay of sperm decondensation (Fig. 25C). Importantly, this delay could be rescued by adding back recombinant Ufd1-Npl4 to depleted extracts and anti-Ufd1-1-treated sperm, confirming specificity of the effect (Fig. 25C).

A

0 min   10 min   30 min

B

C
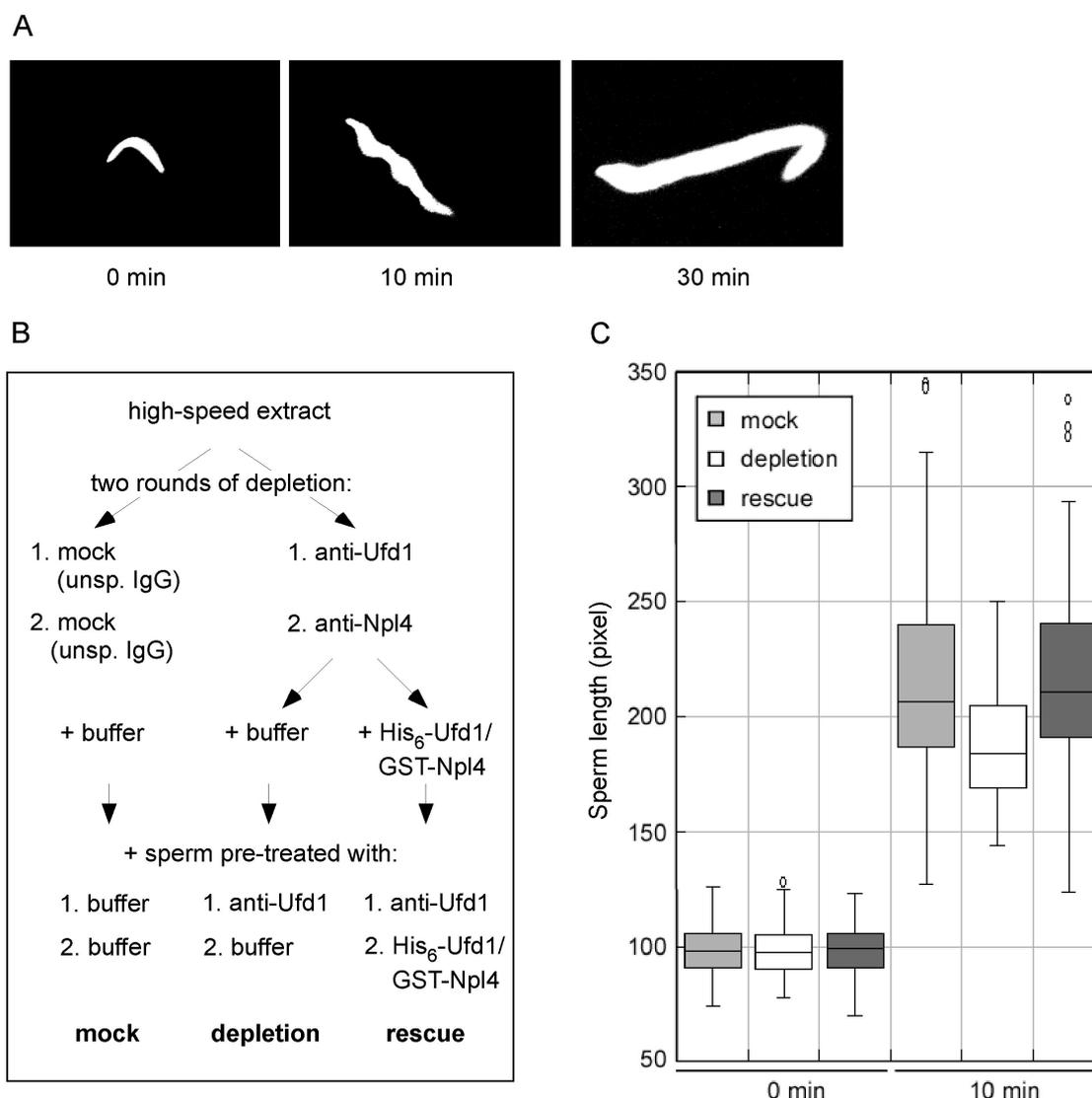
Fig. 25: Sperm decondensation is delayed upon interference with p97 function. **(A)** DAPI-stained *Xenopus* sperm nuclei after incubation in high-speed extract for 0, 10 and 30 min. Pictures were taken at 400x magnification. **(B)** Scheme of experiment evaluated in C, see text for details. **(C)** Length distributions of sperm incubated in high-speed extract for 0 or 10 min. Extracts were mock-depleted (mock), Ufd1-Npl4-depleted (Depletion) or Ufd1-Npl4-depleted and rescued with recombinant His$_6$-Ufd1/GST-Npl4 (Rescue) and then supplemented with sperm pre-treated with buffer or anti-Ufd1-1 antibodies as outlined in B. Successful depletion of Ufd1-Npl4 from high-speed extract was confirmed by immunoblotting (data not shown). Aliquots were taken before (0 min) or 10 min after addition of sperm to extracts, DAPI-stained and analyzed for sperm length (50 nuclei each) at 400x magnification. Data are presented in a Box-Whiskers-plot: Each box encloses 50% of the data with the median value displayed as a line. The top and the bottom of the box mark the limits of +/- 25% of the variable population. The lines extending from the top and bottom of each box mark the minimum and maximum value within the data set that fall within an acceptable range. Any value outside of this range is displayed as an individual point.

The difference in sperm length distribution was most evident at intermediate timepoints, such as 10 min, and eventually disappeared until 30 min (Fig. 25C and data not shown). This could indicate that sperm decondensation, although

delayed, can be completed in the absence of p97. However, it is difficult to fully obliterate p97 function in these assays due to its presence in sperm nuclei that cannot be depleted and might restrict access of anti-Ufd1-1 antibodies used to interfere with p97 function. Thus, incomplete inactivation of p97 constitutes an alternative explanation of why sperm decondensation finally went to completion.

3.2 Securin is not required for chromosomal stability in human cells

To avoid missegregation of chromosomes exact timing of separase activation is essential. By cleaving centromere-associated cohesin, separase resolves the final linkage between sister chromatids thereby triggering anaphase onset. Separase is kept inactive for most of the cell cycle by binding of its inhibitory chaperone securin (Funabiki et al., 1996; Zou et al., 1999) and by phosphorylation-dependent complex formation with Cdk1 (Stemmann et al., 2001; Gorr et al., 2005). Separase is eventually activated by proteolysis of securin and the cyclin B1 subunit of Cdk1, which in both cases is mediated by the APC/C^{Cdc20} (Glotzer et al., 1991; Zur and Brandeis, 2001; Peters, 2002). Thus, securin is a key regulator in anaphase and its exact role for proper chromosome segregation is of great interest. To investigate this question in more detail, Jallepalli et al. (2001) inactivated both copies of the gene encoding human securin via homologous recombination in the karyotypically stable human colorectal cancer cell line HCT110. Their results indicated that securin is needed for chromosomal stability in human cells as securin-deficient cells exhibited massive missegregation of chromosomes. Furthermore, the data suggested that securin plays a crucial positive role for the proper function of separase: Both separase level and activity were greatly reduced in the knockout cell line and *securin*$^{-/-}$ cells suffered from non-disjunction rather than premature separation of sister chromatids. However, the important role of human securin implied by the Jallepalli et al. (2001) study contrasted with the results of other investigations, which found mice lacking securin to be viable, apparently normal and fertile (Mei et al., 2001; Huang et al., 2005; Wirth et al., 2006; Kumada et al., 2006). To solve this discrepancy, our collaborators Katrin Pfleghaar and Michael Speicher conducted further studies with the *securin*$^{-/-}$ cell line obtained from Jallepalli and co-workers. In an initial step, metaphase spreads of the *securin*$^{-/-}$ cell line were

karyotyped by multiplex fluorescence in situ hybridization (M-FISH) after different numbers of passages (Fig. 26). For passages 2 and 3 they confirmed the loss of numerous chromosomes in the majority of analyzed cells (Fig. 26A and B). About 60% (12/20) of metaphase spreads showed losses of at least one chromosome. Surprisingly however, the high rate of chromosome losses in the $securin^{-/-}$ cell line had almost vanished by passage 8 (Fig. 26C), when aberrant chromosome numbers were detectable in only 10% (2/20) of cells. By passage 12, no chromosome losses were observed anymore (Fig. 26D). In the latter two analyses, merely one metaphase spread each had a gain of a single chromosome (Fig. 26C and D). Pfleghaar and Speicher confirmed by interphase FISH that $securin^{-/-}$ cells at passage 12 were indeed chromosomally stable (Pfleghaar et al., 2005). Additionally, normal execution of anaphase in $securin^{-/-}$ cells at passage 12 or higher was demonstrated by examination of centromere distribution during mitosis in immunofluorescence experiments (Pfleghaar et al, 2005). Thus, as quickly as 12 passages after knockout, $securin^{-/-}$ cells displayed normal sister chromatid separation, were chromosomally stable and in this regard indistinguishable from the parental HCT116 cell line. Since Jallepalli et al. (2001) had reported that both separase levels and activity were reduced in $securin^{-/-}$ cells, we wondered whether these biochemical defects were still present in $securin^{-/-}$ cells that had regained chromosomal stability or if level and activity of separase had likewise recovered, thereby providing an explanation for the chromosomally stable phenotype. Therefore separase levels were analyzed in $securin^{+/+}$ and chromosomally stable $securin^{-/-}$ cells synchronized by nocodazole. In both cell lines full-length and the cleaved form of separase were detectable. However, separase signals were consistently 3- to 4-fold weaker in securin$^{-/-}$ cells (Fig. 27A). To compare separase activities, Scc1 cleavage assays were performed as follows: Separase was immunopreciptated by anti-separase antibody from lysates of nocodazole-arrested $securin^{+/+}$ and $securin^{-/-}$ cells and incubated in *Xenopus* lowΔ90-extracts to degrade securin (if present). In case of HCT116 parental cells, incubation of re-isolated separase beads with *in vitro* translated ^{35}S-Scc1 resulted in the typical cleavage fragments (Fig. 27B). In contrast, separase from $securin^{-/-}$ cells displayed no cleavage activity towards Scc1, even after 90 min of incubation and with four times higher amount of starting cell material as compared to the wild type. Despite the absence of activity

in vitro, the presence of separase auto-cleavage products (Fig. 27A and C) demonstrates the presence of at least some separase activity in *securin*^{-/-} cells, which, apparently, is sufficient to execute anaphase normally.
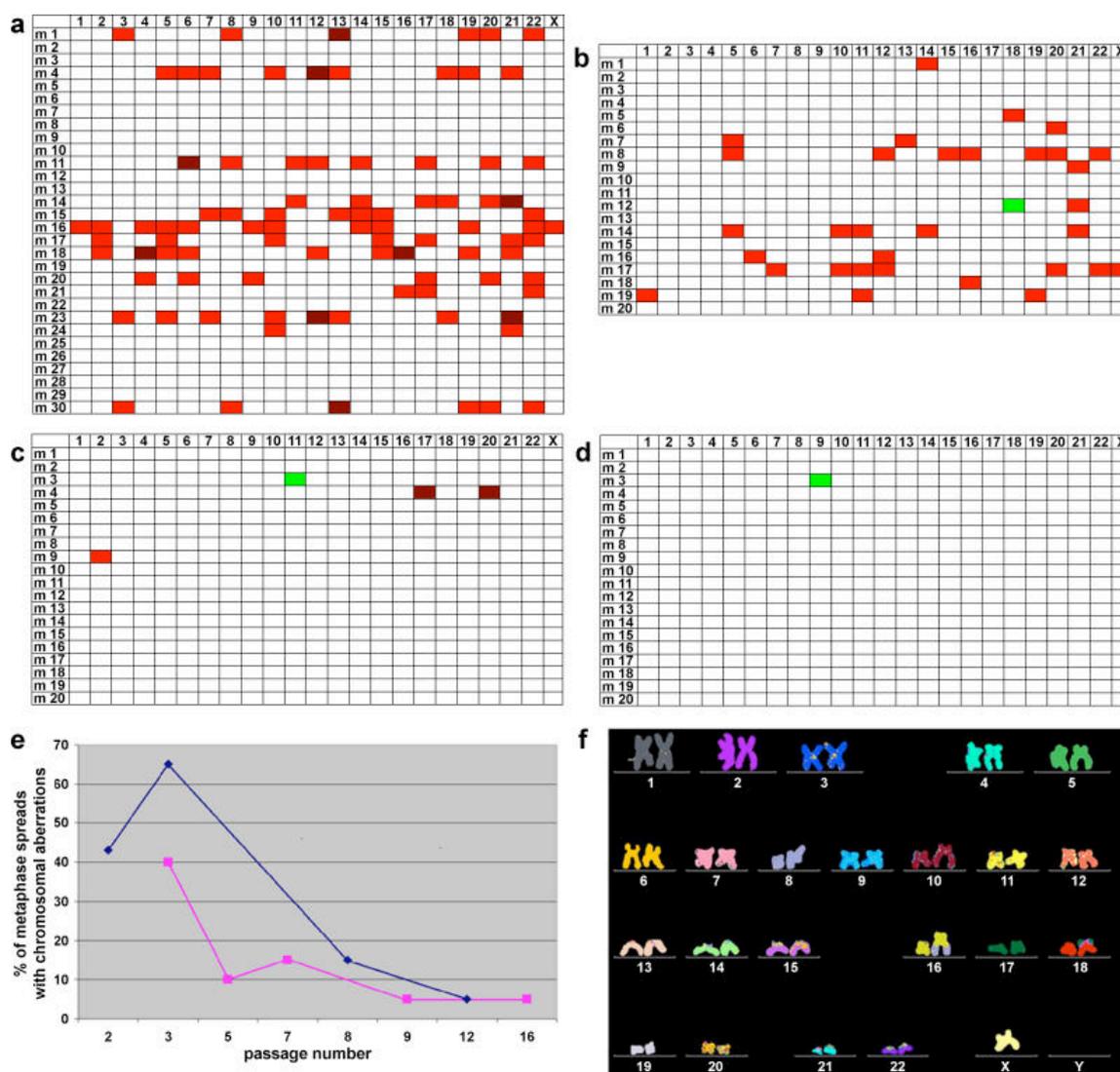
Experiment performed by Katrin Pfleghaar and Michael Speicher

Fig. 26: Human *securin*^{-/-} cells regain chromosomal stability quickly after securin knockout by homologous recombination. **(A-D)** Graphical summary of multiplex FISH data from securin^{-/-} cells at passages 2 (a), 3 (b), 8 (c), and 12 (d). At each passage point 20 or 30 metaphase spreads were painted by M-FISH and analyzed for alterations of chromosome structure and number. Loss of a single copy of a given chromosome is marked in red, loss of both copies is marked in crimson, and gain of a single chromosome is marked in green. Rows indicate the analyzed metaphase spreads (m1 to m30 or m20), columns indicate the chromosome number (1-22 and X). **(E)** Graphic representation of the percentage of metaphase spreads with chromosomal copy number aberrations at different passage number for the series of experiments shown in (a-d) (blue line) and for a repeat experiment (purple line). **(F)** M-FISH karyotype of a passage 12 securin^{-/-} cell, showing that the karyotype is identical to the parent cell line HCT116.

Interestingly, immunoprecipitated separase from nocodazole arrested securin^{-/-} cells even showed a higher degree of self-cleavage as compared to *securin*^{+/+} cells prior to incubation in lowΔ90-extract (Fig. 27C). This suggests that separase might be partly de-regulated in the *securin*^{-/-} cells.
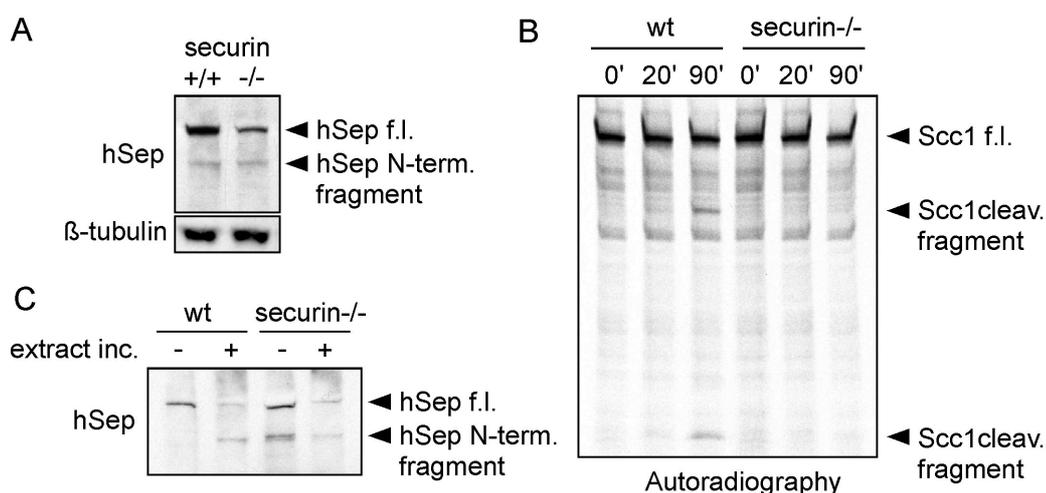
Fig. 27: Chromosomally stable human *securin*^{-/-} cells show reduction in both level and activity of separase.
(A) Quantitation of full length separase and the N-terminal cleavage product in both *securin*^{+/+} and *securin*^{-/-} cells. Lysates from nocodazole arrested cells were analyzed by immunoblotting with anti-Sep-N. The chromosomally stable *securin*^{-/-} cells show reduced levels of both full length and the cleaved N-terminal form of separase. ß-tubulin was used as a loading control. **(B)** Separase was immunoprecipitated from nocodazole-arrested *securin*^{+/+} and *securin*^{-/-} cells, activated by incubation in lowΔ90-extracts, and incubated with ^{35}S-Scc1 for 0, 20, or 90 min before analyses by SDS-PAGE and autoradiography. For these experiments four times the amount of *securin*^{-/-} cells as compared to the *securin*^{+/+} cells was used. **(C)** Separase used for the activity assay in (B) was analyzed by Western before (-) and after (+) exposure to lowΔ90-extracts.

Together, these results showed that separase level and activity were still reduced in chromosomally stable *securin*^{-/-} cells demonstrating that regain of chromosomal stability in *securin*^{-/-} cells was not due to recovery of separase function. To conclude, although deletion of *securin* leads to permanent reduction of separase level and activity, it has no effect on long-term chromosome segregation fidelity. Human securin is thus fully dispensable for maintenance of a stable complement of chromosomes and human cells might be able to up-regulate other mechanisms involved in chromosome segregation to compensate for the loss of securin.

4 DISCUSSION

4.1 Dispensability of p97 for spindle disassembly

Studying specific p97 functions *in vivo* is hampered by its involvement in a multitude of vital cellular activities. Consequently, homozygous deletion of p97 leads to early embryonic lethality (Müller et al., 2007; Sasagawa et al., 2007) and RNAi-mediated knockdown of p97 in higher eukaryotic cells gives rise to complex phenotypes (Wojcik et al., 2004). Cell-free extracts prepared from *Xenopus* eggs generally avoid this kind of problem because they are amenable to biochemical interference of specific protein functions at defined, arrested stages and can then be released to cycle synchronously. Given this power, tools to study p97 function in *Xenopus* egg extracts were developed in this thesis with the ultimate goal of investigating possible roles of p97 in mitosis. Although mainly investigated outside mitosis, several observations indicated that p97 fulfills important tasks also during mitosis (Cao et al., 2003; Hetzer et al., 2001; Wojcik et al., 2004). Importantly, p97 activity was reported to be essential for the transition of mitotic spindles into interphase MT-arrays both in *S. cerevisiae* and the *Xenopus* system (Cao et al., 2003). The publication from Cao et al. (2003) constituted a crucial foundation of this PhD project as it suggested a specific mitotic role of p97, including molecular details of its action. Cao et al. interfered with p97 function in *Xenopus* egg extracts by the addition of a either a dominant-negative mutant (p97-QQ) or a soluble anti-Ufd1 antibody, or by immunodepletion of Ufd1-Npl4 using the same anti-Ufd1 antibody. Spindle disassembly was reported to be completely blocked in response to all these manipulations. However, these results could not be reproduced when repeating their assays and were finally clearly disproved by this thesis (Heubes and Stemmann, 2007). Spindle disassembly was found to be undisturbed by a large variety of dominant-negative p97 mutants over a wide range of concentrations (0.5 to 5 mg/ml) with the highest tested concentration exceeding the p97-QQ concentration used by Cao et al. 10-fold and the endogenous p97 levels 20-fold. Furthermore, spindle disassembly occurred irrespective of whether aster formation was triggered by addition of sperm chromatin or centrosomes. In addition, immunodepletion of Ufd1-Npl4 had no effect on spindle disassembly despite the fact that depletions were performed under a variety of different conditions, using either anti-Ufd1-1,

anti-Npl4-1 or a combination of both antibodies, and that they – at least for Npl4 – were more efficient than those of Cao et al. (2003), who used only anti-Ufd1 for all their experiments. Likewise, while Zheng and colleagues were able to block formation of interphase MT-arrays by adding soluble anti-Ufd1, no such phenotype was observed even when soluble anti-Ufd1-1 or anti-Npl4-1 were added after immunodepletion of the heterodimeric adaptor. By comparing kinetics of spindle disassembly in the absence or presence of p97 function, a slightly accelerated disappearance of both chromatin-associated and centrosome-generated asters in Ufd1-Npl4-depleted extracts could be seen instead. Along this line, very high concentrations of p97-QQ (≥ 4 mg/ml final) were found to result in smaller spindles that depolymerized over time in CSF-extracts while spindles in controls persisted (Heubes and Stemmann, unpublished data). Together, these data suggest that p97 exerts a positive rather than a negative effect, if any, on the mitotic spindle and that blocking p97 function slightly destablizes spindles rather than stabilizes them. Given the fact that all *Xenopus* experiments from the Cao et al. (2003) publication were repeated with great care and by performing many additional controls, it is difficult to reconcile the data from Cao et al. (2003) with the results of this work without assuming inconsistencies in their experiments. Antibody-mediated protein depletion can be prone to errors if the antibody cross-reacts with other proteins, in this case perhaps a factor required for spindle disassembly. However, Cao et al. (2003) reported that their observed defect in Ufd1-depleted extract could be rescued by bacterially expressed Ufd1-Npl4, suggesting that antibody cross-reactivity was not a problem. Therefore, an alternative explanation for the differing results might be that, under their conditions, p97 depletion caused a secondary or indirect effect on spindle stability due to perturbations of other p97-dependent processes such as ERAD. In conclusion, the findings presented in this thesis strongly suggest to re-evaluate the proposed role of p97 in spindle disassembly during exit from mitosis. Supporting the results of this work, p97 was demonstrated very recently to be dispensable for spindle disassembly at the end of *C. elegans* meiosis I (Sasagawa et al., 2007).

4.2 Reconstitution of ERAD in *Xenopus* egg extracts

To demonstrate the effectiveness of dominant-negative mutants in blocking p97 function, p97-dependent ERAD was established for the first time in cell-free egg extracts from *Xenopus*. Although ERAD has been reconstituted using reticulocyte lysates before, this *in vitro*-system suffers from the need to isolate microsomes and from the presence of p97 in both key components, reticulocyte lysate and ER-membrane preparations (Xiong et al., 1999). Within this thesis an alternative approach was developed using just CFTRΔF508-encoding mRNA and standard *Xenopus* egg extracts. Due to the relatively low centrifugal force used for their preparation, these extracts contain sufficient microsomal membranes to fully support ER-associated translation and subsequent ERAD. Addition of dominant-negative p97-QQ at a concentration as low as 0.25 mg/ml inhibited ERAD of CFTRΔF508 almost completely, thereby proving the effectiveness of this approach in blocking p97 function and validating the results regarding spindle disassembly. At the same time this provides a general and easy opportunity to investigate the p97-dependency of ERAD of diverse substrates in a vertebrate model system. Moreover, this simple *in vitro* system should prove valuable for further investigations of other aspects of ERAD like the possible existence of multiple pathways for ubiquitylation and the presentation of substrates to the proteasome.

4.3 No evidence on a connection between p97 and separase in higher eukaryotes

The recent discovery of genetic interaction between Cut1/separase and Cut2/securin with Cdc48/p97 in *S. pombe* (Yuasa et al., 2004; Ikai and Yanagida, 2006) immediately raised the question of whether a similar connection also exists in higher eukaryotes. In their *S. pombe* studies, Yanagida and co-workers not only showed genetic interaction between these proteins but also demonstrated that Cut1/separase was degraded along with Cut2/securin in anaphase in the newly isolated mutant strain *cdc48-353*. Growth defects of the *cdc48-353* mutant strain were rescued by overexpression of Cut1/separase but aggravated by overexpression of Cut2/securin. Based on these observations, Cdc48 was hypothesized to be required for proper destruction of polyubiquitylated

Cut2/securin on the one hand and/or to act as a "stabilizer" of separase after Cut2/securin degradation on the other hand.

Therefore, a possible connection between separase, securin and p97 in higher eukaryotes was investigated. Towards this end, separase stability and activation as well as securin degradation in the absence of functional p97 were examined by incubating purified human separase/securin complexes in *Xenopus* anaphase extracts. However, irrespective of whether p97 function had been blocked, securin was efficiently degraded in these extracts and separase was activated. Furthermore, separase levels remained constant after securin degradation. These results were achieved and confirmed in different experimental setups. Either soluble human separase/securin complexes were incubated in *Xenopus* anaphase extracts supplemented with dominant-negative p97-QQ, or immobilized human separase was activated by degradation of associated securin in extracts depleted of Ufd1-Npl4 or p47. Under all conditions securin degradation and separase activation occurred completely normal demonstrating that p97 is dispensable for these processes in higher eukaryotes. An explanation for the apparent discrepancy to *S. pombe* might be an indirect effect of Cdc48/p97 on Cut1/separase. This is conceivable since Yanagida and co-workers applied a pure genetic approach but were unable to show a direct biochemical interaction between both proteins (Ikai and Yanagida, 2006). Similarly, no direct interaction between human or *Xenopus* separase with *Xenopus* p97 was found (Heubes and Stemmann, unpublished data). Furthermore, regarding the *S. pombe* data, it remains mysterious why *cdc48-353* was the only out of several *cdc48* mutant strains that was rescued by overexpression of Cut1/separase. The *cdc48-353* strain carries a hitherto uncharacterized point mutation of Gly338 (Gly318 in vertebrate p97) to Asp within the D1 domain of Cdc48. This amino acid exchange neither impairs hexamer formation nor ATPase activity of the AAA-ATPase, and hence, does not result in a dominant-like allele. This raises the question of whether the D1 domain of Cdc48/p97 might exert an additional, as yet uncharacterized function. The p97/Cdc48 hexamer bears two chambers formed by the D1 and D2 domains, respectively, with both chambers being connected by a central pore (Fig. 3). The fact that the mutated *S. pombe* Gly338 (vertebrate Gly318) is located on the inside of the central pore led to the proposition and investigation of another model on how p97/Cdc48 might have an impact on

separase: This giant protease likely needs the help of chaperones for proper folding. So far, mainly unfolding activity has been attributed to p97/Cdc48. However, Cdc48 has been reported to be able to recognize denatured proteins and to prevent their aggregation *in vitro* (Thoms, 2002). Additionally, other members of AAA+ familiy such as Hsp104 and ClpB have been demonstrated to promote refolding of denatured proteins (Glover and Lindquist, 1998; Schlieker et al., 2004). It was therefore conceivable that p97/Cdc48 acts as a chaperone that assists separase in adopting a native state, a process that might be disturbed by the Gly338 (vertebrate Gly318) mutation. To investigate this hypothesis, CSF-extracts were supplemented with mRNA encoding human separase instead of purified separase/securin protein complexes, since the requirement of p97 as a chaperone might be co-translational and transient. Again, p97 function was blocked in extracts by either supplementation with p97-QQ or depletion of Ufd1-Npl4. However, interfering with p97 function had no significant effect on separase level and activity as separase was efficiently translated and activated under all conditions. Assuming that the proposed foldase activity is susceptible to the dominant-negative approach or the removal of its heterodimeric adaptor, these findings exclude a model of p97 acting as a chaperone for separase. In accordance with this, the addition of *Xenopus* p97-G318D and p97-H317A to extract also showed no effect (Heubes and Stemmann, unpublished data) although, in this case, the presence of endogenous p97 might mask a potential effect. In summary, these results suggest that there is no connection between p97 and separase in higher eukaryotes.

Interestingly, studying translation of separase led to new insights into the role of securin which had been suggested to act as a chaperone for separase since separase levels and activity are reduced in its absence (Jallepalli et al. 2001; Pfleghaar et al., 2005). Due to low conservation in sequence, *Xenopus* securin binds human separase with at least 10-fold lower affinity than its human counterpart (Fan et al., 2006). Expecting a requirement of human securin for efficient folding of newly synthesized human separase, purified human securin protein was added to the *Xenopus* egg extracts. Surprisingly, levels of translated human separase were unaffected and activities were only slightly enhanced by the presence of human securin. Two explanations are possible: Endogenous *Xenopus* securin might be able to functionally replace human securin despite its

very weak interaction with human separase. Alternatively, securin might affect separase levels not by acting as a chaperone but as a transcriptional activator. Absence of transcription in *Xenopus* egg extracts might thus explain why securin has no effect on separase levels in this model system. Consistent with this latter possibility, securin has been reported to act as a regulator of global and p53-mediated transcription (Tong et al., 2007; Bernal et al., 2002). Measuring separase mRNA levels in *securin*$^{-/-}$ cells and wild type cells by Northern Blotting or real-time RT-PCR and following separase protein levels upon inhibition of transcription/translation will clarify this issue.

4.4 Other putative roles of p97 in mitosis or meiosis of higher eukaryotes?

The results obtained suggest that p97 might play less specific roles in mitosis/meiosis than originally assumed. The major report on a mitotic function of p97, namely its involvement in spindle disassembly, was disproved and no evidence on a connection between separase and p97 in higher eukaryotes was found despite thorough examination. Similarly, p97 was found to be dispensable for both SAC maintenance and override mediated by UbcH10 in *Xenopus*. However, the G2/M arrest of *cdc48-1* mutants from the original *S.cerevisiae* screen that led to the discovery of p97/Cdc48 (Moir et al., 1982; Frohlich et al., 1991) still remains to be explained. Some recent reports make new suggestions on how p97 might act in mitosis or meiosis, but given that they are in parts contradictory to each other, these should be interpreted carefully. Zheng and co-workers reported that p97-Ufd1-Npl4 interacts with survivin, a component of the chromosomal passenger complex (CPC) that also includes Aurora B. In early mitosis the CPC localizes to centromeres and is important for proper chromosome alignment. Zheng and co-workers claimed that Ufd1-mediated ubiquitylation of survivin was necessary for proper localization of both survivin and Aurora B to centromeres. Following knockdown of Ufd1 in HeLa cells, these researchers observed prolonged mitosis caused by problems in chromosome alignment (Vong et al., 2005). In contrast, Wojcik et al. (2004) observed little effect of siRNA-mediated depletion of Ufd1, Npl4 or p47 on cell proliferation using the same cell line. Only after siRNA against p97, Wojcik and collegues obtained significant multiple phenotypes in HeLa cells, including G2/M arrest and

apoptosis. Since apoptosis itself causes a pseudo-mitotic state and inhibits cell proliferation, it is doubtful whether the G2/M arrest is directly caused by a lack of p97 or whether it reflects a secondary effect of apoptosis. Alternatively, mitotic defects after knockdown of p97 might be indirect consequences of defects in other p97-dependent pathways such as ERAD. Importantly, siRNA against p97 in Drospophila S2 cells did not lead to a G2/M arrest in the hands of the same researchers (Wojcik et al., 2004). Furthermore, Wojcik and colleagues observed a low degree of chromosome condensation in p97-defective G2/M-arrested HeLa cells. This is reminiscent of a recent study in *C. elegans* (Sasagawa et al., 2007) that demonstrated defects in meiosis I chromosome condensation as a consequence of RNAi-mediated depletion of Cdc48. However, Sasagawa et al. (2007) were unable to show an interaction between p97/Cdc48 and components of the condensin complexes. Similarly, no genetic interaction between p97/Cdc48 and the condensin subunits SMC4 and SMC2 was found in *S. pombe* (Yuasa et al., 2004). Alternatively, p97 might influence mitotic chromosome condensation by acting as a chromatin-remodelling factor, consistent with its newly discovered role in sperm-specific chromatin remodelling (see below). Future investigations that include examination of this highly speculative model will shed light on the controversial role of p97/Cdc48 in mitosis/meiosis.

4.5 A novel role of p97 in sperm chromatin remodelling at fertilization

During investigation of possible functions of p97 in mitosis, a completely new function of the AAA-ATPase was revealed. p97-Ufd1-Npl4 was found to interact with nucleoplasmin, a nuclear chaperone that plays a major role in fertilization. By catalyzing the exchange of sperm-specific basic proteins to somatic histones H2A and H2B during stage I sperm decondensation, nucleoplasmin is essential for male pronucleus formation and, consequently, successful fertilization. Given the interaction of p97 with nucleoplasmin, an involvement of p97 in stage I decondensation was investigated. Blocking p97-Ufd1-Npl4 function indeed resulted in a delay of sperm swelling, an effect whose specificity was demonstrated in rescue experiments. In the original study, Philpott et al. (1991) had suggested that nucleoplasmin alone was sufficient to bring about sperm decondensation since purified nucleoplasmin efficiently catalyzed sperm swelling.

However, the results obtained in this work argue for a revised model with nucleoplasmin and p97 acting together in mediating the exchange of SBPs for somatic histones (Fig. 28).
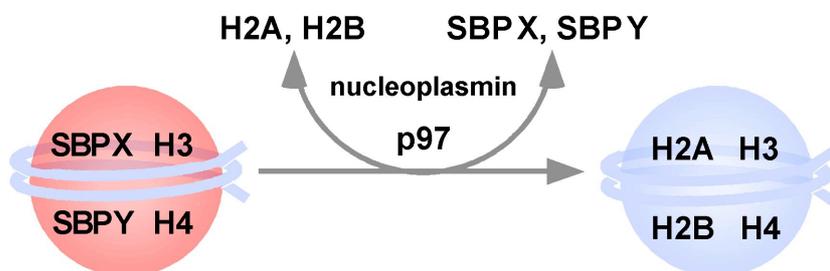
Fig. 28: Revised model of stage I sperm decondensation. p97 assists nucleoplasmin in exchanging sperm-specific histone variants (SBPs) to histones H2A and H2B at fertilization.

The observation that purified nucleoplasmin alone is able to mediate sperm swelling is easily reconciled with the revised model by taking into account that sperm nuclei themselves contain p97, its adaptors and ATP. Further support of a shared function between nucleoplasmin and p97 comes from the report that sperm swelling in extract is more efficient than with purified nucleoplasmin alone (Philpott et al., 1991), consistent with p97 function being limiting in the purified system. The fact that interfering with p97 function only resulted in a small delay of sperm decondensation is likely explained by difficulties in fully obliterating p97 function in sperm nuclei. Residual nuclear membranes might constitute a diffusion barrier for large proteins such as anti-Ufd1 antibodies used to block p97 function. An alternative approach using the small molecule N-ethylmaleimide (NEM) to inhibit p97 in sperm failed due to low specificity of this alkylating reagent and technical difficulties (Heubes and Stemmann, unpublished data).

The newly discovered role of p97 in sperm chromatin remodelling raises many interesting questions. Does p97 also play a role in the reverse process, i.e. hypercondensation of chromatin during spermatogenesis, when somatic histones are replaced by SBPs? Given the preference of p97 for ubiquitylated substrates, it is interesting to note that histones H2A and H2B are ubiquitylated during mouse spermatogenesis shortly before their exchange for SBPs. Is it possible that p97-dependent chromatin remodelling may require histone ubiquitylation? Lastly, nucleoplasmin also participates in other processes such as decondensation of somatic heterochromatin (Tamada et al., 2006; Frehlick et al., 2006) and

regulation of chromatin condensation during apoptosis (Lu et al., 2005), raising the question of an involvement of p97 in these processes.

4.6 Excess of UbcH10 triggers releases from CSF-arrest

Addition of recombinant human UbcH10 to checkpoint-arrested HeLa cell lysates leads to SAC inactivation. This is explained on the molecular level by UbcH10-dependent polyubiquitylation of Cdc20, which in turn triggers disassembly of the MCC. Cdc20 is thus liberated and again able to associate with and activate the APC/C (Reddy et al., 2007). To investigate if p97 was required for dissociating polyubiquitylated Cdc20 from the MCC, SAC inactivation in *Xenopus* egg extracts by human UbcH10 was established. As demonstrated previously in the purely human system, UbcH10 inactivated the SAC also in *Xenopus* egg extracts, indicating that this important mechanism is highly conserved among vertebrates. p97, however, turned out to be dispensable for SAC inactivation both in *Xenopus* and the human system (this work and M. Rape, personal communication). Surprisingly, UbcH10 was found not only to inactivate the SAC but also the CSF-arrest in *Xenopus*. In contrast to the inhibition of the APC/C^{Cdc20} triggered by SAC signaling, less is known of its inhibition by Erp1 during CSF-arrest. Although attempts to show a direct interaction of Erp1 with Cdc20 failed so far (Schmidt et al., 2006), Erp1 was recently demonstrated to bind to APC/C core subunits (Nishiyama et al., 2007). Based on these observations, Erp1 was suggested to act as a pseudosubstrate inhibitor of the APC/C^{Cdc20} as shown for its relative Emi1 (Nishiyama et al., 2007; Miller et al., 2006). At fertilization increase of the cytosolic Ca^{2+} concentration triggers a cascade that ultimately leads to ubiquitylation of Erp1 by the E3 ubiquitin ligase SCF, which in turn results in Erp1 degradation and thus APC/C^{Cdc20} activation. How excess of UbcH10 can cause release from CSF, as discovered in this work, currently remains a mystery. It will be interesting to investigate whether this involves ubiquitylation of Erp1 and if so, whether ubiquitylation is mediated by the E3 ligase SCF or the APC/C^{Cdc20} itself as in SAC inactivation. Furthermore, it will be important to study if UbcH10-dependent CSF inactivation includes Erp1 degradation or solely its dissocation from APC/C^{Cdc20}.

4.7 Faithful chromosome segregation in human cells in the absence of securin

To address securin's function, both copies of its gene were inactivated in an earlier study via homologous recombination in the karyotypically stable human cancer cell line HCT116. A first investigation of these *securin*^{-/-} cells revealed high rates of chromosome missegregation leading to the proposal that securin is essential for maintaining chromosomal stability in humans (Jallepalli et al., 2001). However, this report contrasted with findings in mice. *Securin*^{-/-} mice were found to be viable and only 20% of mouse cells lacking securin exhibited gain or loss of chromosomes (Mei et al., 2001; Huang et al., 2005). Therefore, in collaboration with the group of M. Speicher, the human HCT116 *securin*^{-/-} cells generated by Jallepalli et al. (2001) were investigated in more detail within this thesis. Surprisingly, *securin*^{-/-} cells were found to quickly regain chromosomal stability within just a few passages after gene-knockout showing that they are capable of fully compensating for the loss of securin. However, the initially described defects such as reduced levels and activity of separase persisted also in higher passage *securin*^{-/-} cells. The data obtained in this collaborative effort are fully consistent with the securin knockout mice beeing viable and apparently normal. However, some differences remain: While the percentage of aneuploid *securin*^{-/-} cells was reduced to background levels after a few passages, about 20% of mouse embryonic stem cells lacking securin were aneuploid. Additionally, in contrast to *securin*^{-/-} cells, mouse cells without securin have little change in the level of separase (Huang et al., 2005). Together, this indicates that subtle differences in securin-dependent regulation of separase must exist between human and mouse cells. The reconstitution of chromosomal stability and complete separation of sister chromatids in *securin*^{-/-} cells suggests that significantly lower than normal amounts of separase are sufficient for normal execution of anaphase. This is in agreement with wild-type levels of separase being able to efficiently remove even vastly increased amounts of cohesin from chromosomes (Giménez-Abián et al., 2004).

In conclusion, the findings obtained in collaboration with M. Speicher's group demonstrate that deletion of *securin* has little or no effect on long-term chromosome fidelity in human cells. Therefore, securin-independent mechanisms are apparently sufficient for proper regulation of human separase. Cdk1-

dependent phosphorylation is one such mechanism (Stemmann et al., 2001; Huang et al., 2005). It remains to be elucidated whether the transient chromosomal instability in *securin*$^{-/-}$ cells resulted just from the insult inflicted by the knockout procedure or reflects an up-regulation of compensatory mechanisms that control anaphase onset.

5 MATERIALS AND METHODS

Hard- and software
This work was written on an "Apple iBook G4" (Apple Computer Inc.) using "Microsoft Word 2001" (Microsoft Corporation). "Microsoft Excel 2001" (Microsoft Corporation) was used for generation of diagrams. Exposed films of immunoblots and autoradiographies were digitalized by scanning with a ScanMaker i900 (Microtek). Processing of all images was performed with "Adobe Photoshop 7.0 (Adobe Systems Inc.) and final design was carried out with "Canvas 9.0" (Deneba Software Inc.). DNASTAR Lasergene (DNASTAR Inc.) was used for analysis of DNA and protein sequences. Literature and database searches were done with electronic services provided by the "National Center for Biotechnology Information" (http://www.ncbi.nlm.nih.gov/).

Protocols
The methods described in this section are based on standard techniques (Ausubel et al., 1994; Sambrook et al., 1989) or follow the manufacturer's instructions. When protocols have been modified, detailed information is provided. For all methods, de-ionized sterile water, sterile solutions and sterile flasks were used.

Chemicals and reagents
Unless otherwise noticed, chemicals and reagents (pro analysis grade) were purchased from AppliChem, Biomol, Biorad, Calbiochem, Fermentas, Fluka, Invitrogen, Merck, New England Biolabs (NEB), GE Healthcare, Promega, Roche, Riedel de Haen, Roth, Serva, Sigma and Pierce.

Antibodies
Polyclonal antibodies against *Xenopus* p97, Npl4, Ufd1 and p47 were raised in rabbits as described in section 5.5.2. Polyclonal rabbit antibodies against human securin and the N-terminus of human separase (anti-Sep-N) were characterized in Stemmann et al. (2001) and Zou et al. (1999). Another polyclonal rabbit antibody was raised against the peptide sequence GSDGEDSASGGKTPA of human separase (anti-Sep-M). Other antibodies and affinity matrices were as follows: Mouse monoclonal anti-hCFTR (Upstate, clone M3A7), mouse monoclonal anti-Myc (Upstate, clone 4A6), mouse monoclonal anti-Flag (M2, Sigma), mouse monoclonal anti-nucleoplasmin (Developmental Studies Hybridoma Bank, clone b7-1A9), mouse monoclonal anti-*Xenopus*-p97 (PROGEN Biotechnik), mouse monoclonal anti-β-tubulin (Developmental Studies Hybridoma Bank, clone E7), unspecific rabbit and mouse IgG (Sigma) and IgG sepharose (4 Fast Flow, GE Healthcare). Polyclonal goat anti-mouse-IgG or anti-rabbit-IgG coupled to peroxidase (Dianova) were used as secondary antibodies in immunoblotting.

5.1 Microbiological techniques

E. coli strains

XL-1 blue: *E. coli sup*E44, *hsd*R17, *rec*A1, *end*A1, *gyr*A46, *thi*, *rel*A1, *lac* ⁻,
                                    [F' *pro* AB, *lac*Iq, *Lac* ZΔM15, Tn10 (*Tet* r)] (Stratagene)

BL21(DE3)/RIL: *E. coli* B F⁻ *omp*T *hsd*S(rB⁻ mB⁻) *dcm*⁺ Tetr galλ (DE3) *End*A *The*
                                    [*arg*U *ile*Y *leu*W *Cam*r] (Stratagene)

E.coli vectors

pGEX4T1 (GE Healthcare) with modified MCS (FseI/AscI sites inserted)
pQE80 (Quiagen) with modified MCS (FseI/AscI sites inserted)
pQE9 (Qiagen)
pQE30 (Qiagen)
pRSF-Duet-1 (Merck KGaA) with modified MCS (FseI/AscI sites inserted)

E. coli media

LB medium   1% Trypton (Difco)
                           0,5% yeast extract (Difco)
                           1% NaCl
                           sterilized by autoclaving

LB agar   LB-medium with 1.5% agar

SOB medium   2% Trypton (Difco)
                           0.5% yeast extract (Difco)
                           0.05% NaCl
                           0.02% KCl
                           sterilized by autoclaving

Cultivation and storage of *E. coli*

E. coli strains were grown in LB medium by shaking at 200 rpm at 37°C, LB agar plates were incubated at 37°C. Antibiotics for selection of transformed bacteria were added to media at 100 μg/ml (ampicillin) and 30 μg/ml (kanamycin) final. Culture densities were determined by measuring the absorbance at a wavelength of 600 nm (OD_{600}). Cultures on agar plates were stored at 4°C for up to 14 days. For long-term storage, liquid cultures were supplemented with glycerol to 20% final concentration, subsequently snap-frozen and stored at -80°C.

Preparation of competent bacteria

Tbf1 buffer   30 mM KAc
                           50 mM $MnCl_2$
                           100 mM KCl
                           15% glycerol
                           pH adjusted to 5.8

Tbf2 buffer	10 mM MOPS/NaOH
	75 mM $CaCl_2$
	10 mM KCl
	15% glycerol
	pH adjusted to 7.0

For preparation of chemical-competent bacteria, 300 ml SOB medium was inoculated with 4 ml of an overnight culture derived from a single *E. coli* colony and grown at 37°C to an OD_{600} of 0.5. After chilling the culture flask on ice for 15 min, cells were harvested by centrifugation (4°C, 3500 rpm, 15 min). All following steps were performed with pre-chilled sterile materials and solutions at 4°C. Sedimented bacteria were carefully resuspended in 90 ml Tbf1 buffer and chilled on ice for 15 min (XL-1 blue) or 45 min (BL21(DE3)RIL). After a second centrifugation (4°C, 2500 rpm, 15 min), bacteria were resuspended in 15 ml Tbf2 buffer and chilled on ice for 5 min. Finally, suspension of bacteria was aliquoted, snap-frozen and stored at -80°C.

Transformation of plasmid DNA into bacterial cells
Competent bacteria were thawed on ice. For chemical transformation, 50 µl of competent bacteria were mixed with 1 µl of plasmid DNA or 5 µl ligation reaction and incubated on ice for 30 min. A heat shock at 42°C was performed for 45 s. Subsequently, the cell suspension was incubated on ice for 2 min and after addition of 1 ml SOB medium without antibiotics incubated on a shaker at 37°C for 45 min. After recovery, transformed cells were selected by streaking out the bacteria suspension on LB agar plates containing the respective antibiotic(s) and incubated overnight at 37°C.

Expression of proteins in *E. coli*
For expression of recombinant proteins exclusively, the *E. coli* strain BL21(DE3)RIL was used. LB medium was inoculated with a dilution of 1:100 of an overnight culture from a freshly transformed colony. The culture was grown at 37°C and expression of protein(s) was induced by addition of IPTG (0.5 mM final concentration) at an OD_{600} of 0.6 - 0.8. After shaking for 3h at 37°C or overnight at RT, cells were harvested by centrifugation (4°C, 5000 g, 10 min) and pellets were stored at -80°C after snap-freezing.

5.2 Molecular biological methods

Isolation of plasmid DNA from *E. coli*
4ml of LB medium containing the appropriate antibiotic was inoculated with a single *E. coli* colony harboring the DNA plasmid of interest and shaken for 8-14h at 37°C. Plasmid-DNA was purified via alkaline lysis of the bacteria and subsequent isolation by anion exchange columns according to the manufacturer's instructions (Qiagen Plasmid Purification Handbook, Plasmid Mini Preparation for up to 20 µg DNA). Larger amounts of DNA for transfection of human cells were isolated from a 500 ml overnight culture according to the manufacturer's protocol (Qiagen Plasmid Purification Handbook, Plasmid Maxi Preparation for up to 800 µg DNA).

Determination of DNA/RNA concentration in solution

DNA/RNA concentration was determined by measuring the absorbance at a wavelength of 260 nm (OD_{260}) with a ND-1000 Spectrophotometer (Peqlab). An OD_{260} = 1 equals a concentration of 50 μg/ml double-stranded DNA or 40 μg/ml RNA.

Restriction digestion of DNA

Sequence-specific cleavage of DNA with restriction enzymes was performed according to standard protocols (Sambrook et al., 1989) and the instructions of the manufacturer (New England Biolabs, NEB). Usually, 5-10 units of restriction enzyme were used for digestion of 1 μg DNA. Reaction samples were incubated in appropriate buffer at the recommended temperature for 1-2 h. Restriction digestion was then stopped by heat inactivation of the enzymes.

Dephosphorylation of DNA fragments

To avoid recirculation of linearized vectors, the 5' end of vector DNA was dephosphorylated by adding 0.1 units of shrimp alkaline phosphatase (Roche) and incubating for 30 min at 37°C. The required alkaline pH for the reaction was adjusted by addition of 0.1 µl Tris Base to 30 µl reaction mix. Finally, shrimp alkaline phosphatase was heat-inactivated at for 15 min at 70°C.

Separation of DNA fragments by gel electrophoresis

TBE buffer	90 mM Tris
	90 mM Boric acid
	2.5 mM EDTA

DNA loading buffer (5x)	0.5% SDS
	0.25% Orange G
	25% Glycerol
	25 mM EDTA, pH 8,0

For analytical analysis and preparative isolation, DNA fragments were electrophoretically separated on agarose gels (0.8-2.0% of agarose in TBE) containing ethidium bromide (0.5 µg/ml final concentration). DNA samples were mixed with DNA loading buffer and separated at 100 V in TBE buffer. DNA fragments could be visualized by intercalation of ethidium bromide into DNA by using a UV transilluminator (324 nm). The size of the fragments was estimated by standard size markers (O'GeneRuler 1kb or 100 bp DNA-Ladder, Fermentas).

Isolation of DNA from agarose gels

After gel electrophoresis DNA fragments were isolated by excising the respective piece of agarose using a razor blade. DNA was extracted from the agarose block using QiaExII Gel Extraction kit (Qiagen) according to manufacturer's instructions and eluted with TE buffer (5 mM Tris pH 8.0, 1mM EDTA).

Ligation of DNA fragments

Amounts of isolated DNA fragments ("insert") and linearized vectors were estimated on a ethidium bromide-containing agarose gel. For ligation reaction a molar ratio of 1:2 of vector to insert was used. The reaction sample with a total volume of 10 µl usually contained 100 ng of vector DNA and 4 units of T4 DNA Ligase (NEB) and was incubated overnight at 16°C in recommended amounts of reaction buffer (NEB).

Sequencing of DNA

Sequencing PCR and sample preparation were performed with the DYEnamic ET Terminator Cycle Sequencing Premix kit according to the manufacturer's instructions (GE Healthcare). One sample usually contained 0.5 µg of plasmid DNA and 5 pmol of primer. DNA sequencing was then carried out by the core facility of the institute with an Abi-Prism 377 sequencer (Perkin Elmer).

Site-directed mutagenesis of DNA

Specific point mutations in gene sequences were inserted by the GeneEditor *in vitro* Site-directed Mutagenesis System (Promega) according to the manufacturer's instructions. The underlying principle is the use of two oligonucleotides, one containing the desired point mutation and the other one introducing a mutation into the *Amp*R gene leading to resistance against the "GeneEditor" antibiotic. After denaturation of the plasmid of interest, both oligos are allowed to anneal and the second strand is completed by PCR. Subsequently, the double stranded plasmid is transformed into bacteria that are then selected on "GeneEditor" antibiotic containing agar plates. Introduced mutations were verified by sequencing.

Polymerase chain reaction (PCR)

PCRs were usually performed in a total volume of 50 µl with 50 ng of plasmid DNA, 2.5 µl of the respective forward and reverse oligonucleotide primer (10 µM each), 5 µl deoxynucleotide mix (each 10 mM, NEB) and 0.5 µl of DNA polymerase (Phusion, Finnzyme) in the corresponding PCR buffer (Phusion HF buffer, Finnzyme). For amplification, a PCR Mastercycler (Eppendorf) was used. The reaction profile was adjusted according to quantity and quality of template DNA, length and G/C content of the oligonucleotides, the length of the amplified sequences and in view of the manufacturer's instructions (Finnzyme).

Reverse transcription (RT)-PCRs from *Xenopus* mRNA were performed as follows: Reverse transcription was carried out in a total volume of 20 µl by incubation of 50 - 100 ng of *Xenopus* mRNA with 1 µl of M-MuLV Reverse Transcriptase (200 U/µl, Fermentas), 2 µl of the respective reverse oligonucleotide primer (10 µM), 2 µl of deoxynucleotide mix (10 mM each, NEB), 0.5 µl of RNasin (Promega) and in the corresponding M-MuLV buffer (Fermentas). The reaction mix was incubated for 1h at 42°C. Subsequently, 1-3 µl were used as template (instead of plasmid DNA) in a PCR carried out as described above.

mRNA synthesis *in vitro*

For generation of human CFTRΔF508 mRNA and human Myc$_6$-Tev$_2$-separase mRNA, corresponding genes were first linked to T7-promoters by PCR. Towards this end, the ORF of CFTRΔF508 was amplified from a plasmid kindly provided by P.J. Thomas using oligonucleotide primers

5'-TAATACGACTCACTATAGGGACTACCATGCAGAGGTCGCCTCT-3' and
5'-CTAAAGCCTTGTATCTTGCACCTCTTC-3'.

The ORF of Myc$_6$-Tev$_2$-separase was amplified from plasmid pOS111 (kind gift from O. Stemmann) using oligonucleotide primers

5'-TAATACGACTCACTATAGGGATCCCATCGATTTAAAGCTATGG-3' and
5'-ATGGCGCGCCTTACCGCAGAGAGACAGGCAAGCCATA-3'.

Starting with the purified PCR products, capped, poly-adenylated mRNAs were generated and purified using the mMESSAGEmMachineT7Ultrakit and MEGAclear columns (both Ambion) according to the manufacturer's instructions.

5.3 Cell biological methods

Cell lines and expression vector

HCT116	Human colorectal cancer cell line
293T	Human embryonic kidney cell line transformed with SV40 large T antigen

pCS2 (Turner and Weintraub, 1994) with modified MCS (FseI, AscI sites inserted)

Cultivation of mammalian cells

PBS	137 mM NaCl
	2.7 mM KCl
	8 mM Na$_2$HPO$_4$
	1.4 mM KH$_2$PO$_4$, pH 7.4

HCT116 and 293T cells were cultured in McCoy's 5A medium (Gibco, Invitrogen) and Dulbecco's Modified Eagle Medium (DMEM, Gibco, Invitrogen), respectively. Media were supplemented with 10% heat-inactivated (56°C, 30 min) fetal bovine serum (Biochrom), 100 units/ml penicillin and 0.1 mg/ml streptomycin (Gibco, Invitrogen). Monolayer cultures were grown in cell culture dishes (Falcon) at 37°C in a 5% CO$_2$ atmosphere and were split in a ration of 1:3 to 1:5 twice a week. Towards this end, medium was removed, cells were washed with PBS and subsequently incubated for 5 min with 1-3 ml of Trypsin/EDTA solution (Gibco, Invitrogen). After removal of the Trypsin/EDTA solution, cells were detached by rinsing the cell culture dish with fresh medium. Subsequently, cells were appropriately diluted in fresh medium and distributed on new cell culture dishes. Cell number of cell suspensions was determined by using a Neubauer counting chamber.

Storage of mammalian cells

For long-term storage living cells were kept in liquid nitrogen. Towards this end, cells were harvested at 80% confluence as described above, resuspended in freezing medium (10% DMSO, 20% fetal bovine serum in DMEM or McCoy's 5A), and aliquoted in cryovials (Nalgene). The cell suspension was then slowly frozen in an isopropanol-containing freezing device (Nalgene) at –80°C. After two days, cells were finally transferred to liquid nitrogen. For thawing, frozen cells were rapidly diluted with pre-warmed medium and spread on a cell culture dish ($\varnothing$ 10 cm). To remove residual DMSO, the medium was exchanged after attachment of the cells (usually 10 to 12 h after spreading).

Transfection of mammalian cells

2x HBS (50 ml)	800 mg NaCl
	37 mg KCl
	10.65 mg Na_2HPO_4
	100 mg Glucose
	500 mg HEPES
	pH 7.05 adjusted with NaOH

293T cells were transfected with different expression constructs for human separase and securin according to the calcium phosphate method. Along this line 3×10^6 cells per cell culture dish ($\varnothing$ 10 cm) were spread and grown overnight. Shortly before transfection the next day, chloroquin was added to the medium to a final concentration of 25 μM. For one transfection mix, 40 μg of separase-encoding and 20 μg of securin-encoding plasmid DNA were mixed with 99.2 μl 2M $CaCl_2$ solution and filled up with water to 800 μl. Then, 800 μl of 2x HBS solution were slowly added in small drops. After mixing and incubating for 15 min at RT, the transfection mix was dropped onto the medium of the prepared cells. 12 h later medium was exchanged. 24 h after transfection, nocodazole was added to the medium in a final concentration of 0.2 μg/ml to arrest cells in mitosis. After another 12 h cells were harvested by rinsing the cell culture dish with PBS. Following centrifugation (1500 rpm, 10 min, RT), pelleted cells were either directly lysed or snap-frozen and stored at –80°C.

5.4 *Xenopus* protocols

5.4.1 Preparation of *Xenopus* egg extracts

Xenopus egg extracts and *Xenopus* sperm nuclei were prepared as described (Murray, 1991).

Buffers

CSF-XB	100 mM KCl
	0,1 mM $CaCl_2$
	2 mM $MgCl_2$
	10 mM HEPES/KOH, pH 7.7
	50 mM sucrose
	5 mM EGTA/KOH, pH 8.0
	pH 7.7, adjusted with KOH

MMR (25x)	2,5 M NaCl
	50 mM KCl
	25 mM MgCl$_2$
	50 mM CaCl$_2$
	2.5 mM EDTA/NaOH, pH 8.0
	125 mM HEPES/NaOH, pH 7.8
	pH 7.8, adjusted with NaOH
DAPI-Fix	48% Glycerol
	11% Formaldehyde
	1x MMR (see above)
	1 µg/ml Hoechst 33342 (Sigma B-2261)
XB-salts (20x):	2 M KCl
	2 mM CaCl$_2$
	20 mM MgCl$_2$
Cysteine solution	2% (w/v) cysteine (free base)
	0,5x XB-salts
	pH 7.8, adjusted with KOH
Sperm dilution buffer	5 mM HEPES/KOH, pH 7.7
	100 mM KCl
	150 mM Sucrose
	1 mM MgCl$_2$

Prior to extract preparation all vessels were rinsed with bidestilled water in order to avoid contamination with Ca^{2+}. Work with frogs or frog eggs were performed at 18°C. Prepared extracts were kept on ice and were exclusively pipetted with cutted tips. The day before extract preparation, female frogs were injected each of which with 1 ml solution of human chorionic gonadotropin (Sigma CG-10, 1000 U/ml in H$_2$0) into the dorsal lymph sac. 16 h later frogs were transferred to 1x MMR buffer. Frogs laid mature oocytes 20-24 h after injection being sufficient for up to 1 ml of low-speed extract per frog. The jelly coats (zona pellucida) of the eggs were removed by incubation in cysteine solution for 10 min at maximum. Eggs were then extensively washed with CSF-XB. After all apoptotic, activated and abnormal eggs had been removed, eggs were transferred to a centrifuge tube containing 1 ml of CSF-XB and 10 µl of cytochalasin B (10 mg/ml in DMSO). By centrifugation in a JS 13.1 swing-out rotor (Beckmann) for 1 min at 200 g and 1 min at 600 g, eggs were tightly packed. Surplus of buffer on top of the packed eggs was removed. Eggs were then lysed by centrifugation at 13 000 g for 10 min. The light brown cytoplasmic fraction was isolated by puncturing the centrifuge tube with a needle and was transferred to an eppendorf tube. To block actin polymerisation, cytochalasin B was added in a final concentration of 10 µg/ml. At this stage, the extract was arrested in metaphase of meiosis II (CSF-extract). In some cases cycloheximide (Calbiochem 239764, dissolved in H$_2$O) was added in a final concentration of 100 µg/ml to inhibit translation. The CSF-arrest of all extracts was tested by incubation of an aliquot with sperm nuclei at 27°C. After 30 min, 2 µl of the sperm-supplemented aliquot were mixed

with 5 μl of DAPI-Fix and investigated by microscopy regarding the chromatin morphology. To produce lowΔ90 or highΔ90 anaphase extracts, CSF-extracts were supplemented with human cyclin B1Δ90 at 80 nM or 550 nM final, respectively. After incubation for 10 min at 18°C, Ca^{2+} (stock solution: 15 mM CaCl$_2$ in sperm dilution buffer) was added in a final concentration of 0.6 mM and the extract was further incubated for 15 min at 18°C. Anaphase extracts were either directly used or shock-frozen in aliquots of 200 μl and stored at –80°C. To prepare high-speed extracts, CSF-extracts were released into interphase by addition of Ca^{2+} in a final concentration of 0.6 mM following incubation for 30 min at 18°C. Then, interpase extracts were subjected to a second centrifugation (100 000 g, 1h, 4°C) in a SW60 swing-out rotor. The membrane-free fraction was recovered by punctuation of the centrifuge tube, aliquoted, snap-frozen and stored at –80°C.

5.4.2 Isolation of mRNA from *Xenopus* eggs

25 freshly laid *Xenopus* eggs were incubated in cysteine solution and subsequently washed in CSF-XB as described (see above). After removal of the jelly coats, eggs were packed by centrifugation (1 min, 2000 rpm, 18°C). Surplus of buffer on top of the eggs was removed. Eggs were then lysed and homogenized in 750 μl of Lysis/Binding solution (RNAqueous-4PCR kit, Ambion) by pulling through a syringe (connected to a 27-G needle). Following steps for isolation and washing of total RNA via silica-based filters were carried out with the RNAqueous-4PCR kit (Ambion) according to the manufacturer's instructions. Typically, 30 μg of total RNA from 25 eggs were obtained. The Poly(A)Purist MAG kit (Ambion) was used to purify mRNA from the total RNA preparation. Towards this end, total RNA was 1:2 diluted with Binding Solution (Poly(A)Purist MAG kit, Ambion). Enrichment of mRNA via oligo(dT) beads, washing and elution was carried out according to the manufacturer's instructions (Poly(A)Purist MAG kit, Ambion). Usually, 2 μg of mRNA were obtained starting with 30 μg of total RNA.

5.5 Protein methods

5.5.1 Standard protocols

SDS-polyacrylamide gel electrophoresis (SDS-PAGE)

7x Bis-Tris/HCl	2.5 M Bis-Tris
	1.5 M HCl
	adjusted to pH 6.5
6% gel solution	42.2 ml H$_2$O
	13 ml 30% acrylamide; 0.8% bisacrylamide
	9.3 ml 7x Bis-Tris/HCl
	163 µl 20% SDS (w/v)
	54.2 µl TEMED
	325 µl 10% APS (w/v)

15% gel solution	16.5 ml H_2O
	4.6 ml 2,5 M sucrose
	30 ml 30% acrylamide; 0.8% bisacrylamide
	8.6 ml 7x Bis-Tris/HCl
	150 µl 20% SDS
	25 µl TEMED
	300 µl 10% APS
MOPS running buffer	50 mM MOPS
	1 mM EDTA
	0.1% SDS
	50 mM Tris base
Sample buffer (4x)	40% glycerol
	564 mM Tris base
	424 mM HCl
	8% SDS
	2.04 mM EDTA/NaOH
	0.88 mM Coomassie G250
	0.7 mM Phenol red
	800 mM DTT

For the separation of proteins under denaturing conditions, SDS-PAGE was performed with the NuPAGE system (Invitrogen). 6-15% gradient gels were poored with a gradient mixer using pre-cooled 6% and 15% gel solutions. This type of gel does not require an additional stacking gel since protein samples are concentrated in the upper, low percentage part of the gel. Prior to loading, protein samples were mixed with sample buffer and denatured at 95°C for 5 min. In case of sperm nuclei, samples were additionally sonicated (10 sec, 20% intensity constant, Bandelin Sonoplus) to reduce their viscosity. As a molecular weight standard, PageRuler Prestained Protein Ladder (Fermentas) was loaded onto the gels. Electrophoresis was carried out at constant current (40 mA) in MOPS running buffer.

Immunoblotting

Blotting buffer	25 mM Tris
	192 mM glycine
	0.01% SDS
TBS-w	25 mM Tris, pH 7.5
	137 mM NaCl
	2.6 mM KCl
	0.05% Tween-20 (v/v)

After resolving proteins by SDS-PAGE they were transferred to a polyvinylidene fluoride (PVDF) membrane (Immobilon P, Millipore) in a "semi-dry" blotting apparatus (Biorad). Prior to blotting, the membrane was covered with 100% methanol that was then diluted with water to 5% under continous shaking. Protein transfer was carried out at a constant

voltage of 15 V for 30-45 min at RT. Subsequently, the membrane was blocked for 15 min at RT in TBS-w milk (5% skim milk powder (w/v) in TBS-w) followed by incubation with the primary antibody in TBS-w for 1 h at RT or overnight at 4°C. The membrane was then washed three times with TBS-w and afterwards incubated with the secondary antibody coupled to horseradish peroxidase (anti-mouse or anti-rabbit IgG) at a dilution of 1: 7000 in TBS-w. Finally, the membrane was washed as before and detection was carried out as described in the protocol for the chemiluminescence kit (ECL, Amersham) followed by exposure to an ECL hyperfilm (Amersham).

Coomassie staining

Coomassie solution	0.4% Coomassie Billiant Blue R250,
	0.4% Coomassie Billiant Blue G250
	40% MeOH (commercially pure)
	10% HAc
Destaining solution	30% MeOH (technisch)
	7% HAc

For coomassie staining, gels were incubated in coomassie solution after SDS-PAGE for at least 2 h. To remove unspecific stain, gels were subsequently transferred to destaining solution for 5 to 12 h. For long-term storage, coomassie-stained gels were dried on a whatman paper in a slab gel dryer (GD2000, Hoefer).

Autoradiography

After SDS-PAGE, gels were incubated in destaining solution for 20 min and subsequently washed with water. Gels were then dried on a whatman paper in a slab gel dryer (GD2000, Hoefer) and exposed to a film (BioMax MR, Kodak) for 3 h to 3 days depending on the intensity of the expected signals.

Determination of protein concentration

Protein concentrations were determined using the Bradford method (BioRad protein assay, BioRad) and compared to BSA standard dilution series by measuring the OD_{595}.

In vitro translation (IVT)

Coupled transcription and translation of plasmid DNA (from pCS2-based plasmids) *in vitro* was performed with rabbit reticulocyte lysate and SP6 RNA polymerase (TNT SP6 Quick, Promega). For radioactive labelling of proteins, the reaction mix was supplemented with ^{35}S-methione instead of unlabelled methione. *In vitro*-generated mRNAs were translated as described above with the alteration that mRNA instead of plasmid DNA was used as template.

5.5.2 Purification of proteins

Buffers (alphabetical order)

Antibody elution buffer	0.1 M glycine-HCl, pH 2.5
	0.1 M NaCl

Bacterial lysis buffer	150 mM Na-phosphate, pH 7.4
	300 mM NaCl
	5 mM ß-mercaptoethanol
	10 mM imidazole
	+ Complete protease inhibitor mix/ EDTA-free (Roche)

Bacterial lysis buffer 2	100 mM Tris-HCl, pH 7.4
	300 mM NaCl
	5 mM $MgCl_2$
	10 mM DTT
	+ Complete protease inhibitor mix (Roche)

Coupling buffer	0.2 M $NaHCO_3$, pH 8.3
	0.5 M NaCl

Elution buffer GST	50 mM reduced glutathione (Merck)
	10 mM DTT
	50 mM Tris/HCl pH 8.0
	300 mM NaCl
	5 mM $MgCl_2$
	+ Complete protease inhibitor mix (Roche)
	pH adjusted to 8 with NaOH

Elution buffer NTA	1 mM $MgCl_2$
	100 mM KCl
	150 mM sucrose
	5 mM Hepes/KOH, pH 7.4
	250 mM imidazole
	1 mM DTT
	pH adjusted to 7.4 with HCl

Glycine buffer	100mM glycine, pH 2.5
	100 mM NaCl

Lysis buffer 2 (LP2)   20 mM Tris/HCl, pH7.7
100 mM NaCl
10 mM NaF
20 mM ß-glycerophosphate
5 mM MgCl$_2$
0.1% Triton X100
5% glycerol
1 mM EGTA
1 µM microcystin-LR
+ Complete protease inhibitor mix (Roche)

Lysis buffer 2A (LP2A)   20 mM Tris/HCl, pH7.7
300 mM NaCl
10 mM NaF
20 mM ß-glycerophosphate
5 mM MgCl$_2$
0.1% Triton X100
5% glycerol
1 mM EGTA
1 µM microcystin-LR
10 mM imidazole
+ Complete protease inhibitor mix/EDTA-free (Roche)

Lysis buffer 2B (LP2B)   20 mM Tris/HCl, pH7.7
300 mM NaCl
10 mM NaF
20 mM ß-glycerophosphate
5 mM MgCl$_2$
0.1% Triton X100
5% glycerol
1 mM EGTA
1 µM microcystin-LR
30 mM imidazole
+ complete protease inhibitor mix/EDTA-free (Roche)

Lysis buffer 2C (LP2C)   50 mM Na-phosphate pH 6.5
300 mM NaCl
10 mM NaF
20 mM ß-glycerophosphate
5 mM MgCl$_2$
0.1% Triton X100
5% glycerol
1 mM EGTA
1 µM microcystin-LR
250 mM imidazole
2 mM DTT

Lysis buffer B	500 mM KCl
	100 mM Tris-HCl, pH 7.4
	5 mM $MgCl_2$
	1 mM ATP
	5% glycerol
	2 mM ß-mercaptoethanol
	+ Complete protease inhibitor mix (Roche)
SA buffer	50 mM Na-phosphate buffer pH 8.0
	100 mM NaCl
	20 mM NaF
	10 mM ß-glycerophosphate
	0.01% NP-40
	10 mM DTT
	1 mM EDTA
	1 mM EGTA
	1 µM microcystin-LR
	+ Complete protease inhibitor mix (Roche)
SB buffer	50 mM Na-phosphate buffer pH 8.0
	1 M NaCl
	20 mM NaF
	10 mM ß-glycerophosphate
	0.01% NP-40
	10 mM DTT
	1mM EDTA
	1 mM EGTA
	1 µM microcystin-LR
	+ Complete protease inhibitor mix (Roche)
Storage buffer	50% glycerol
	10 mM Na-phosphate pH 7.4
	150 mM NaCl
	0.02% NaN_3
	2 mM DTT
Urea elution buffer	8M urea
	20 mM Tris-HCl, pH 7.5
	250 mM imidazole
	pH adjusted to 7.5 with HCl
Urea lysis buffer	8M urea
	20 mM Tris-HCl, pH 8.0

Urea wash buffer	8M urea
	20 mM Tris-HCl, pH 7.5
	60 mM imidazole
	pH adjusted to 7.5 with HCl
Wash buffer 1	150 mM KCl
	50 mM Hepes/KOH, pH 7.4
	5 mM $MgCl_2$
	1 mM ATP
	5% glycerol
	2 mM ß-mercaptotethanol
	+ Complete protease inhibitor mix (Roche)
Wash buffer 2	1M KCl
	50 mM Hepes/KOH, pH 7.4
	5 mM $MgCl_2$
	1 mM ATP
	5% glycerol
	2 mM ß-mercaptotethanol
	+ Complete protease inhibitor mix (Roche)
Wash buffer NHS	5 mM Tris-HCl, pH 6.8
	150 mM NaCl
Wash buffer NTA	50 mM Na-phosphate, pH 7.4
	300 mM NaCl
	5 mM ß-mercaptoethanol
	60 mM imidazole
	pH adjusted to 7.4 with HCl
XB buffer	100 mM KCl
	0.1 mM $CaCl_2$
	1 mM $MgCl_2$
	10 mM HEPES/KOH, pH 7.7
	50 mM sucrose

Xenopus, murine and human His$_6$-p97 wt and mutants from _E. coli_
Expression constructs were generated as follows: Wildtype _Xenopus_ p97 ORF was linked to 5'-FseI and 3'-AscI-sites by PCR using oligonucleotide primers

5'-AATGGCCGGCCGATGGCTTCCGGATCAGATACCA-3' and
5'-TAAGGCGCGCCTTAACCATAGAGATCGTCGTCTTC-3'

on a plasmid kindly provided by J.M. Peters (Peters et al., 1990). The PCR-fragment was FseI/AscI-cloned into a modified pQE80 resulting in plasmid pSH355 and an N-terminal MRGS(H)$_6$GSGRP-tag. _Xenopus_ p97-E305,578Q, p97-E305,578Q,K524A, p97-E578Q, and p97-E578Q,K524A were generated from pSH355 by GeneEditor mutagenesis (see

5.2) giving rise to plasmids pSH431, pSH462, pSH421, and pSH463, respectively. Human p97-E305,578Q was generated by GeneEditor mutagenesis on a pQE30-based plasmid encoding MRGS(H)$_6$GS-tagged wildtype human p97 (obtained from H. Richly and S. Jentsch). N-terminally MRGS(H)$_6$GS-tagged murine p97-wt and p97-E305,578Q on pQE9-derived plasmids with constitutive promoters were obtained from Y. Ye.

Xenopus and human p97 proteins were expressed in BL21-DE3-RIL as described in section 5.1, murine proteins were similarly expressed in XL-1 blue but without IPTG induction (since the proteins were expressed from constitutive promoters). Pelleted bacteria were resuspended in a 10-fold volume of bacterial lysis buffer 1 and lysed in an EmulsiFlex-C5 (Avestin) according to the manufacturer's instructions. Following ultracentrifugation (35 000 rpm in a Ti45 rotor (Beckmann), 4°C, 45 min), supernatants were incubated with Ni^{2+}-NTA agarose (Qiagen) overnight at 4°C. Beads were then washed with a 20-fold volume of wash buffer NTA. Finally, bound proteins were eluted from the beads with a 2-fold volume of elution buffer NTA and dialyzed against sperm dilution buffer (human and *Xenopus* proteins) or XB buffer (murine proteins). All proteins were snap-frozen and stored in aliquots at –80°C.

Xenopus GST-p97 wt from *E. coli*
The expression construct was generated by FseI/AscI-subcloning of the *Xenopus* p97 ORF from pSH355 into a modified pGEX4T1.

After expression in BL21-DE3-RIL as described (5.1), pelleted bacteria were resuspended in a 10-fold volume of bacterial lysis buffer 2. After lysis and centrifugation as described above (purification of His$_6$-tagged p97), supernatants were incubated with gluthathione sepharose 4 Fast Flow (GE Healthcare) for 6 h at 4°C. After washing with a 20-fold volume of bacterial lysis buffer 2 (without Complete®), beads were eluted by incubation in a 1-fold volume of elution buffer GST overnight at 4°C. Eluted GST-p97 was thoroughly dialyzed against coupling buffer (4x against a 50-fold volume of coupling buffer for 30 min, 1h, 2h and 3h) to completely remove residual glutathione. Finally, the purified protein was snap-frozen and stored in aliquots at –80°C.

Xenopus His$_6$-Ufd1, His$_6$-Npl4 and His$_6$-p47 from *E. coli*
Xenopus Ufd1, Npl4, and p47 ORFs were amplified and tagged with Fse1- and Asc1-linkers by RT-PCR from *Xenopus* egg mRNA using the following oligonucleotide primers:

5'-TATGGCCGGCCCGCAATGTTTTCCTTCAACATGTTTGACCA-3' and
5'-TTAGGCGCGCCTTATGGTTTTCTGCCTTTCTTCC-3' (Ufd1)

5'-TATGGCCGGCCGATGTCGGAGAGCATTATAATTCG-3' and
5'- AATGGCGCGCCTTAGGTGTGAGGCAGCCGGCA-3' (Npl4)

5'- TAAGGCCGGCCGATGGCAGGGCAGCCGGA-3' and
5'- TATGGCGCGCCTCATATTAATCGCTGCACAATGAC-3' (p47)

The obtained PCR-products were FseI/AscI-cloned into a modified pQE80 giving rise to plasmids pSH512, pSH513, and pSH514, respectively. Additionally, Ufd1 was FseI/AscI-

subcloned from pSH512 into a modified pRSF-Duet-1 resulting in pSH694 compatible for co-transformation and expression with pSH516 (encoding GST-Npl4, see below).

Following expression in BL21-DE3-RIL (see 5.1), His_6-Npl4 and His_6-p47 were purified over Ni^{2+}-NTA agarose as described above (purification of His_6-tagged p97) and dialyzed against sperm dilution buffer. His_6-Ufd1 (as GST-Ufd1) was largely insoluble and therefore purified under denaturing conditions after expression in BL21-DE3-RIL. Towards this end, pelleted bacteria from a 1l culture were washed in 20 ml of PBS, centrifuged again (10 000 rpm, 10 min, 4°C) and resuspended in 12 ml of urea lysis buffer. After sonification in an ultrasonic bath (Branson 2510, 60% intensity) for 10 min, an ultracentrifugation (35 000 rpm, 45 min, RT) was carried out. Supernatants were incubated with 3 ml of Ni^{2+}-NTA agarose overnight at RT. After washing of the beads with a 20-fold volume of urea wash buffer, bound His_6-Ufd1 was eluted with 2 ml of urea elution buffer and dialyzed against PBS at RT. To obtain soluble recombinant His_6-Ufd1, pSH694 and pSH516 (encoding GST-Npl4, see below) were transformed and expressed together in BL21-DE3-RIL. A significant fraction of the resulting His_6-Ufd1/GST-Npl4 complex was soluble and could be purified via Ni^{2+}-NTA-agarose under native conditions as described (purification of His_6-tagged p97). Purified His_6-Ufd1/GST-Npl4 was dialyzed against coupling buffer and against sperm dilution buffer. All proteins were snap-frozen and stored in aliquots at –80°C.

Xenopus GST-Ufd1, GST-Npl4 and GST-p47 from *E. coli*
The expression constructs were generated by FseI/AscI-subcloning of the *Xenopus* Ufd1, Npl4 and p47 ORFs from pSH512, pSH513, and pSH514 into a modified pGEX4T1 resulting in plasmids pSH515, pSH516 and pSH517, respectively.

Following expression in BL21-DE3-RIL, proteins were purified over glutathione sepharose 4 Fast Flow and dialyzed against coupling buffer as described (purification of GST-p97). All proteins were snap-frozen and stored in aliquots at –80°C.

Xenopus GST-UT6 from *E.coli*
Xenopus UT6 (Hetzer et al., 2001) was amplified and tagged with Fse1- and Asc1-linkers (5'- ATTGGCCGGCCAGACCACAGTGAGTATGCTGTAG-3' and 5'-TATGGCGCGCCAGTTATGGTTTTCTGCCTTTCTTCC-3') by RT-PCR from *Xenopus* egg mRNA and cloned into a modified pGEX4T1 resulting in pSH347.

Following expression in BL21-DE3-RIL, GST-UT6 was purified and immobilized on beads as described in Meyer at al. (2000). Pelleted bacteria from a 1l culture were resuspended in 30 ml of lysis buffer B and lysed with an EmulsiFlex-C5 (Avestin). After ultracentrifugation (35 000 rpm, 45 min, 4°C), supernatants were incubated with 2 ml of gluathione sepharose 4 Fast Flow overnight at 4°C. Beads were then washed with 40 ml of wash buffer 1, 10 ml of wash buffer 2 and again 10 ml of wash buffer 1. Finally, beads were resuspended in 5 ml of storage buffer, centrifuged (700 rpm, 2 min, 4°C) and supplemented with another 2 ml of storage buffer after discarding supernatants. The 1:1 suspension of beads loaded with GST-UT6 was stored at –20°C.

Human separase/securin from 293T cells

Expression constructs (all pCS2-based) for HA$_3$-tagged human separase (plasmid pOS187.1), ZZ-Tev$_4$-tagged human separase (plasmid pOS22), human securin with a C-terminal His$_6$-Flag-His$_6$-Flag-tag (plasmid pOS237.8) and untagged human securin (plasmid pSX100) were kind gifts from O. Stemmann.

Purification of HA$_3$-separase/securin-His$_6$-Flag-His$_6$-Flag:

293T cells were transfected with pOS187.1 and pOS237.8 and sychnronized as described (see 5.3) to express HA$_3$-separase and securin-His$_6$-Flag-His$_6$-Flag. 1.5 g of harvested cells were resuspended in a 10-fold volume of LP2-A and lysed with a glass homogenisator (Dounce). Following ultracentrifugation (40 000 rpm, 30 min, 4°C) supernatants were incubated with 1 ml of Ni^{2+}-NTA agarose overnight at 4°C. Beads were washed with a 20-fold volume of LP2-B and subsequently eluted with 1 ml of LP2-C. Then, the eluate containing both separase/securin complex and free securin was dialysed against SA buffer and loaded onto a MiniS/Smart column. First, the column was washed with 5 ml of SA buffer and then eluted by linearly raising the NaCl concentration from 0.1 to 1 M (SB buffer) in 4 ml (flow rate of 30 µl/min) while collecting 50 µl-fractions (300 µl-fractions in case of flow through during washing). Subsequently, fractions were analyzed by immunoblotting using anti-Sep-M and anti-Flag antibodies. While free securin was in the flow-through fractions, separase/securin complexes eluted only at higher salt concentrations (appr. 150 mM NaCl). Fractions containing securin and separase/securin were pooled, respectively, and dialyzed against sperm dilution buffer. Finally, proteins were snap-frozen and stored at –80°C.

Purification of ZZ-Tev$_4$-separase/Flag-securin:

For expression of ZZ-Tev$_4$-separase and untagged securin, 293T cells were transfected with pOS22 and pSX100 and harvested as described (see 5.3). Cells were lysed in a 10-fold volume of LP2 using a glass homogenisator (Dounce). After ultracentrifugation (45 000 rpm, 30 min, 4°C), supernatants were incubated overnight at 4°C with IgG Sepharose 6 Fast Flow (GE Healtcare) which binds to the ZZ-tag of separase. Usually, 50 µl beads were incubated with the lysate obtained from a 10 cm cell culture dish of transfected cells. Finally, beads with immobilized separase/securin complexes were washed twice with LP2 and twice with XB prior to their incubation in *Xenopus* egg extract (see 5.6.6).

Human cyclin B1Δ90 from Sf9 cells

Kind gift from O. Stemmann. Stored in sperm dilution buffer at –80°C. Expressed and purified as described (Stemmann et al., 2001).

Human His$_6$-UbcH10 from *E. coli*

Kind gift from M. Rape. Stored in PBS, 1 mM DTT at –80°C.

Polyclonal antibodies from rabbit serum

Antibodies against *Xenopus* p97, Ufd1, Npl4, and p47 were raised in rabbits by injection of the respective His-tagged protein. Each rabbit was immunized three times with 0.5-1 mg of antigen in buffer (sperm dilution buffer in case of p97, Npl4, p47; PBS in case of Ufd1) mixed with a similar volume of TiterMax Gold adjuvant (Sigma). Intervals between

immunizations were as recommended by the manufacturer. Finally, rabbits were narcotized and bleeded to death by a veterinarian. To separate the serum, the blood was incubated at 37°C for 1h and then at 4°C overnight. After centrifugation (10 000g, 30 min, 4°C), the serum was obtained as supernatant. Usually, 60-80 ml serumwere obtained per rabbit. 10 ml were kept at 4°C for subsequent affinity purification while the remaining serum was snap-frozen and stored at –80°C. For purification of the antibodies, immunoaffinity columns with corresponding antigens were generated. Towards this end, GST-tagged proteins (GST-p97, GST-Npl4 or GST-p47) were covalently bound to N-hydroxysuccinimide (NHS-) columns (GE Healthcare) according to manufacturer's recommendations. In case of anti-Ufd1-1 and anti-Ufd1-1 antibodies, a mixture of His-tagged Ufd1 (in complex with GST-Npl4) and GST-UT6 was used for preparation of the affinity column. Columns were incubated with the respective serum overnight by slow circular flow (< 0.5 ml/min). This incubation as well as all subsequent purification steps were carried out at 4°C. Then, columns were washed with 20 ml of PBS and 1ml of wash buffer NHS and eluted with 10 ml of glycine buffer. Eluats were collected and immediately neutralized as 1ml-fractions in Eppendorf tubes containing 90 μl of 1M Tris pH 8.5. Columns were re-generated by extensive washing with PBS and stored at 4°C in PBS containing 0.1% azide. Finally, fractions were analyzed by coomassie staining. Antibody-containing fractions were pooled and dialyzed against sperm dilution buffer (anti-p97, anti-p47, anti-Npl4-1 and anti-Npl4-1) or XB-buffer (anti-Ufd1-1 and anti-Ufd1-2). Since some experiments required highly concentrated anti-Ufd1 or anti-Npl4-1 antibodies, fractions of these antibodies were further concentrated in Microcon Centrifuge Devices (YM-10, Millipore). All antibodies were snap-frozen in aliquots and stored at –80°C.

5.6 Biochemical assays

5.6.1 Pulldown experiments

To characterize the antibodies anti-Ufd1-1, anti-Ufd1-2, anti-Npl4-1, anti-Npl4-2 and anti-p47 by immunoprecipiation, 10 μg of antibody were bound each to 50 μl magnetic protein A beads (DYNAL) and washed with XB buffer prior to incubation in 35 μl of *Xenopus* highΔ90-extract for 30 min at 18°C. Beads were then washed three times with XB buffer (+0.05% Tween 20) and resuspended in sample buffer. To investigate interactions between p97 and nucleoplasmin or tubulin, the following pulldown experiments were performed: 30 μg of anti-Npl4-2 were coupled to 20 μl of protein G sepharose (GE Healthcare). Beads were blocked by incubation with 50 mg/ml BSA in TBS-w for 2 h and washed twice with XB. Following incubation in 90 μl of *Xenopus* high-speed extract for 1 h at 18°C, beads were washed three times with XB buffer (+0.01% Tween 20, + 200mM NaCl) and resuspended in sample buffer. Similarly, 100 μg of anti-p97 were bound to 20 μl of protein G sepharose. Beads were blocked with BSA as described and washed with XB buffer. After incubation in 120 μl of *Xenopus* high-speed extract for 1 h at 18°C, beads were washed twice with XB buffer (+1% Tween 20) and twice with XB buffer (+500 mM NaCl). Finally, beads were resuspended in sample buffer. For all immunoprecipiation experiments, controls were performed by using corresponding amounts of unspecific IgG. For UT6-pulldowns, 60 μl of glutathione sepharose with coupled GST-UT6 (see 5.5.2) or GST as control were washed with XB buffer and incubated in 60 μl of CSF-extract for 1h at 18°C. Beads were then washed

twice with XB buffer (+1% Tween 20) and twice with XB buffer (+300 mM salt) and were finally resuspended in sample buffer. Beads from all experiments were analyzed by SDS-PAGE and immunoblotting.

5.6.2 Depletion of p97 and its adaptors

For depletion of p97 from *Xenopus* high-speed extract, GST-UT6 immobilized on glutathione sepharose (see section 5.5.2) was used while glutathione sepharose coupled to GST alone served as control. To deplete 60μl of high-speed extracts, two rounds of 30 min-depletion at 18°C were performed each with 60μl of GST-UT6 beads or GST beads. For depletion of Ufd1, Npl4 or p47 from CSF-extracts, antibodies were coupled to magnetic protein A beads (DYNAL) at a ratio of 1 mg per 4 ml suspension. Beads were washed with XB buffer before performing two rounds of 30-min depletion at 12°C. Optimal depletion of 50 μl *Xenopus* egg extract was achieved by using 2x 15 μg anti-Ufd1-1, 2x 20 μg anti-Npl4-1, or 2x 10 μg anti-p47. Co-depletion of Ufd1 and Npl4 was done with 15 μg anti-Ufd1-1 in the first and 20 μg anti-Npl4-1 in the second round. As controls, egg extracts were mock-depleted using the corresponding amounts of unspecific rabbit IgG.

5.6.3 Malachit-green ATPase assay

To confirm eliminated ATPase activity of mutant p97 proteins, malachite green assays were performed as follows: Two or five μg of recombinant p97 in 40 μl sperm dilution buffer were supplemented with ATP to 0.4 mM and incubated at 37°C. After 0, 15 and 30 min, 10 μl aliquots were mixed with 40 μl of 1 M perchloric acid. Stopped reactions were finally combined with 40μl of malachite green solution (4.2 g ammonium moldybdate in 100 ml 4M HCl mixed with 0.135 g malachite green in 300 ml H_2O) and incubated for 20 min at room temperature before measuring extinctions at 615 nm.

5.6.4 ATP bioluminescense assay

5 μl and 10 μl of sperm preparation (1.3x10^8/ml) were filled up each to a total volume of 25 μl with dilution buffer (ATP Bioluminescence Assay Kit HS II, Roche). ATP determination by the ATP Bioluminescence Assay Kit HS II (Roche) is based on the ATP dependency of the light emitting oxidation of luciferin catalyzed by luciferase. This technique allows the measurement of extremely low concentrations of ATP. Sperm samples were processed according to the manufacturer's instructions and compared to standard ATP solutions. ATP concentration of the sperm preparation was finally calculated as the mean value of the 5 and 10 μl sperm sample.

5.6.5 Analysis of endogenous separase from HCT116 cells

HCT116 wt and HCT116 securin$^{-/-}$ cells were grown as described (see section 5.3) and synchronized at a confluence of 70% by the addition of nocodazole (0.2 μg/ml final concentration) for 14 h. For quantification and comparison of separase levels, cells from six 75 ml dishes of each cell line were lysed in 2 ml of LP2 using a glass homogenisator (Dounce). Following ultracentrifugation (45 000 rpm, 4°C, 30 min) supernatants were analyzed by immunoblotting using anti-Sep-N and anti-tubulin antibodies. Separase signals were quantified by normalizing to ß-tubulin. For activity assays, comparable

amounts of separase were immunoprecipitated from both cell lines. Towards this end, four 75 ml dishes of HCT116 wt and 12 75 ml dishes of hSecurin$^{-/-}$ were lysed and centrifuged as described above. Supernatants were incubated each with 8 μg of anti-Sep-M antibody bound to 30 μl of Protein G Sepharose 4 Fast Flow (GE Healthcare) overnight at 4°C. After washing the beads twice with LP2 and twice with XB, 5 μl of the beads were removed to check amounts of immunoprecipitated separase by immunoblotting. Remaining beads were incubated in *Xenopus* egg extract and put into an Scc1 cleavage assay (see section 5.6.8).

5.6.6 Separase activity assays

Activation of purified human separase/securin complexes in *Xenopus* egg extract and Scc1 cleavage assays were performed as described (Stemmann et al., 2001). The role of p97 during separase activation was investigated by modification of the protocol as outlined below.

Cleavage buffer	30 mM Hepes/KOH pH 7.7
	30% glycerol
	25 mM NaF
	25 mM KCl
	5 mM MgCl$_2$
	1 mM EGTA/KOH pH 7.5

Endogenous separase from HCT116 wt or securin$^{-/-}$ cells:
Endogenous separase immunopreciptated with anti-Sep-M antibody coupled to protein G sepharose (see 5.6.5) was activated as follows: 25 μl of the beads were were washed with XB buffer and incubated in 250 μl of lowΔ90-extract for 1 h at 18°C. Then, beads were washed with XB buffer and cleavage buffer. After removal of 5 μl of beads for immunoblotting, remaining beads were supplemented with 2 μl of antigenic peptide (GSDGEDSASGGKTPA), 20 μl of cleavage buffer and 4 μl of *in-vitro* translated ^{35}S-Scc1. Aliquots were taken 0, 20 and 60 min thereafter and analyzed by autoradiography.

Human ZZ-Tev$_4$-separase from 293T cells (activity assay with re-isolated separase):
ZZ-Tev$_4$-separase was bound to IgG sepharose as described (see section 5.5.2) was activated in *Xenopus* egg extracts as follows: 10 μl of beads were incubated in 90 μl of freshly prepared lowΔ90-extract that had been either depleted from Ufd1-Npl4 (see section 5.6.2) or p47. As control, 10 μl of beads were incubated in mock-depleted extract using unspecific IgG. After incubation for 1h at 18°C, beads were re-isolated and washed three times with XB buffer. Then, separase was eluted from the beads by incubation with Tev protease for 30 min at 18°C resulting in clipping of the ZZ-tag. Finally, 3 μl of the eluted separase were mixed with 6 μl of cleavage buffer and 2 μl of *in-vitro* translated ^{35}S-Scc1. Aliquots were taken 0, 10 and 60 min after addition of ^{35}S-Scc1 and analyzed by autoradiography.

HA$_3$-separase from 293T cells (in-extract cleavage assay):
Free HA$_3$-separase/securin complexes were activated in *Xenopus* egg extract as follows: 30 μl of lowΔ90-extract were supplemented with p97-QQ (2μg/μl final) and 1.6 μl of

purified separase/securin complexes (see 5.5.2). During incubation for 1h at 18°C, aliquots were taken after 0 and 30 min for analysis by immunoblotting. Then, 1.2 µl of *in-vitro* translated ^{35}S-Scc1 were added to the extract. Aliquots were taken 0,10, 20 and 60 min thereafter and analyzed by immunoblotting and autoradiography.

5.6.7 Translation and activation of separase from *in vitro*-generated mRNA

For translation and activation of separase in *Xenopus* egg extract and investigation of an involvement of p97 in these processes, the following experiments were carried out: 24 µl of CSF-extract were supplemented either with 2 µl of Myc$_6$-Tev$_2$-separase-encoding mRNA (200 ng/µl, generated as described in 5.2) alone or together with 0.6 µl of human securin protein (see 5.5.2). Buffer supplementations instead of mRNA served as controls. To investigate a putative requirement of p97, the same samples were prepared but additionally contained human p97-QQ at a final concentration of 2 mg/ml. All extracts were incubated for 75 min at RT to allow for translation and then supplemented with cyclin B1Δ90 (80 nM) After 10 min, extracts were released from CSF by addition of Ca^{2+} to 0.6 mM final and were incubated for another 120 min. Aliquots were taken 0, 60 and 90 min after release and analyzed by immunoblotting. In an alternative approach, CSF-extracts were depleted from Ufd1-Npl4 and then supplemented with 2 µl of Myc$_6$-Tev$_2$-separase-encoding mRNA and 0.6 µl of human securin protein. Mock-depleted extracts served as controls. Incubation, release and analysis of extracts was carried out as described above.

5.7 Cell biological *in-vitro* assays

5.7.1 Spindle disassembly assays

CSF-extracts were supplemented with recombinant p97 or human cyclin B1Δ90 at final concentrations of 0.5 to 5 mg/ml or 0.03 mg/ml, respectively, and incubated for 30 to 60 min at 4°C. For kinetic evaluation of spindle disassembly (Fig. 15), extracts were pre-incubated with murine p97-wt or -QQ at 1 mg/ml final for 30 min. Alternatively, Ufd1-Npl4 or p47 were immunodepleted from CSF-extract (see 5.6.2). In two experiments shown in Tab. 1 and in Fig. 15, soluble anti-Npl4-1 antibody or anti-Ufd1-1 antibody were additionally added to depleted extract (each 0.25 mg/ml final). To generate and visualize spindles, CSF extracts were then combined with rhodamine-labelled tubulin (Cytoskeleton, Denver, USA) and sperm nuclei in final concentrations of 200 – 2000 per µl extract. To facilitate quantification of chromatin-associated asters, experiments shown in Fig. 15 were performed at 500 sperm nuclei per ml extract. After incubation for 30 min at 20°C, extracts were released into interphase at 25°C by two additions of Ca^{2+} (0.6 mM final each) 5 min after one another. Aliquots taken every 5 to 15 min after release were fixed and DAPI-stained as described (Philpott et al., 1991). To determine the kinetics of mitotic exit, 100 to 150 sperm nuclei per aliquot were analyzed for condensation status and associated spindle. Disassembly of chromatin-independent MT-asters was investigated by using purified human centrosomes (kind gift of T. Mayer) instead of sperm nuclei. In these experiments, spindles were allowed to form for 30 min at 25°C instead of 20°C.

5.7.2 ERAD in *Xenopus* egg extracts

To compare translation of CFTRΔF508-encoding mRNA in *Xenopus* egg extract with its translation in reticulocyte lysate (carried out as described in 5.2), the mRNA was incubated in CSF-extract at x 0.05 mg/ml final for 3h at 20°C. Reaction products were analyzed by immunoblotting. Shut-off experiments were performed at 20°C as follows: CSF-arrested extracts (without cycloheximide) were released by adding Ca^{2+} to 0.6 mM. Ten min thereafter, extracts were supplemented with mRNA to 0.05 mg/ml and incubated for additional 80 min to allow for translation of CFTRΔF508. Then, *Xenopus* p97-QQ (0.25 - 1 mg/ml final concentration) or sperm dilution buffer were added and extracts were incubated for another 15 min. Thereafter, translation was stopped by addition of cycloheximide to 0.2 µg/µl. Aliquots were taken at 0, 30, 45, 60, 75, and 90 min after inhibition of translation and subjected to immunoblotting against CFTR and ß-tubulin.

5.7.3 Mitotic checkpoint assays

To establish a SAC in *Xenopus* egg extracts, a suitable sperm concentration was determined in the following setup: CSF-extract was supplemented with rhodamine-labelled tubulin (250x, Cytoskeleton) and *in-vitro* translated human ^{35}S-securin (1/20 of extract volume). Then, the extract was partitioned and additionally supplemented with *Xenopus* sperm nuclei in different final concentrations. All extracts were released by the addition of Ca^{2+} (0.6 mM final) in the presence of nocodazole (0.01 mg/ml final). Aliquots were taken 0, 15, 30 and 45 min after release and analyzed for ^{35}S-securin levels and for chromatin morphology after DAPI-staining. A concentration of 5000 sperm/µl extract turned out to be sufficient to activate the SAC as judged by unchanged ^{35}S-securin levels and (mitotic) chromatin morphology 45 min after release. Therefore, a sperm concentration of 5000 sperm/µl was used in the following experiments. To test if recombinant UbcH10 can inactivate the SAC in *Xenopus* egg extracts, CSF-extracts containing rhodamine-labelled tubulin, ^{35}S-securin, 5000 sperm/µl and nocodazole (0.01 mg/ml) were additionally supplemented with human UbcH10 or buffer as control. After addition of Ca^{2+}, ^{35}S-securin levels and chromatin morphology were again monitored by taking aliquots after 0, 15, 30 and 60 min. A final UbcH10 concentration of 0.5 mg/ml turned out to efficiently inactivate the SAC. Finally, an involvement of p97 in UbcH10-dependent checkpoint inactivation was investigated as follows: CSF-extracts were supplemented with rhodamine-labelled tubulin, ^{35}S-securin, sperm and nocodazole as described and were released by addition of Ca^{2+} in the presence or absence of *Xenopus* p97-QQ (final 1 µg/µl). Extracts supplemented with buffer instead of nocodazole and/or buffer instead of p97-QQ served as controls. ^{35}S-securin levels and chromatin morphology were investigated as described. In an alternative approach, p97 function was blocked in CSF-extracts by depleting Ufd1-Npl4 or p47. Mock-depleted extracts served as controls. All extracts were then supplemented and tested for SAC inactivation as described above. Release from CSF by addition of UbcH10 was tested by adding UbcH10 (0.5 mg/ml final) to CSF-extracts containing rhodamine-labelled tubulin, ^{35}S-securin and sperm nuclei as described. Aliquots were taken 0, 15, 30, 45 and 60 min after UbcH10 addition. Extracts released by addition of Ca^{2+} served as controls for these experiments.

5.7.4 Sperm decondensation assay

The role of p97 in stage I sperm decondensation was investigated as follows (outlined in Fig. 25B): *Xenopus* high-speed extract was depleted from Ufd-Npl4 (see x.x.x) or mock-depleted. Ufd1-Npl4 depleted extract was partitioned. One half was supplemented with recombinant His-Ufd1/GST-Npl4 to 0.8 μg/μl final (rescued extract) while the other half remained untreated (depleted extract). In parallel, sperm nuclei were prepared: 1 μl of sperm nuclei (1.3x10^8/ml) was incubated with anti-Ufd1-1 antibody (1.5 μg/μl final) in a total volume of 10 μl. After incubation for 45 min at RT, the sample was mixed and partitioned. One half was incubated with 2 μl of His-Ufd1/GST-Npl4 (corresponding to 4.2 μg/μl final, rescued sperm) for 15 min at RT while the other half was similarly incubated with 2 μl of sperm dilution buffer (depleted sperm). To prepare mock-treated sperm, 1 μl of sperm nuclei was incubated with XB buffer in a total volume of 10 μl and incubated for 45 min at RT. Then, 4 μl sperm dilution buffer were added following another incubation for 15 min at RT (mock-depleted sperm). 1 μl-aliquots of all three sperm samples were taken and DAPI-fixed (0 min). Finally, sperm swelling was started by adding 1.4 μl of mock-depleted, depleted and rescued sperm to 20 μl of correspondingly treated extracts. 2 μl -aliquots were taken after 1.5, 3, 4.5, 6, 10, 15 and 30 min. Samples were DAPI-fixed and analyzed for sperm length (50 nuclei each) at 400x magnification.

6 REFERENCES

Alberts, B., Johnson, A., Lewis, J., Raff, M., Roberts, K. and Walter, P. (2002) Molecular biology of the cell. 4th edition. New York, Garland.

Aristarkhov, A., Eytan, E., Moghe, A., Admon, A., Hershko, A. and Ruderman, J. V. (1996). E2-C, a cyclin-selective ubiquitin carrier protein required for the destruction of mitotic cyclins. *Proc Natl Acad Sci USA* 93, 4294-4299.

Ausio, J. (1999). Histone H1 and evolution of sperm nuclear basic proteins. *J Biol Chem* 274, 31115-31118.

Ausubel, F. M., Brent, R., Kingston, R. E., Moore, D. D., Seidman, J. G., Smith, J. A. and Struhl, K. (1998). Current protocols in molecular biology (New York, Greene publishing associates).

Bergmann, M. (2005). [Spermatogenesis--physiology and pathophysiology]. *Urologe A* 44, 1131-1132, 1134-1138.

Bernal, J. A., Luna, R., Espina, A., Lazaro, I., Ramos-Morales, F., Romero, F., Arias, C., Silva, A., Tortolero, M. and Pintor-Toro, J. A. (2002). Human securin interacts with p53 and modulates p53-mediated transcriptional activity and apoptosis. *Nat Genet* 32, 306-311.

Bruderer, R. M., Brasseur, C. and Meyer, H. H. (2004). The AAA ATPase p97/VCP interacts with its alternative co-factors, Ufd1-Npl4 and p47, through a common bipartite binding mechanism. *J Biol Chem* 279, 49609-16.

Cao, K., Nakajima, R., Meyer, H. H. and Zheng, Y. (2003). The AAA-ATPase Cdc48/p97 regulates spindle disassembly at the end of mitosis. *Cell* 115, 355-67.

Ciosk, R., Shirayama, M., Shevchenko, A., Tanaka, T., Toth, A. and Nasmyth, K. (2000). Cohesin's binding to chromosomes depends on a separate complex consisting of Scc2 and Scc4 proteins. *Mol Cell* 5, 243-54.

De Antoni, A., Pearson, C. G., Cimini, D., Canman, J. C., Sala, V., Nezi, L., Mapelli, M., Sironi, L., Faretta, M., Salmon, E. D. et al. (2005). The Mad1/Mad2 complex as a template for Mad2 activation in the spindle assembly checkpoint. *Curr Biol* 15, 214-25.

DeLaBarre, B. and Brunger, A. T. (2003). Complete structure of p97/valosin-containing protein reveals communication between nucleotide domains. *Nat Struct Biol* 10, 856-63.

Fan, H. Y., Sun, Q. Y. and Zou, H. (2006). Regulation of Separase in meiosis: Separase is activated at the metaphase I-II transition in Xenopus oocytes during meiosis. *Cell Cycle* 5, 198-204.

Frehlick, L. J., Eirin-Lopez, J. M., Jeffery, E. D., Hunt, D. F. and Ausio, J. (2006). The

characterization of amphibian nucleoplasmins yields new insight into their role in sperm chromatin remodeling. *BMC Genomics* 7, 99.

Frohlich, K. U., Fries, H. W., Rudiger, M., Erdmann, R., Botstein, D. and Mecke, D. (1991). Yeast cell cycle protein CDC48p shows full-length homology to the mammalian protein VCP and is a member of a protein family involved in secretion, peroxisome formation, and gene expression. *J Cell Biol* 114, 443-53.

Funabiki, H., Yamano, H., Kumada, K., Nagao, K., Hunt, T. and Yanagida, M. (1996). Cut2 proteolysis required for sister-chromatid seperation in fission yeast. *Nature* 381, 438-41.

Gimenez-Abian, J. F., Sumara, I., Hirota, T., Hauf, S., Gerlich, D., de la Torre, C., Ellenberg, J. and Peters, J. M. (2004). Regulation of sister chromatid cohesion between chromosome arms. *Curr Biol* 14, 1187-93.

Glotzer, M., Murray, A. W. and Kirschner, M. W. (1991). Cyclin is degraded by the ubiquitin pathway. *Nature* 349, 132-8.

Gorr, I. H., Boos, D. and Stemmann, O. (2005). Mutual inhibition of separase and Cdk1 by two-step complex formation. *Mol Cell* 19, 135-41.

Glover, J. R. and Lindquist, S. (1998). Hsp104, Hsp70, and Hsp40: a novel chaperone system that rescues previously aggregated proteins. *Cell* 94, 73-82.

Hauf, S., Roitinger, E., Koch, B., Dittrich, C. M., Mechtler, K. and Peters, J. M. (2005). Dissociation of cohesin from chromosome arms and loss of arm cohesion during early mitosis depends on phosphorylation of SA2. *PLoS Biol* 3, e69.

Heald, R., Tournebize, R., Blank, T., Sandaltzopoulos, R., Becker, P., Hyman, A. and Karsenti, E. (1996). Self-organization of microtubules into bipolar spindles around artificial chromosomes in Xenopus egg extracts. *Nature* 382, 420-5.

Hetzer, M., Gruss, O. J. and Mattaj, I. W. (2002). The Ran GTPase as a marker of chromosome position in spindle formation and nuclear envelope assembly. *Nat Cell Biol* 4, E177-84.

Hetzer, M., Meyer, H. H., Walther, T. C., Bilbao-Cortes, D., Warren, G. and Mattaj, I. W. (2001). Distinct AAA-ATPase p97 complexes function in discrete steps of nuclear assembly. *Nat Cell Biol* 3, 1086-91.

Heubes, S. and Stemmann, O. (2007). The AAA-ATPase p97-Ufd1-Npl4 is required for ERAD but not for spindle disassembly in Xenopus egg extracts. *J Cell Sci* 120, 1325-9.

Holland, A. J. and Taylor, S. S. (2006). Cyclin-B1-mediated inhibition of excess separase is required for timely chromosome disjunction. *J Cell Sci* 119, 3325-3336.

Holloway, S. L., Glotzer, M., King, R. W. and Murray, A. W. (1993). Anaphase is initiated by proteolysis rather than by the inactivation of maturation-promoting factor. *Cell* 73, 1393-402.

Huang, X., Hatcher, R., York, J. P. and Zhang, P. (2005). Securin and separase phosphorylation act redundantly to maintain sister chromatid cohesion in Mammalian cells. *Mol Biol Cell* 16, 4725-32.

Ikai, N. and Yanagida, M. (2006). Cdc48 is required for the stability of Cut1/separase in mitotic anaphase. *J Struct Biol* 156, 50-61.

Ivanov, D. and Nasmyth, K. (2005). A topological interaction between cohesin rings and a circular minichromosome. *Cell* 122, 849-60.

Jager, H., Herzig, B., Herzig, A., Sticht, H., Lehner, C. F. and Heidmann, S. (2004). Structure predictions and interaction studies indicate homology of separase N-terminal regulatory domains and Drosophila THR. *Cell Cycle* 3, 182-8.

Jallepalli, P. V., Waizenegger, I. C., Bunz, F., Langer, S., Speicher, M. R., Peters, J., Kinzler, K. W., Vogelstein, B. and Lengauer, C. (2001). Securin is required for chromosomal stability in human cells. *Cell* 105, 445-57.

Jensen, S., Segal, M., Clarke, D. J. and Reed, S. I. (2001). A novel role of the budding yeast separin Esp1 in anaphase spindle elongation: evidence that proper spindle association of Esp1 is regulated by Pds1. *J Cell Biol* 152, 27-40.

Kirschner, M. and Mitchison, T. (1986). Beyond self-assembly: from microtubules to morphogenesis. *Cell* 45, 329-42.

Kitajima, T. S., Kawashima, S. A. and Watanabe, Y. (2004). The conserved kinetochore protein shugoshin protects centromeric cohesion during meiosis. *Nature* 427, 510-7.

Kitami, M. I., Kitami, T., Nagahama, M., Tagaya, M., Hori, S., Kakizuka, A., Mizuno, Y. and Hattori, N. (2006). Dominant-negative effect of mutant valosin-containing protein in aggresome formation. *FEBS Lett* 580, 474-8.

Kunkle, M. and Longo, F. J. (1975). Cytological events leading to the cleavage of golden hamster zygotes. *J Morphol* 146, 197-213.

Kumada, K., Yao, R., Kawaguchi, T., Karasawa, M., Hoshikawa, Y., Ichikawa, K., Sugitani, Y., Imoto, I., Inazawa, J., Sugawara, M. et al. (2006). The selective continued linkage of centromeres from mitosis to interphase in the absence of mammalian separase. *J Cell Biol* 172, 835-46.

Laskey, R. A., Honda, B. M., Mills, A. D. and Finch, J. T. (1978). Nucleosomes are assembled by an acidic protein which binds histones and transfers them to DNA. *Nature* 275, 416-20.

Lu, Z., Zhang, C. and Zhai, Z. (2005). Nucleoplasmin regulates chromatin condensation during apoptosis. *Proc Natl Acad Sci U S A* 102, 2778-83.

Mathe, E., Kraft, C., Giet, R., Deak, P., Peters, J. M. and Glover, D. M. (2004). The E2-C vihar is required for the correct spatiotemporal proteolysis of cyclin B and itself undergoes cyclical degradation. *Curr Biol* 14, 1723-33.

Mei, J., Huang, X. and Zhang, P. (2001). Securin is not required for cellular viability, but is required for normal growth of mouse embryonic fibroblasts. *Curr Biol* 11, 1197-201.

Meusser, B., Hirsch, C., Jarosch, E. and Sommer, T. (2005). ERAD: the long road to destruction. *Nat Cell Biol* 7, 766-772.

Meyer, H. H., Shorter, J. G., Seemann, J., Pappin, D. and Warren, G. (2000). A complex of mammalian ufd1 and npl4 links the AAA-ATPase, p97, to ubiquitin and nuclear transport pathways. *EMBO J* 19, 2181-2192.

Meyer, H. H., Wang, Y. and Warren, G. (2002). Direct binding of ubiquitin conjugates by the mammalian p97 adaptor complexes, p47 and Ufd1-Npl4. *EMBO J* 21, 5645-5652.

Miller, J. J., Summers, M. K., Hansen, D. V., Nachury, M. V., Lehman, N. L., Loktev, A. and Jackson, P. K. (2006). Emi1 stably binds and inhibits the anaphase-promoting complex/cyclosome as a pseudosubstrate inhibitor. *Genes Dev* 20, 2410-20.

Mills, A. D., Laskey, R. A., Black, P. and De Robertis, E. M. (1980). An acidic protein which assembles nucleosomes in vitro is the most abundant protein in Xenopus oocyte nuclei. *J Mol Biol* 139, 561-8.

Minshull, J., Sun, H., Tonks, N. K. and Murray, A. W. (1994). A MAP kinase-dependent spindle assembly checkpoint in Xenopus egg extracts. *Cell* 79, 475-486.

Moir, D., Stewart, S. E., Osmond, B. C. and Botstein, D. (1982). Cold-sensitive cell-division-cycle mutants of yeast: isolation, properties, and pseudoreversion studies. *Genetics* 100, 547-63.

Muller, J. M., Deinhardt, K., Rosewell, I., Warren, G. and Shima, D. T. (2007). Targeted deletion of p97 (VCP/CDC48) in mouse results in early embryonic lethality. *Biochem Biophys Res Commun* 354, 459-65.

Murray, A. W. (1989). Cell biology: the cell cycle as a cdc2 cycle. *Nature* 342, 14-5.

Murray, A. W. and Kirschner, M. W. (1989). Cyclin synthesis drives the early embryonic cell cycle. *Nature* 339, 275-280.

Nagao, K., Adachi, Y. and Yanagida, M. (2004). Separase-mediated cleavage of cohesin at interphase is required for DNA repair. *Nature* 430, 1044-8.

Nasmyth, K. (2005). How do so few control so many? *Cell* 120, 739-46.

Nasmyth, K. and Haering, C. H. (2005). The structure and function of SMC and kleisin complexes. *Annu Rev Biochem* 74, 595-648.

Nishiyama, T., Ohsumi, K. and Kishimoto, T. (2007). Phosphorylation of Erp1 by p90rsk is required for cytostatic factor arrest in Xenopus laevis eggs. *Nature* 446, 1096-9.

Okiyoneda, T., Harada, K., Takeya, M., Yamahira, K., Wada, I., Shuto, T., Suico, M. A., Hashimoto, Y. and Kai, H. (2004). Delta F508 CFTR pool in the endoplasmic reticulum is increased by calnexin overexpression. *Mol Biol Cell* 15, 563-574.

Papi, M., Berdougo, E., Randall, C. L., Ganguly, S. and Jallepalli, P. V. (2005). Multiple roles for separase auto-cleavage during the G2/M transition. *Nat Cell Biol* 7, 1029-35.

Peters, J. M., Walsh, M. J. and Franke, W. W. (1990). An abundant and ubiquitous homo-oligomeric ring-shaped ATPase particle related to the putative vesicle fusion proteins Sec18p and NSF. *EMBO J* 9, 1757-1767.

Peters, J. M. (2002). The anaphase-promoting complex: proteolysis in mitosis and beyond. *Mol Cell* 9, 931-43.

Pfleghaar, K., Heubes, S., Cox, J., Stemmann, O. and Speicher, M. R. (2005). Securin is not required for chromosomal stability in human cells. *PLoS Biol* 3, e416.

Philpott, A. and Leno, G. H. (1992). Nucleoplasmin remodels sperm chromatin in Xenopus egg extracts. *Cell* 69, 759-67.

Philpott, A., Leno, G. H. and Laskey, R. A. (1991). Sperm decondensation in Xenopus egg cytoplasm is mediated by nucleoplasmin. *Cell* 65, 569-78.

Pickart, C. M. and Eddins, M. J. (2004). Ubiquitin: structures, functions, mechanisms. *Biochim Biophys Acta* 1695, 55-72.

Pye, V. E., Dreveny, I., Briggs, L. C., Sands, C., Beuron, F., Zhang, X. and Freemont, P. S. (2006). Going through the motions: The ATPase cycle of p97. *J Struct Biol* 156, 12-28.

Rabinovich, E., Kerem, A., Frohlich, K. U., Diamant, N. and Bar-Nun, S. (2002). AAA-ATPase p97/Cdc48p, a cytosolic chaperone required for endoplasmic reticulum-associated protein degradation. *Mol Cell Biol* 22, 626-34.

Rape, M. and Kirschner, M. W. (2004). Autonomous regulation of the anaphase-promoting complex couples mitosis to S-phase entry. *Nature* 432, 588-95.

Rape, M., Hoppe, T., Gorr, I., Kalocay, M., Richly, H. and Jentsch, S. (2001). Mobilization of processed, membrane-tethered SPT23 transcription factor by CDC48(UFD1/NPL4), a ubiquitin-selective chaperone. *Cell* 107, 667-77.

Rauh, N. R., Schmidt, A., Bormann, J., Nigg, E. A. and Mayer, T. U. (2005). Calcium triggers exit from meiosis II by targeting the APC/C inhibitor XErp1 for degradation. *Nature* 437, 1048-52.

Reddy, S. K., Rape, M., Margansky, W. A. and Kirschner, M. W. (2007). Ubiquitination by the anaphase-promoting complex drives spindle checkpoint inactivation. *Nature* 446, 921-5.

Riedel, C. G., Katis, V. L., Katou, Y., Mori, S., Itoh, T., Helmhart, W., Galova, M., Petronczki, M., Gregan, J., Cetin, B. et al. (2006). Protein phosphatase 2A protects centromeric sister chromatid cohesion during meiosis I. *Nature* 441, 53-61.

Sambrook, J., Fritsch, E. F. and Maniatis, T. (1989). Molecular Cloning (Cold Spring Harbor, *CSH Laboratory Press*).

Sasagawa, Y., Yamanaka, K., Nishikori, S. and Ogura, T. (2007). Caenorhabditis elegans p97/CDC-48 is crucial for progression of meiosis I. *Biochem Biophys Res Commun* 358, 920-4.

Schlieker, C., Weibezahn, J., Patzelt, H., Tessarz, P., Strub, C., Zeth, K., Erbse, A., Schneider-Mergener, J., Chin, J. W., Schultz, P. G., Bukau, B. and Mogk, A. (2004). Substrate recognition by the AAA+ chaperone ClpB. *Nat Struct Mol Biol* 11, 607-615.

Schmidt, A., Duncan, P. I., Rauh, N. R., Sauer, G., Fry, A. M., Nigg, E. A. and Mayer, T. U. (2005). Xenopus polo-like kinase Plx1 regulates XErp1, a novel inhibitor of APC/C activity. *Genes Dev* 19, 502-13.

Schmidt, A., Rauh, N. R., Nigg, E. A. and Mayer, T. U. (2006). Cytostatic factor: an activity that puts the cell cycle on hold. *J Cell Sci* 119, 1213-8.

Seino, H., Kishi, T., Nishitani, H. and Yamao, F. (2003). Two ubiquitin-conjugating enzymes, UbcP1/Ubc4 and UbcP4/Ubc11, have distinct functions for ubiquitination of mitotic cyclin. *Mol Cell Biol* 23, 3497-505.

Skibbens, R. V., Corson, L. B., Koshland, D. and Hieter, P. (1999). Ctf7p is essential for sister chromatid cohesion and links mitotic chromosome structure to the DNA replication machinery. *Genes Dev* 13, 307-19.

Song, C., Wang, Q. and Li, C. C. (2003). ATPase activity of p97-valosin-containing protein (VCP). D2 mediates the major enzyme activity, and D1 contributes to the heat-induced activity. *J Biol Chem* 278, 3648-3655.

Stegmeier, F., Rape, M., Draviam, V. M., Nalepa, G., Sowa, M. E., Ang, X. L., McDonald, E. R., 3rd, Li, M. Z., Hannon, G. J., Sorger, P. K. et al. (2007). Anaphase initiation is regulated by antagonistic ubiquitination and deubiquitination activities. *Nature* 446, 876-81.

Stemmann, O., Zou, H., Gerber, S. A., Gygi, S. P. and Kirschner, M. W. (2001). Dual inhibition of sister chromatid separation at metaphase. *Cell* 107, 715-26.

Sudakin, V., Chan, G. K. and Yen, T. J. (2001). Checkpoint inhibition of the APC/C in HeLa cells is mediated by a complex of BUBR1, BUB3, CDC20, and MAD2. *J Cell Biol* 154, 925-936.

Tamada, H., Van Thuan, N., Reed, P., Nelson, D., Katoku-Kikyo, N., Wudel, J., Wakayama, T. and Kikyo, N. (2006). Chromatin decondensation and nuclear reprogramming by nucleoplasmin. *Mol Cell Biol* 26, 1259-71.

Thoms, S. (2002). Cdc48 can distinguish between native and non-native proteins in the absence of cofactors. *FEBS Lett* 520, 107-110.

Tong, Y., Tan, Y., Zhou, C. and Melmed, S. (2007). Pituitary tumor transforming gene interacts with Sp1 to modulate G1/S cell phase transition. *Oncogene*.

Townsley, F. M., Aristarkhov, A., Beck, S., Hershko, A. and Ruderman, J. V. (1997). Dominant-negative cyclin-selective ubiquitin carrier protein E2-C/UbcH10 blocks cells in metaphase. *Proc Natl Acad Sci U S A* 94, 2362-7.

Turner, D. L. and Weintraub, H. (1994). Expression of achaete-scute homolog 3 in Xenopus embryos converts ectodermal cells to a neural fate. *Genes Dev* 8, 1434-1447.

Uchiyama, K. and Kondo, H. (2005). p97/p47-Mediated biogenesis of Golgi and ER. *J Biochem (Tokyo)* 137, 115-9.

Uhlmann, F., Wernic, D., Poupart, M. A., Koonin, E. V. and Nasmyth, K. (2000). Cleavage of cohesin by the CD clan protease separin triggers anaphase in yeast. *Cell* 103, 375-86.

Varga, K., Jurkuvenaite, A., Wakefield, J., Hong, J. S., Guimbellot, J. S., Venglarik, C. J., Niraj, A., Mazur, M., Sorscher, E. J., Collawn, J. F. and Bebok, Z. (2004). Efficient intracellular processing of the endogenous cystic fibrosis transmembrane conductance regulator in epithelial cell lines. *J Biol Chem* 279, 22578-22584.

Verde, F., Dogterom, M., Stelzer, E., Karsenti, E. and Leibler, S. (1992). Control of microtubule dynamics and length by cyclin A- and cyclin B-dependent kinases in Xenopus egg extracts. *J Cell Biol* 118, 1097-108.

Verde, F., Labbe, J. C., Doree, M. and Karsenti, E. (1990). Regulation of microtubule dynamics by cdc2 protein kinase in cell-free extracts of Xenopus eggs. *Nature* 343, 233-8.

Vong, Q. P., Cao, K., Li, H. Y., Iglesias, P. A. and Zheng, Y. (2005). Chromosome alignment and segregation regulated by ubiquitination of survivin. *Science* 310, 1499-504.

Waizenegger, I. C., Hauf, S., Meinke, A. and Peters, J. M. (2000). Two distinct pathways remove mammalian cohesin from chromosome arms in prophase and from centromeres in anaphase. *Cell* 103, 399-410.

Wang, Q., Song, C. and Li, C. C. (2003). Hexamerization of p97-VCP is promoted by ATP binding to the D1 domain and required for ATPase and biological activities. *Biochem Biophys Res Commun* 300, 253-260.

Wang, Q., Song, C., Yang, X. and Li, C. C. (2003). D1 ring is stable and nucleotide-independent, whereas D2 ring undergoes major conformational changes during the ATPase cycle of p97-VCP. *J Biol Chem* 278, 32784-32793.

Wassmann, K., Liberal, V. and Benezra, R. (2003). Mad2 phosphorylation regulates its association with Mad1 and the APC/C. *EMBO J* 22, 797-806.

Weihl, C. C., Dalal, S., Pestronk, A. and Hanson, P. I. (2006). Inclusion body myopathy-associated mutations in p97/VCP impair endoplasmic reticulum-associated degradation. *Hum Mol Genet* 15, 189-99.

Wheatley, S. P., Hinchcliffe, E. H., Glotzer, M., Hyman, A. A., Sluder, G. and Wang, Y. (1997). CDK1 inactivation regulates anaphase spindle dynamics and cytokinesis in vivo. *J Cell Biol* 138, 385-93.

Wirth, K. G., Wutz, G., Kudo, N. R., Desdouets, C., Zetterberg, A., Taghybeeglu, S., Seznec, J., Ducos, G. M., Ricci, R., Firnberg, N. et al. (2006). Separase: a universal trigger for sister chromatid disjunction but not chromosome cycle progression. *J Cell Biol* 172, 847-60.

Wojcik, C., Yano, M. and DeMartino, G. N. (2004). RNA interference of valosin-containing protein (VCP/p97) reveals multiple cellular roles linked to ubiquitin/proteasome-dependent proteolysis. *J Cell Sci* 117, 281-92.

Xia, G., Luo, X., Habu, T., Rizo, J., Matsumoto, T. and Yu, H. (2004). Conformation-specific binding of p31(comet) antagonizes the function of Mad2 in the spindle checkpoint. *EMBO J* 23, 3133-3143.

Xiong, X., Chong, E. and Skach, W. R. (1999). Evidence that endoplasmic reticulum (ER)-associated degradation of cystic fibrosis transmembrane conductance regulator is linked to retrograde translocation from the ER membrane. *J Biol Chem* 274, 2616-24.

Yamamoto, A., Guacci, V. and Koshland, D. (1996). Pds1p is required for faithful execution of anaphase in the yeast, Saccharomyces cerevisiae. *J Cell Biol* 133, 85-97.

Ye, Y. (2006). Diverse functions with a common regulator: Ubiquitin takes command of an AAA ATPase. *J Struct Biol* 156, 29-40.

Ye, Y., Meyer, H. H. and Rapoport, T. A. (2003). Function of the p97-Ufd1-Npl4 complex in retrotranslocation from the ER to the cytosol: dual recognition of nonubiquitinated polypeptide segments and polyubiquitin chains. *J Cell Biol* 162, 71-84.

Ye, Y., Meyer, H. H. and Rapoport, T. A. (2001). The AAA ATPase Cdc48/p97 and its partners transport proteins from the ER into the cytosol. *Nature* 414, 652-6.

Yu, H., King, R. W., Peters, J. M. and Kirschner, M. W. (1996). Identification of a novel ubiquitin-conjugating enzyme involved in mitotic cyclin degradation. *Curr Biol* 6, 455-66.

Yuasa, T., Hayashi, T., Ikai, N., Katayama, T., Aoki, K., Obara, T., Toyoda, Y., Maruyama, T., Kitagawa, D., Takahashi, K. et al. (2004). An interactive gene network for securin-separase, condensin, cohesin, Dis1/Mtc1 and histones constructed by mass transformation. *Genes Cells* 9, 1069-82.

Zhang, D., Yin, S., Jiang, M. X., Ma, W., Hou, Y., Liang, C. G., Yu, L. Z., Wang, W. H. and Sun, Q. Y. (2007). Cytoplasmic dynein participates in meiotic checkpoint inactivation in mouse oocytes by transporting cytoplasmic mitotic arrest-deficient (Mad) proteins from kinetochores to spindle poles. *Reproduction* 133, 685-695.

Zhang, Y., Nijbroek, G., Sullivan, M. L., McCracken, A. A., Watkins, S. C., Michaelis, S.and Brodsky, J. L. (2001). Hsp70 molecular chaperone facilitates endoplasmic reticulum-associated protein degradation of cystic fibrosis transmembrane conductance regulator in yeast. *Mol Biol Cell* 12, 1303-1314.

Zou, H., McGarry, T. J., Bernal, T. and Kirschner, M. W. (1999). Identification of a vertebrate sister-chromatid separation inhibitor involved in transformation and tumorigenesis. *Science* 285, 418-22.

Zur, A. and Brandeis, M. (2001). Securin degradation is mediated by fzy and fzr, and is required for complete chromatid separation but not for cytokinesis. *Embo J* 20, 792-801.

ABBREVIATIONS

aa	amino acid(s)
amp	ampicillin
APS	ammonium peroxodisulfate
ATP	adenosine 5'-triphosphate
bp	base pairs
BSA	bovine serum albumin
CHX	cycloheximide
CLD	Cdc6-like domain
CSF	cytostatic factor
C-terminal	carboxyterminal
C-terminus	carboxy terminus
DAPI	4',6'-diamino-2-phenylindol
DMSO	dimethylsulfoxide
DNA	deoxyribonucleic acid
dNTP	deoxynucleotide
DTT	dithiothreitol
E. coli	*Escherichia coli*
EDTA	ethylendiamine tetraacetic acid
EGTA	ethylen glycol tetraacetic acid
ERAD	endoplasmic reticulum associated protein degradation
Fig.	figure
FISH	Fluorescence In Situ Hybridization
f.l.	full length
g	gram or gravitational constant (9.81 m/sec^2)
GST	glutathione S transferase
h	hour or human
HA	hemagglutinin
HAc	acetic acid
HEPES	4-(2-hydroxyethyl)-1piperazineethansulfonic acid
H.s.	*Homo sapiens*
Ig	immunoglobulin
IP	immunoprecipitation
IPTG	isopropyl-β-D-thiogalactopyranoside
IVT	*in vitro* translation
k	kilo
kb	kilo base pairs
kDa	kilo dalton
kDa	kilo dalton
LB	Luria-Bertani
m	milli
μ	micro
M	molar
MCS	multiple cloning site
min	minutes
MMR	Marc's modified Ringer

MOPS	3-N-morpholinopropane sulfonic acid
MT	microtubules
mRNA	messenger RNA
n	nano
NEM	N-ethylmaleimide
NHS	N-hydroxysuccinimid
NTA	nitrilo tri acetic acid
N-terminal	aminoterminal
N-terminus	amino terminus
OD	optical density
ORF	open reading frame
p.a.	*pro analysi*
PAGE	polyacrylamide gel electrophoresis
PBS	phoshate buffered saline
PCR	polymerase chain reaction
PVDF	polyvinylidene fluoride
rpm	rounds per minute
RT	room temperature
SAC	spindle assembly checkpoint
S. cerevisiae	*Saccharomyces cerevisiae* (budding yeast)
SDS	sodium dodecylsulfate
sec	seconds or securing
hSep	human separase
S. pombe	*Saccharomyces pombe* (fission yeast)
Tab	Table
TEMED	N,N,N',N'-tetramethylethylendiamine
Tev	protease of tobacco etch virus
Tris	tris(hydroxymethyl)aminomethane
U	unit
Ub	ubiquitin
V	volt
v/v	volume per volume
w/v	weight per volume
wt	wild type
ZZ	IgG binding domain of protein A

Unless stated otherwise, "extract" is used to describe *Xenopus* low-speed extracts. "HighΔ90"- or "lowΔ90"-extracts describe *Xenopus* (low-speed) anaphase extracts containing high (>120 nM) or low (80 nM) concentrations of non-degradable cyclin B1 (cyclin B1Δ90).

OVERVIEW OF PROTEINS AND PROTEIN COMPLEXES

AAA	ATPases associated with various cellular activities (protein family)
APC/C	Anaphase promoting complex/cyclosome (E3 ligase)
Bub1, R1, 3	Budding uninhibited by benzimidazole 1, R1, 3 (checkpoint proteins)
Cdc20	Co-activator of the APC/C
Cdc48	p97 in yeast
Cdh1	Co-activator of the APC/C
Cdk1	Cyclin-dependent kinase 1
CFTR	Cystic fibrosis transmembrane conductance regulator
CPC	Chromosomal passenger complex (consisting of Aurora B, INCENP, Survivin and Borealin)
Cut1	Separase in fission yeast
Cut2	Securin in fission yeast
Δ90	Cyclin B1 mutant stabilized via an N-terminal deletion of 90 aa
Emi1	Early mitotic inhibitor 1
H2A, B	Histone 2A, B
Mad1, 2	Mitotic arrest deficient 1, 2 (checkpoint proteins)
MCC	Mitotic checkpoint complex (consisting of Cdc20, Mad2, BubR1 and Bub3)
Npl4	Nuclear protein localization 4 (p97 adaptor)
p47	p97 adaptor
SBP	Sperm-specific basic protein
SCF	Skp1/Cullin/F-Box (E3 ligase)
UbcH5, 10	E2 enzymes of the APC/C
Ufd1	Ubiquitin-fusion degradation 1 (p97 adaptor)
VCP	Valosin-containing protein (= p97)
(X)Erp1	(*Xenopus*)Emi1-related protein 1

DANKSAGUNG

LEBENSLAUF

Name: Simone Heubes
Geburtsdatum: 18. Januar 1978
Geburtsort: Konstanz

Schulbildung

1984 - 1988   Volksschule Poxdorf
1988 - 1997   Ehrenbürg-Gymnasium Forchheim
                  Abschluss mit Abitur im Juli 1997

Studium

1997 - 2003   Universität Bayreuth
                  Diplomstudiengang Biochemie
2002 - 2003   Diplomarbeit am Deutschen Krebsforschungszentrum,
                  Heidelberg, Abteilung Molekularbiologie der Zelle I
                  (Prof. Ingrid Grummt)
                  Thema: „Epigenetische Mechanismen der Transkriptions-
                      regulation: Nachweis spezifischer Histon-
                      modifikationen an transkriptionell aktiven und
                      inaktiven rRNA Genen"
                  Abschluss mit Diplom im Februar 2003

Promotion

2003 - 2007   Max-Planck-Institut für Biochemie, Martinsried
                  AG Chromosome Segregation in Mitosis and Meiosis
                  (Dr. Olaf Stemmann)
                  Thema: „The AAA-ATPase p97 in mitosis and fertilization"

Stipendien

1997 - 2002   Bayerisches Hochbegabten-Stipendium
2000 - 2002   Stipendium der Studienstiftung des deutschen Volkes
2004 - 2006   Promotionsstipendium der Boehringer Ingelheim Fonds
2004 - 2006   Promotionsstipendium der Studienstiftung des deutschen
                  Volkes